جمهورية العراق
وزارة التعليم العالي و البحث العلمي
جامعة بابل/ كلية العلوم
قسم الفيزياء

دراسة الخصائص الفيزيائية لـ TiO_2 / PANI لتطبيقات الخلايا الشمسية باستخدام تقنية البرم المغزلي

رسالة
مقدمة إلى مجلس كلية العلوم في جامعة بابل كجزء من متطلبات
نيل درجة الماجستير في العلوم/ الفيزياء

من قبل

حسن راسم محمد عويز

(بكالوريوس علوم فيزياء / ٢٠١٠)

إشراف

أ. د. محمد هادي شنين

٢٠٢١ م ١٤٤٣هـ

بسم الله الرحمن الرحيم

(فَتَعَالَى اللَّهُ الْمَلِكُ الْحَقُّ ۗ وَلَا تَعْجَلْ
بِالْقُرْآنِ مِن قَبْلِ أَن يُقْضَىٰ
إِلَيْكَ وَحْيُهُ ۖ وَقُل رَّبِّ زِدْنِي عِلْمًا)

صدق الله العظيم

سورة طه الآية (١١٤)

Supervisor Certification

I certify that this thesis is titled (**Study Physical Properties of TiO_2/PANI For Solar Cells Applications Using Spin Coating Technique)** Was prepared by (**Hassan Rasim Mohammed Aweiz**) under my supervision at the Department of Physics, College of Science, University of Babylon, as partial fulfillment of the requirements for practical degree of Physics Master thesis in (Physics) .

Signature

Supervisor : Dr.Mohammed Hadi Shinen

Title : prof .

Address : Department of physics / College of science / University of Babylon .

Date: / / 2021

Certification of the Head of the Department

In view of the available recommendation , I forward this thesis for debate by the examination committee .

Signature:

Name : Dr. Abdulazeez O. Mousa Al-Ogaili

Title: prof.

Address: Head of Department of physics /College of science / University of Babylon .

Date: / / 2021

Examining Committee Certificate

We certify that we have read this thesis entitled (**Study Physical Properties of TiO_2/PANI For Solar Cells Applications Using Spin Coating Technique**) and as an examining committee, examined the M.Sc. student "**Hassan Rasim Mohammed Aweiz** " in its content and that , in our opinion it meets the standards of a Thesis for the degree of master in science of physics.

Signature :

Name : **Dr. Raheem Gaid Kadhim**
Title : Professor
Address : Department of Physics/
College of Science / University of Babylon
Date : / / 2021
(Chairman)

Signature :

Name : **Dr. Hussein Falih Hussein**
Title : Professor
Address : Department of Physics /
College of Education for pure Science
University of Basrah
Date : / / 2021
(Member)

Signature :

Name : **Dr. Maan Abd-Alameer Salih**
Title : Lecturer
Address : Department of Physics /
College of Science/University of Babylon
Date : / / 2021
(Member)

Signature :

Name **Dr. Mohammed Hadi Shenin**
Title : Professor
Address : Department of Physics /
College of Science/University of Babylon
Date : / / 2021
(Member and Supervisor)

Approved by the College committee on graduate studies

Signature:

Name **: Dr. Enas Mohammed Al-Robayi**

Title: Professor

Address: Dean of the College of science /University of Babylon

Date: / / 2021

Dedication

To My:

Dears Father, Mother,

Wife, Brothers, Sisters and Sons

with My Great Love.

Hassan

Acknowledgements

First of all, my deepest gratitude goes to ALLAH (The Almighty), The compassionate, and the merciful for everything. Many thanks to the College of Science in University of Babylon and the Department of Physics for offering me the opportunity to complete my study.

My deep thanks and gratitude go to my supervisor**,** ***Prof.Dr. Mohammed Hadi Shinen*** for the valuable guidance and support to bring this thesis to light.

Finally, I shall always be grateful to all those who helped me in the preparation of this research and all my colleagues postgraduate masters.

Hassan

الخلاصة

في هذه الدراسة، تم تحضير ثاني اوكسيد التيتانيوم بطريقة السول- جل ، تم تحضير اغشية رقيقة بواسطة تقنية البرم المغزلي على شرائح ITO بثلاث سماكات (١٠٦، ٨٧،٦٣) نانومتر. تم تلدين الاغشية المحضرة عند درجة حرارة ٥٥٠س° لمدة ٣٠ دقيقة، اظهرت نتائج حيود الاشعة السينية (XRD) للاغشية المحضرة ان طور anatase هو الطور السائد عند تلدين الاغشية في درجة حرارة ٥٥٠س° ، اظهرت نتائج المجهر الالكتروني الماسح (SEM) ان جميع الاغشية ذات تجانس جيد وان معدل الخشونة ومعدل الحجم الحبيبي يزداد مع تناقص السمك، بواسطة مطياف الاشعة تحت الحمراء (FT-IR) تم تشخيص الاواصر الفعالة لبوليمر بولي انلين النانوي، تم ترسيب اغشية بوليمر بولي انلين النانوي بثلاث سماكات (١٠٦،٨٧، ٦٣) نانومتر باستخدام تقنية البرم المغزلي.

درست الخصائص البصرية لاغشية ثاني اوكسيد التيتانيوم وبولي انلين باستخدام مطياف UV-VIS من خلال قياس طيف الامتصاصية كدالة للطول الموجي في مدى الاطوال الموجية (٢٠٠ - ١١٠٠) نانومتر. اظهرت النتائج ان نفاذية الاغشية تزداد مع تناقص السمك، مما جعلها مناسبة لاستخدامها في تطبيقات الخلايا الشمسية، تتناقص الامتصاصية ومعامل الانكسار ومعامل الامتصاص مع تناقص السمك. تزداد فجوة الطاقة مع تناقص السمك .

كتطبيق عملي تم استخدام هذه الاغشية في تصنيع خلية شمسية ، تم دراسة كفاءة هذه الخلية الشمسية، حيث اظهرت النتائج ان كفاءة الخلية الشمسية تزداد عند تناقص السمك من (١٠٦الى٨٧) نانومتر ،ثم تنخفض عند سمك ٦٣ نانو متر ، وجد أن اقصى كفاءة كانت عند سمك ٨٧ نانومتر وكانت قيمتها (٠،٦١%).

Republic of Iraq
Ministry of Higher Education and Scientific Research
University of Babylon
College of Science
Department of Physics

Study Physical Properties of TiO_2/PANI For Solar Cells Applications Using Spin Coating Technique

A Thesis

Submitted to the Council of College of Science, University of Babylon in Partial Fulfillment of the Requirements of the Degree of Master in Science / Physics.

By

Hassan Rasim Mohammed Aweiz

(B.Sc. in Physics /2010)

Supervised by

Prof . Dr. Mohammed Hadi Shinen

2021A.D. 1443A.H.

Summary

In this study, Titanium dioxide have been prepared using a sol-gel method. Thin films were prepared by Spin Coating technology on glass slides and on ITO slides at three thickness (106,87,63) nm. The prepared films were annealed at 550 °C for 30 minutes. The results of X-ray diffraction (XRD) for the prepared films Observed that anatase phase is the predominant phase when annealing the films at a temperature of 550 °C. The results of a scanning electron microscope (SEM) showed that all the films had good homogeneity, and that the roughness rate and the rate of grain size increased with decreasing of thickness. by infrared Spectrophotometer (FT-IR) the active bonds of the nano polyaniline polymer were diagnosed, the nano polymer polyaniline films were deposited with three thickness (106,87,63) nm using spin coating technology.

The optical properties of Titanium dioxide and Polyaniline films were studied using UV-VIS spectrophotometer by recording the absorbance spectrum as a function of wavelength in the wavelength range (200-1100) nm. The results showed that the Transmittance of the films increases with the decrease in the thickness , making it suitable for use in solar cell applications .The absorbance, refractive index and absorption coefficient decrease with the decrease in thickness. The energy gap increases with decreasing thickness.

As a practical application, these films were used in the manufacture of a solar cell. The efficiency of this solar cell was studied, as the results showed that the efficiency of the solar cell increases when the thickness is decreased from (106 to 87) nm and then decreases at the thickness 63 nm , found that the maximum efficiency was at a thickness (87) nm and its value was (0.61%).

Contents

List of Symbols and Abbreviations

Symbol	Physical meaning
PANI	Polyaniline
TiO_2	Titanium Dioxide
A	Absorbance
CR39	Columbia Resin
PLD	Pulsed Laser Deposition
a	Lattice Constant
ITO	Indium Tin Oxide
A^*	Richardson Constant
A_j	Effective Area
AFM	Atomic Force Microscope
FT-IR	Fourier Transform of Infrared
α_{op}	Absorption Coefficient
E_g	Energy Gap
C.B.	Conduction Band
V.B.	Valence Band
c	Velocity of Light
$d_{(hkl)}$	The Inter-Plane Distance
D_s	Crystallite Size
E	Electric Field Vector
E_a	Electrical Activation Energy
$E_{C.B}$	Conduction Band Energy

Symbol	Physical meaning
CPs	Conducting Polymers
E_F	Fermi Level Energy
ΔE_v	Discontinuity in the Valence Band
ΔE_c	Discontinuity in the Conduction Band
OLEDs	Organic Light Emitting Diodes
$E_{V.B}$	Valence Band Energy
E_u	Urbach Energy
h	Plank Constant
I-V	Current-Voltage
IR	Infrared Radiation
I_f	Forward Current
I_A	Absorbed Light Intensity
I_o	Incident Intensity of Light
I_{sc}	Short Circuit Current
I_{ph}	Photocurrent
I_s	Saturation Current
I_d	Dark Current
I_T	Intensity of the Transmitting Rays
J	Current Density
J_s	Reverse Saturation Current Density
J_{sc}	Short – Circuit Photocurrent Density
J_o	Dark Current Density
J_R	Photocurrent Density
k_o	Extinction Coefficient
k	Wave vector
$K_ß$	Boltzmann's Constant
HJ	Hetero Junction
L_n	Diffusion Length of Electrons

Symbol	Physical meaning
L	**Distance Between The Opposite poles**
λ	**Wavelength**
m_e^*	**Effective Mass of Electron**
m_o	**Rest Mass of Electron**
a	**Pole Width**
N	**Electrons Concentration**
n	**Refractive Index**
n^*	**Complex Refractive Index**
n_e	**Carrier Concentration**
N_D	**Donors Concentration**
N_A	**Acceptors Concentration**
N_l	**Number of Layers**
$N(E_F)$	**Density of Localized States Near Fermi Level**
NIR	**Near-Infrared Region**
n_i	**Intrinsic Carrier Concentration**
S	**Micro Strain**
P_{in}	**Incident Power**
P	**Radiation Power**
PEM	**Photo Electromagnetic**
RMS	**Root Mean Square**
R	**Reflectance**
R_H	**Hall Coefficient**
ε	**Dielectric Constant**
ε_i	**Imaginary Part of Dielectric Constant**
ε_r	**Real Part of Dielectric Constant**
ε_s	**Static Dielectric Constant**
T	**Transmittance**
t	**Thin Film Thickness**
T_s	**Substrate Temperature**
T_g	**Glass Transition Temperature**
UV	**Ultra Violet**
V_F	**Forward Voltage**
V_R	**Reverse Voltage**
V_d	**Drift Velocity**

Symbol	Physical meaning
υ	Frequency
V_{oc}	Open Circuit Voltage
W_D	Junction Width
SEM	Scanning Electron Microscope
XRD	X-ray Diffraction
ρ	Resistivity
ρ_o	Density of Material
μ	Mobility
μ_p	Hole Mobility
μ_n	Electron Mobility
σ	Electrical Conductivity
σ_o	Minimum Electrical Conductivity
$\sigma_{D.c}$	Direct - Current
σ_n	Electron Conductivity
σ_p	Hole Conductivity
β	Ideality Factor
Φ	Work Function
η	Efficiency
F.F	Fill Factor
L	The distance between opposite poles (cm)
R	Resistant Films

List of Figures

List of Tables

1.1- General Introduction

Nanotechnology is a very important part of science and technology, as it is possible to control atoms and molecules of materials whose size ranges from (1 to 100) nm. Within this technology, devices and products can be made using small parts, such as optical and electronic devices, sensors, and other devices. There is a lot of research and attempts aimed at developing this technology at the present time. There are also many applications of this technology in the production of materials with magnetic and optical properties [1].

Titanium dioxide, also referred to as titania or titanium quaternary oxide can be defined as a naturally-occurring titanium dioxide, chemically denoted by TiO_2. This material has many and wide applications in solar cells, painting, food coloring, and other applications in other fields. Due to titanium dioxide's physical and chemical advantages, it received great attention from researchers and specialists in this technology, and these features made it suitable for many scientific applications. In TiO_2, a major feature is that it has chemical stability and its resistance to corrosion significantly; in addition to that, it is transparent to visible light and infrared rays and has a high refractive index, which makes it used in anti-reflection coatings in optical applications [2]. Among its other uses, as it was used as a pigment in coatings, to protect against harmful sun rays and toothpaste and other uses, the aim of the present work is to examine the optical and structural properties of TiO_2 and its applications in optical and electronic devices. In recent years, nano films have been produced of TiO_2, which is a major oxide of materials with optical, electrical, and electrochemical properties. Many studies have been conducted regarding the preparation of TiO_2 and the possibility of using it as thin films, which are prepared via a sol-gel approach. Through a review of previous studies that specialize in this technique, it has been indicated that the TiO_2

properties are largely depending on the preparation conditions and the materials utilized in preparation. Many researchers have used the sol-gel method to prepare TiO_2. For example, nanostructured titanium dioxide was produced at low temperatures through a sol-gel approach with the use of nitric acid and titanium isopropoxide, with 50 nm as grain size, also when annealing of TiO_2 films at a temperature of 600 °C that gives rise to the rutile phase [3]. The optical properties of TiO_2 nanoparticles have been shown by sol-gel preparation by means of titanium isopropoxide, aqueous solution, and ethanol [4]. The size of the obtained particles is 7.8 nm and 7.4 nm, respectively [5]. Likewise, the characteristics of TiO_2 nanoparticles prepared through the sol-gel technique have been described, where the particles' average size was approximately 10 nm after annealing. At different temperatures, and after making some measurements that fit with these films, many of the properties of these films were known [6]. TiO_2 films were prepared with a granular size from 13 to 34 nm after being annealed at temperatures at (550) ^oC; in addition, through the sol-gel process, TiO_2 Thin Films were prepared and annealed. It was observed that these films crystallize with the increase in annealing temperature [7].

1.2- Classification of Polymers

Polymers are frequently separated according to whether they can be melted and reshaped throughout purpose of heat and pressure, called thermoplastics, or whether they decompose previous to they can be melted or reshaped, called thermosets. While , together thermoset polymers and thermoplastics can be recycled, because thermoplastics can be reshaped simply throughout the submission of heat and pressure, recycling of thermoplastics is easier [8,9] . There is also conductive polymers, such as (polyaniline) and other non-conductive.Therefore, polymers classify into diverse types of dissimilar sources [10].

1- Classification based on source.

2- Classification based on structure of polymers such as linear.

3- Classification based on mode of polymerization.

4- Classification based on molecular forces.

1.3- Conducting Polymers (CPs)

Organic polymers are normally insulators, they can be presumed that conducting polymers (CPs) must have an unusual structure. Polymers with conjugated π-electron (i. e. system have C=C conjugated bonds) display unusual electronic properties such as low energy optical transition, low ionization potentials, and high electron affinities. The result is a class of polymers that can be oxidized or reduced more easily and more reversibly than conventional polymers.

The effect of this oxidation or reduction on polymer is called doping, i. e. convert an insulating polymer to conducting one [11]. Conducting polymers (CPs) such as polypyrrole, polythiophene and polyanilines are complex dynamic structures that captivate the imagination of those involved in intelligent materials research. The application of electrical stimuli can result in drastic changes in the chemical, electrical and mechanical properties of CPs. These complex properties can be controlled only if we understand, first, the nature of the processes that regulate them during the synthesis of the conducting polymers, and second, the extent to which these properties are changed by the application of an electrical stimulus. Polyaniline and its derivative is one of important conducting polymer, it has many application such as organic light emitting diodes [12].

1.4- Nanomaterials

It can be defined nanomaterials as those distinct category of advanced materials that can be produced so ranging dimensions or the dimensions of the internal grain size gauges between (1-100) nm ,small

gauges of this volume of materials has led to behave different from conventional materials oversize with dimensions greater than 100 nm, for example, add strength and flexibility to protect thermal plastics, ceramics and metals [13,14].

1.5- Polyaniline (PANI)

The polymer polyaniline (PANI), is one of conductive polymers which received much interest in recently because of its optical properties and electrically [15]. The polyaniline exists in a diversity of forms that vary in chemical and physical properties the most common green protonated emeraldine has conductivity on a semiconductor rank of the array of (10^{-10}) s cm^{-1}, many orders of degree higher than that of common polymers ($<10^{-9}$ s cm^{-1}) but lower than that of typical metals ($>10^{4}$ s cm^{-1}). Protonated PANI, (PANI hydrochloride) converts to a nonconducting blue emeraldine base when treated with ammonium hydroxide, figure (1-1) [16].

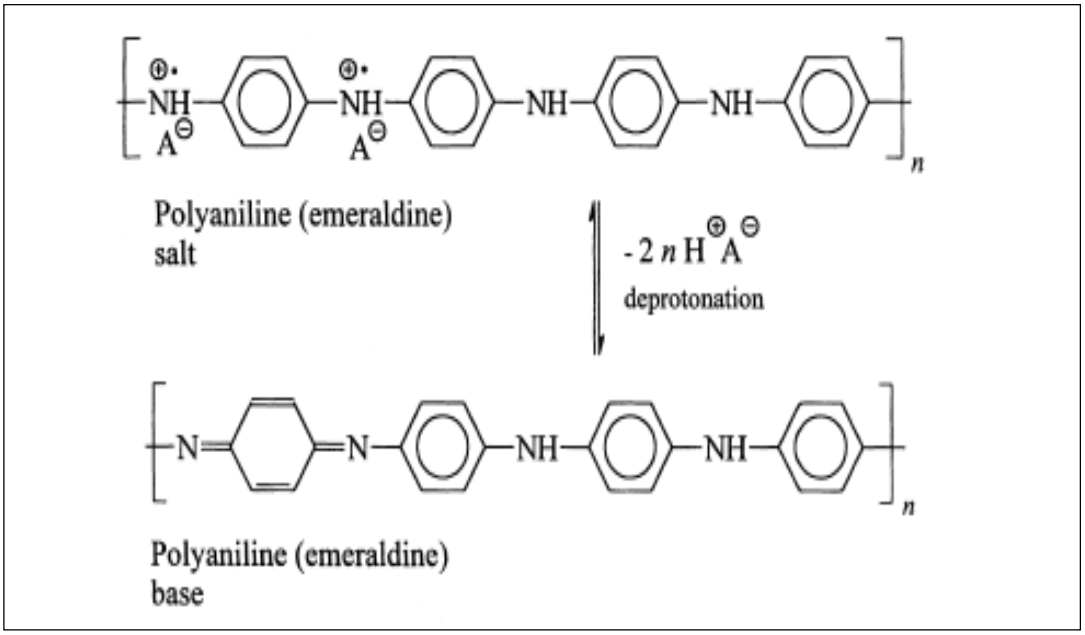

Figure (1-1): Polyaniline (emeraldine) salt is deprotonated in the alkaline medium to polyaniline (emeraldine) base. A– is an arbitrary anion, e.g., chloride [16].

Polyaniline is one of the majority which investigate conducting polymers, due to its high chemical and thermal stability and the simplicity of

polymerization, collectively with the relative low expense of production it also has the latent of many scientific applications [17].

1.6- Applications of Polyaniline

Polyaniline has many applications in several areas, including [18,19]

a- Optical emission diodes industry.

b- Protect metals from corrosion.

c - Solar cells industry.

d - Industry energy storage tools.

e - Enters in smart windows industry.

f- Industry gas separation membranes.

1.7- Methods of Preparation Polymer Thin Films

There are many ways to deposited thin films, the methods employed for thin film deposition can be divided into two groups based on the nature of deposition process, namely physical and chemical [20,21] :

1.8- Literature Review

- In 2010 D.K. Dwivedi, and M. Dayashankar, [22] Nanostructure composite and thin film of titanium dioxide coatings on glass have been prepared by the sol-gel method. TiO_2 sol suspension was prepared by first adding titanium tetra isopropoxide to a mixture of ethanol and HCl and then adding a 2 wt.% solution of hydroxyl ethyl cellulose as dispersant followed by of stirring. Precalcined TiO_2 nano powder was mixed with a sol and heat treated. Thin and composite films were deposited on the glass substrate (microscope glass slide) by spin coating at ambient conditions. After drying, samples were heated to 500 °C. The resulting films were characterized by UV-Vis spectroscopy, X-ray diffraction (XRD) and Atomic Force Microscopy (AFM). The purpose of this study was to determine if thin and composite TiO_2 films with ultraviolet light have any

effect on the growth of Escherichia coli, Staphylococcus aureus and Bacillus species were unusual results in which TiO_2 thin and composite films protect E. coli, S. aureus and Bacillus sp from UV light. The survival of E. coli with UV alone was 3.2 % while with UV and TiO_2 composite film was 91%. The UV absorbing coatings are transparent, colorless, and exhibit high optical quality. The UV-protective coatings offer an easy method to protect the living organisms against UV.

- In 2011 A. Hateef, [23] Thin films of titanium dioxide with high surface area are prepared by sol-gel dip-coating technique. Inthis regards, Titania nano sols with high photo catalytic activity were prepared by dissolving titanium alkoxide inalcohol and water under acidic conditions. Photo catalytic activities of titanium dioxide thin films were measured in the presence of methylene blue. Microstructure and photo catalytic activity of the films, nano powders and titanium dioxide sols were investigated using X-ray diffraction, scanning electron microscopy, specific surface area, zeta sizerand ultraviolet–visible spectrometry techniques. Particle size analysis of sols showed that the mean particle sizes were15 to 128 nm. X-ray diffraction analyses revealed that anatase crystal structure was produced with crystallite size below 11 nm. Increasing mass percent of anatase phase and specific surface area, enhance the photo catalytic activity. Scanning electron microscopy images showed that the addition of methylcellulose as a dispersant, not only produce drough texture in the thin film, but also enhanced photo catalytic activity. The thin films prepared by using nitric acid asa stabilizer, revealed higher photo catalytic activity, surface area and sol stability and these data were more than those prepared with acetic acid.
- In 2012 D.A. Hanaor *et al* .,[24] Nano crystalline TiO_2 thin films were prepared at ambient conditions and titanium tetra iso propoxide [C12H28O4Ti] was used as a Ti-precursor. The effect of annealing temperature on optical properties of nano crystalline TiO_2 thin films was

studied. The as-deposited films were dried at 100 ^{o}C for 1 hr. The films formed were further heated in temperature between (200 and 500) ^{o}C for 1 hr. The films were characterized by different techniques: XRD, UV-visible spectroscopy, FT-IR spectroscopy. The characterization studies revealed that the films are crystallized as anatase phase and nano-structured with better optical properties $\alpha = 0.89$ as compared to reported data. The optical measurement showed the indirect band gap between 3.31 and 3.35 eV with corresponding crystallite sizes between 8.9 and 3.7 nm. The SEM image of film annealed at 400 ^{o}C showed spherical nano crystalline structure of TiO_2 particles. The crystallite sizes obtained from SEM image are found to be between 30 and 100 nm. It is also observed that refractive index of the film increases with increasing the annealing temperature. The smaller crystallite size gives larger band gap due to quantum size effects. It is also observed that refractive index of the film increases with increasing the annealing temperature and hence the crystallite size. Hence, the nano crystalline TiO_2 thin films prepared in the present work might be having tremendous potential for the applications like photo anodes, photo-electrochemical devices and dye sensitized solar cells.

- In 2012 K . M. Ziadan *et al* ., [25] Thin films TiO_2 were prepared by magnetron sputtering through deposition of metal Ti on Si substrates and subsequent gas-solid state reaction. Structural evolution of the thin film TiO_2 has been investigated from room temperature to 500 °C. Amorphous TiO_2 and its local crystallization in the thin films were observed by X-ray diffraction and transmission electron microscope (SEM). X-ray reflectivity experiments indicate that the expansion ratio of the thickness is 1.4 after oxidation at the temperature 300 °C. Dielectric constant of the amorphous TiO_2 thin film is about 18 at room temperature
- In 2013 S. Reda Al-Ghannam, [26] Thin films of anatase titanium dioxide are deposited on Indium-doped tin Oxide (ITO) glass substrates utilizing

the electric field-assisted aerosol reaction of titanium isopropoxide in toluene at 450 °C. The as-deposited films are characterized using scanning electron microscopy (SEM), X-ray diffraction (XRD), Raman spectroscopy (RS), and UV-vis spectroscopy. The photoactivity and antibacterial activity of the films are also assessed. The characterization analysis reveals that the use of an electric field affects the film microstructure, its preferential orientation, and the functional properties. XRD of the anatase films reveals that the application of electric fields causes a change in the preferential orientation of the films from (101) to (004) or (211) planes, depending on the strength of the applied field during the deposition.

- In 2014 M. Abd-Alkadum, [27] Titanium dioxide (TiO_2) thin films are deposited on silicon substrates by using sol-gel dip coating technique. Annealing temperature was varied to investigate its effect on the surface morphology, structural and electrical properties of the film. The crystalline structure, surface morphology and the electrical properties were investigated by X-ray diffraction, field emission scanning electron microscopy (SEM), atomic force microscope (AFM), and four point probe. The results show that with an increase in annealing temperature, the value of the intensity of (101) peak increases while the value of the full-width at half maximum decreases. Thin films deposited at high annealing temperatures result in an increase in surface roughness and grain size. The electrical properties of these films show that the resistivity varies between 1.40 x 105 and 7.19 x 102 Ω.cm when the annealing temperature changes from 300 to 900°C, respectively. The TiO_2 thin films annealed at 900°C exhibited lower resistivity than other films. It found that the annealing temperature influences the surface morphology, structural and electrical properties of TiO_2 thin films.
- In 2015 A.N.Daghman *et al* ., [28] Nanocrystalline titanium dioxide (TiO_2) thin films were prepared by using sol-gel through spincoating method. An

assembly of indium tin oxide (ITO)/TiO_2/polyaniline (PANI)/Ag was made in a sandwich panel structure. The obtained junction shows rectifying behavior. Additionally, the I/V characteristic indicates that a P-N junction at nanocrystalline PANI/TiO_2 interface has been created. In this experimental study, we depended only on the ratio between titanium and PANI in the process of preparing sol-gel (PANi/TiO_2 at 20% wt). The largest open circuit voltage of 656 mV and short current density of 0.00315 mA/cm^2 produce 0.0004% power conversion solar cell (η) under simulated solar radiation (50 mW/cm^2). The thin films of PANI and titanium oxide (TiO_2)/ PANI composites were synthesized by sol-gel technique. Pure TiO_2 powder with nanoparticle size of less than 25 nm and PANI were synthesized through chemical oxidative polymerization of aniline monomers. The composite films were characterized by high resolution X-ray diffraction, Fourier transform infrared spectroscopy, field effect scanning electron microscopy, and UV-vis spectroscopy. The results were compared with the corresponding data on pure PANI films. The intensity of diffraction peaks for PANI/TiO_2 composites is lower than that for TiO_2. The characteristic of the FT-IR peaks of pure PANI shifts to a higher wave number in TiO_2/PANI composite, which is attributed to the interaction of TiO2 nanoparticles with PANI molecular chains.

- In 2015 Y. M. Evtushenko *et al.*, [29] Studies the impact of substrate type on crystallinity related to TiO_2 thin films which are synthesized by the process of the PLD. The investigated substrates were Si (100), titanium, and cover glass, while depositions have been made at temperatures in the range from (300 to 450) ºC. It has been identified through using XRD approaches that the rutile phase might be acquired, in a majorly pure phase, at temperatures more than 400 ºC, yet just for titanium and glass substrate. With regard to the case of silicon (100) substrate, it has been specified that the phase of the anatase has been preponderant for the two investigated

process temperature values. The results are highlighting that less expensive Titanium or SiO_2 thin film might be acting as an excellent seed layer for the growth of good-quality rutile TiO_2 phase through the use of the PLD process on the Silicon substrate and utilizing the pre-cursors like H_2O and $TiCl_4$.

- In 2016 S. Demirci *et al*., [30] The thin films of TiO_2 were deposited into the n-Si substrate at a temperature of 100 ºC via the use of a sputtering approach; also, the films were subjected to annealing in air atmosphere between (500-1000) °C. Also, the morphological and structural properties regarding all films are examined via XRD , gas sensor with the inter-digitated platinum electrodes has been fabricated with photolithographic approaches by means of as-deposited and subjected to annealing TiO_2 thin films as an active material. Sensor's sensitivity is evaluated via changing the conductivity regarding such materials within methane gas with different concentrations at various working temperatures. It is indicated that the fabricated sensors utilizing as-deposited TiO_2 thin films with a particle size of 10 nm have fast recovery/response time and high sensitivity. A sensor operating at a temperature of 50 ºC has a high sensitivity to the methane gas, while there is an increase in its detection performance with temperatures. Also, it is identified that the fabricated sensors showed stable and reproducible results.
- In 2017 S.Mukherjee *et al*., [31] The thin films of TiO_2 have been deposited on the silicon substrates by means of a sol-gel spin-coating approach and subjected to annealing at temperatures between (400-900) °C. FT-IR results indicated the formed phases' dependence (rutile, anatase, or mixed anatase-rutile phase) related to TiO_2 films on annealing temperatures. showed peaks at 486 nm (2.55 eV) based on the rutile phase, whereas the 585 nm band (2.11 eV) confirmed the existence of anatase and gradually disappeared for temperatures more than 600 °C. The TiO_2 thin

films' deposition allows controlling the ant reflecting properties regarding the silicon substrate in the range of (13-37) % in the 400-800 nm region.

- In 2018 M. K. Al-hashimi *et al*.,[32] TiO_2 (metal oxide semiconductor) were synthesized effectively with the use of a hydrothermal approach for sensor application. NaOH and TiO_2 were utilized as pre-cursors; such reactants were mixed as well as calcinated at a temperature of 400 ^oC for producing TiO_2 nanoparticles. In addition, the crystalline structure, the morphology regarding the synthesized TiO_2 were examined by means of XRD, FT-IR analysis, and SEM. Also, the XRD results specified that the prepared sample of the Titanium dioxide was highly-crystalline with anatase crystal structure. The peak of the FT-IR spectra at $475cm^{-1}$ specified a characteristic absorption band of TiO_2. FT-IR and XRD results verified the formation of TiO_2 of high-purity. SEM images are showing that the shape of the TiO_2 prepared in the study were spherical. The synthesized TiO_2 have been deposited on the glass substrate at the temperature of the room with the use of E-beam evaporation approach for determining the gauge factor and identified to be 4.70. Furthermore, the deposited thin films of the TiO_2 are offering significant possibilities in applications of magneto-electric and electronic devices.
- In 2019 M. Q. Hamzah *et al*., [33] The thin films of TiO_2 have been deposited on CR39 through sol-gel dip-coating route with various speeds of withdrawal between (250 mm/s and 350 mm/s). Also, the thin films of TiO_2 have been specified through XRD, SEM, ellipsometry, FT-IR, and UV-VIS-NIR spectrophotometry. In addition, the withdrawal speed's role on the thin film thickness to the tailor characteristics regarding TiO_2 thin films is examined. The results of XRD indicated that all films were amorphous in-nature. Yet, the thin films of TiO_2, which are deposited at various withdrawal speed levels showing a decrement in the transmission when the speed is increased. Furthermore, the direct optical bandgap

related to films was evaluated between (3.48 and 3.00) eV through UV-VIS-NIR spectrophotometry and (3.52 and 3.38) eV through ellipsometry. TiO_2 can be defined as one of the possible prospects in microelectronic applications and might be serving as an absorber layer with regard to the PV devices. Surface morphology was granular with the increase in withdrawal speed and the gain size.

- In 2019 E. P. Athisayaraj and C.Vedhi,[34] A nanocomposite material of Polyaniline and Copper oxide was synthesized.The prepared nanocomposites were characterized by UV-Vis, FT-IR, AFM, SEM and electrochemical studies. The FT-IR spectral studies indicated the presence of metal oxide and polymer in nanocomposites. From the FT-IR spectra of nanocomposites, the peak around 512 cm^{-1} and 606 cm-1 indicated the bonding between Cu and O, the peak around 1571 cm^{-1} and 1502 cm^{-1} due to stretching vibrations of the quinonoid and benzenoid rings of polyaniline respectively. The surface morphology was characterized by AFM and SEM. Optical and electrochemical properties were determined using UV-visible spectroscopy and cyclic voltammetry respectively. These characterisations indicated that Polyaniline/CuO was a new semiconductor photoelectric material, and the solar cell prepared with Polyaniline/CuO performed well.
- In 2020 D.K. Muthee nad B.F. Dejene, [35] Studies the report anatase, along with the rutile TiO_2 NPs thin films which are fabricated on the silica and ITO substrates with the use of PLD. Also, the depositions have been conducted at substrate temperatures of 25 ^oC, 400 ^oC, and 600 ^oC from the anatase and rutile phase target materials. The substrate temperature's effect on surface morphology, electrical, optical, and microstructural regarding such films have been examined (systematically) by means of different range of SEM measurements, XRD measurements, and UV-Vis-NIR spectroscopy. It has been indicated that the Titanium dioxide thin film

surface was pre-dominated with nano-particulates with diameter not more than 35 nm, constituting approximately ~ 70%, whereas the electrical resistivity and optical band gaps are decreased with the increase in substrate temperature. The mixed phase (anatase/rutile) Titanium dioxide thin films were formed at substrate temperatures of 400 ^{o}C when the samples were fabricated with rutile and anatase target materials. The results of the paper indicated that the crystallinity and structural, electrical, and optical characteristics might be regulated through different process parameters of PLD for preparing the thin films of TiO_2, which were accountable for applications in photo catalysis, solar cells, and photo voltaic.

- In 2020 F. M. El-Hossary *et al*., [36] Severe research attempts are still in progress to improve the performance of polyaniline (Pani) based photoactive layers as one of the cheapest materials used for manufacturing organic solar cells. Herein, polymer solar cells were fabricated with ITO/(PANI-TiO_2)/Au system. The photoactive layers (PANI-TiO_2) were treated with a hydrogen-plasma discharge for low processing time of 0, 3 and 5 min to enhance the synthesized solar cells efficiency. The morphology, microstructure and optical properties of the prepared samples and plasma treated nanocomposite layers were investigated and discussed. The performance of bulk heterojunction cell samples have been systematically investigated before and after plasma treatment. The absorption and optical band gap energy is increased after the treated PAni-TiO_2 photoactive layers. It is found that, the efficiency was enhanced to 0.7% after 5 min of hydrogen plasma process compared to 0.36% for the pristine cell. The efficiency increase is ascribed to a structural change that accompanied by a rapid increase in surface roughness, which leaded to a decrease in the reflected photons and in turn an increase in the produced charge carriers.

- In 2021 A. A. Al Dairy *et al* ., [37] TiO_2 films were acquired through spray pyrolysis approach onto the glass substrates and kept at temperatures between (300 and 400) ^oC . Also, the conditions were enhanced for obtaining quality films. The acquired films were specified for their structure via x-ray diffract to grams. In addition, the films' optical absorption studies were made by UV-VIS spectroscopy in a spectral range (300-1100) nm. The substrate temperature effect on the optical and structure properties regarding such films was examined. The results are indicating that the acquired films were excellent candidates for the solar cells.

1.9- Aim of the Study

The following points are summarizing the objectives of the presented work:

1. Preparation of Titanium Dioxide (TiO_2) by the sol- gel method.
2. Deposition of Solution of Titanium Dioxide (TiO_2) and polymer (PANI) by Spin coating technique.
3. Studying of optical, electrical, and structural properties of TiO_2 and polymer PANI and using it in solar cell application.

2.1- Introduction

The present chapter is concerned with the mathematical equations and Theoretical foundations ,through which the optical, structural and electrical properties expense are calculated.

2.2- Crystal Structure of Semiconductors

Semiconductor materials can be classified according to their crystal structure or the nature of the arrangement of their atoms into two main classes:

2.2.1- Amorphous Semiconductor Materials

They are called semiconducting materials with atoms randomly distributed within the material, amorphous semiconductor materials[38].

2.2.2- Crystalline Semiconductors

The arrangement of the atoms in crystalline semiconductors is in a periodic geometric manner that repeats cyclically in three directions. The crystalline semiconductor materials are divided into two parts[٣٨]:

2.2.2.1- Monocrystalline Semiconductors

These materials are characterized in the ideal case that their atoms or molecules are arranged in such a way that they repeat themselves periodically and infinitely repeatedly in the three dimensions to be a regular geometric structure, so they have a kind of symmetry.

This arrangement of atoms in the crystal is called the Long Range Order (LRO) [38, 39]. As in figure (2-1a), the atoms of the substance are arranged in all directions in a regular and periodic manner. The atoms' periodic arrangement in the crystal is referred to as the lattice, which consists of units repeating throughout the crystal, and each of these units is called the unit cell [40].

2.2.2.2- Polycrystalline Semiconductors

It is a group of crystals that contain a relatively large number of atoms called granules, each of which has a long-term arrangement unit. Still, the granules as a whole have a Short Rang Order (SRO) because the granules are oriented almost randomly relative to each other, which makes similar properties. polycrystalline semiconductors are equidirectional, unlike monocrystalline whose properties are often asymmetric directions. The meeting surfaces of the crystalline granules with each other are called. Then the periodic arrangement of each granule is interrupted by the boundaries of the granules as shown in figure (2-1b), and the polycrystalline semiconductors are less stable. Thermodynamics of mono crystallization, because the internal minimum free energy is determined by the energy of the boundary of the granules [41].

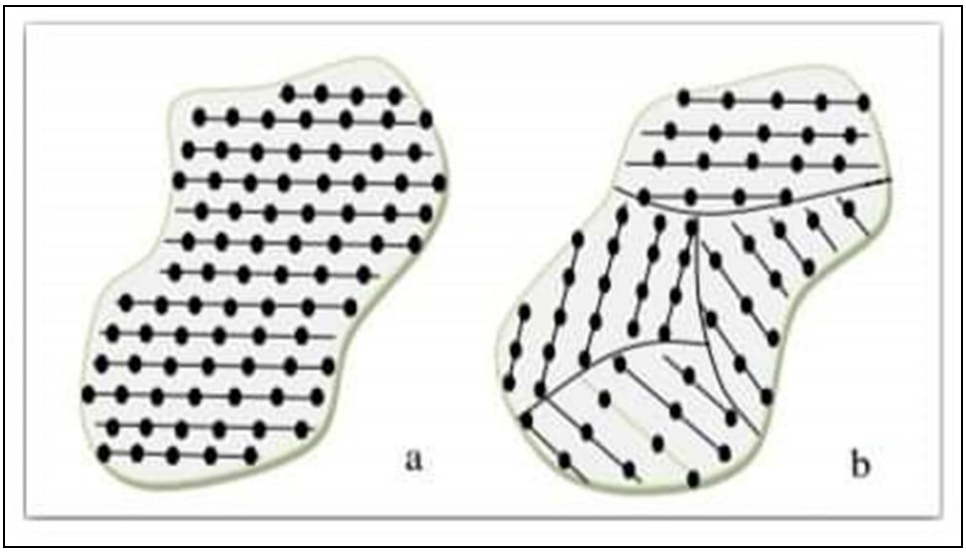

Figure (2-1): Structure of solids according to the arrangement of their atoms: a - monocrystalline b - polycrystalline [42].

2.3- physical and Chemical Properties of Titanium dioxide

Titanium dioxide is an n-type semiconductor material, meaning that the majority charge carriers are electrons, and TiO_2 has a wide energy gap. There are many reasons for choosing titanium dioxide (TiO_2) in our work

as an active material that is used in solar cells, hybrid joints, and anti-reflective coatings [43]. In addition, it is inexpensive and has good transmittance in the visible spectrum region, and has a high refractive index and chemical stability, so it is preferred for use in modern technological industries [44].

Titanium dioxide is found in nature in three phases: anatase, brookite, and rutile. Titanium dioxide with the rutile phase is more stable than the rest of the phases and is more common. The brookite phase is rare in nature. The TiO_2 Thin Films are amorphous in the case of being deposited at a temperature below 300 ^oC, the brookite phase begins to format it, and the rutile phase is formed at higher temperatures [45–47].

2.3.1- General Properties of TiO_2 with Anatase Phase

This phase is characterized by being semi-stable and having multiple forms. When the temperature is increased to 700 ^oC, this phase turns into a rutile phase, but under certain conditions, it turns at a temperature of 400 ^oC Where anatase has a quadruple crystal structure and its lattice constants, a = b = 3.771 Å, c= 9.430 Å, $\frac{c}{a}$ = 2.5007, as in Figure (2-2) [84].

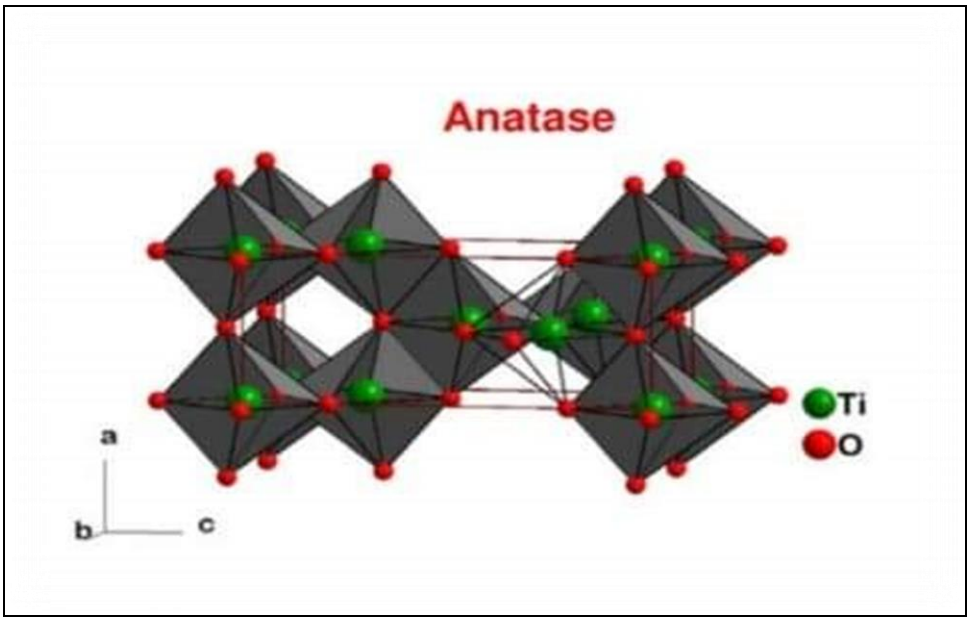

Figure (2-2): Anatase Phase of Titanium dioxide [48].

2.3.2- General Properties of TiO_2 with Rutile Phase

This type is considered one of the most stable phases due to its chemical and mechanical properties' stability. The unit cell of this phase is made up of atoms (Ti), which occupies a basic center in the crystal structure, surrounded by six oxygen atoms, which are Stationed in the corners of the octahedron, The crystalline structure of a rutile phase is a tetragonal right, as in Figure (2-3). the lattice constants have, a = b = 4.593 Å, c = 2.959 Å, and the value, c / a = 0.6442 [48].

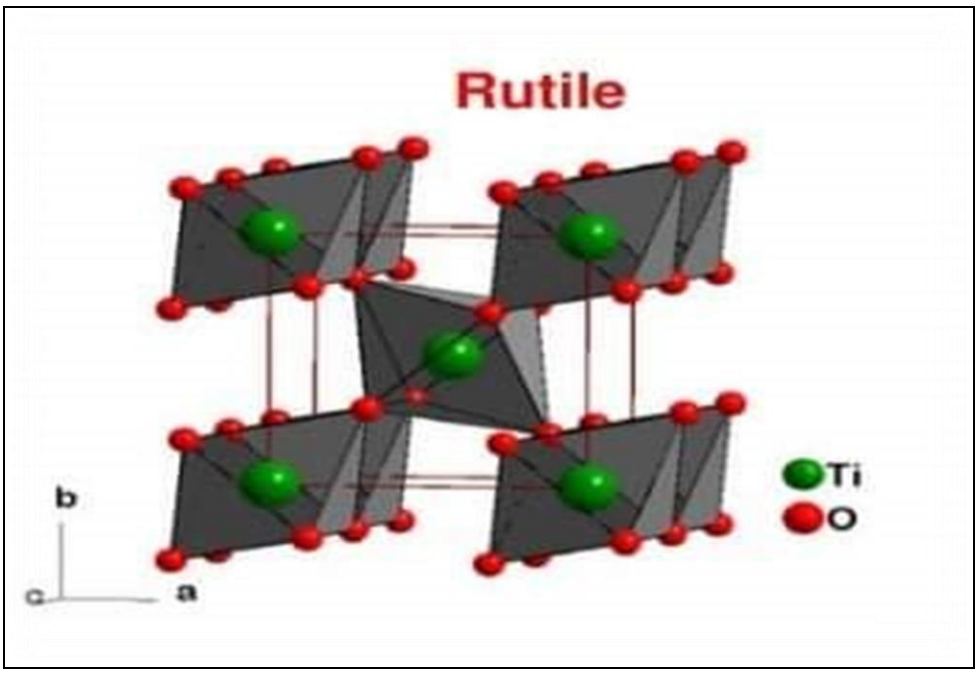

Figure (2-3): Rutile Phase of Titanium dioxide [48].

2.3.3-General Properties of TiO_2 with Brookite Phase

The crystal structure of this phase is more complex; it has a larger cell size than the rutile phase and is less dense than it. It consists of eight cell units and an eight-surface polygon sharing edge similar to a rutile phase, as shown in Figure (2-4). The crystal structure of brookite is Orthorhombic, and the lattice constants have, a = 9.180 Å, b = 5.447 Å, c=145.5 Å [25].

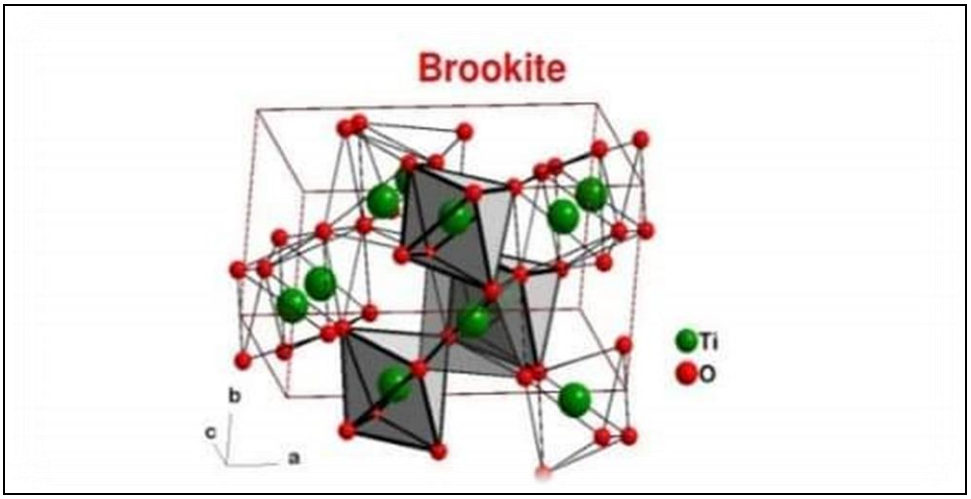

Figure (2-4): Brookite Phase of Titanium dioxide [48].

2.4- Sol-gel Method

The Sol-gel technique is one of the techniques discovered in the past, but its work began in the sixties of the last century with the increasing use of this technology because of its advantages that are not found in the traditional methods of synthetic. This approach has been referred to as the directed approach for the formation of inorganic oxides, with gel-like structures, which are transformed into glassy (amorphous) solid structures at low temperatures, and can be defined from a thermodynamic point of view as the formation of a relatively stable solid phase at a certain temperature, starting from the phase Liquid (solution) one of the advanced ceramic material production techniques.

It is one of the methods of manufacturing ceramic materials. The sol-gel process has a number of advantages. Due to the ease with which liquids are purified (being the starting material for the process), materials of high purity can be produced. It is also possible to produce materials with exceptionally good chemical homogeneity, which is very desirable, especially in the case of complex oxides, because the mixing of components occurs at the molecular level during chemical reactions. Lower condensation temperatures are another good feature. We must not forget that there are real disadvantages. Primary starting materials (such as metal

alkoxides) are somewhat expensive. The difficulties are in the usual drying stage, during which the noticeable cracks, bends, and shrinkage are common problems Because of these problems during the drying phase, the slur-gel method is used little in the manufacture of mono-ceramic materials. However, it has seen significant use in the manufacture of small or thin products such as Films, fibers, and powders. Its use in these areas is expected to grow steadily in the future [49].

2.5- Spin Coating Technique

The spin coating method is an easy and fast way for preparing the homogeneous organic thin-Film types; it's utilized for applying uniform thin Films to the flat substrates. Where have been placed a specific solution amount upon a substrate that is rotating at high speeds (usually about 3000 rpm) to spread liquid through the centrifugal force and the machine that is utilized for spin coating has been referred to as the spinner or the spin coater. Such an approach was explained first by [50]. In spite of the fact that spin coating is utilized all over the world in semi-conductor industry before long, it barely began a theory study. The exact spin coating theory provides the ability for better designing and controlling processes in a variety of applications. It utilizes the paint spin on a large scale in a precise manufacturing area, in which it may be utilized for the creation of thin Films with thickness < 10nm [51], where the thickness of the Film is dependent upon the rotational speed.

2.6- Annealing

Suppose the sample or Thin Film is exposed to a specific temperature for a limited period of time. In that case, this process is referred to as annealing, and it is usually performed either by vacuum or in the presence of a specific gas or with air as needed. The process of annealing may help reduce structural defects, as it gives kinetic energy to

the atoms of the material, and thus it will try to rearrange them and take their place within the crystal structure [52], or lead to the interaction of the Thin Film material with oxygen when the annealing is carried out in the space of air. Therefore, the annealing process varies its effects on the material according to the type of plasticizer and the annealing conditions of the temperature and the surrounding gas. The annealing process is one of the successful methods in preparing some material oxides such as TiO_2. The purpose of this process is to reduce the defects by removing the stresses generated in the material, returning the atoms and the material, and creating a diffusion process for impurities to increase their electrical efficiency. It is also used to convert a thin Film consisting of several materials or one substance from a random state to a polycrystalline or from a polycrystalline to a mono crystalline, as well as most defects such as compaction defects and dislocations are eliminated by the annealing process [53].

In general, the thermal annealing processes are divided into two types, one of them: the traditional thermal annealing by using the furnace and the other the rapid thermal annealing, especially those that employ halogen lamps [52].

2.7- Analysis Techniques

The information obtained by the researcher when studying the structure of the thin Films varies according to the technique adopted in that Measurement that can support one another. It can be divided into three main techniques.

2.7.1- Spectral Techniques: meaning that they provide us with a spectral plot when passing the sample under test. Among these techniques are X-ray diffraction (XRD), FT-IR, and X-ray energy dispersion diffusion (EDX) [54].

2.7.1.1- X-Ray Diffraction (XRD)

The technique of XRD is typically utilized to study the crystal structure of precipitating Thin Films. The location of peaks provides us with information on a lattice structure and the preferred growth direction, while the width of the peaks shows the crystal size of the crystals formed in the Thin Film. Figure (2-5) shows a simple sample of the crystal structure that represents the diffraction pattern of X-rays when they fall on the surface of the crystal by means of W. Bragg's inferring his law [55, 56].

$$n\lambda = 2d_{hkl} \sin\theta \qquad (2\text{-}1)$$

where :

n: integer representing the rank of interference

θ: the angle of incidence of the x-ray

λ: wave length

d_{hk1}: distance between levels (hk1)

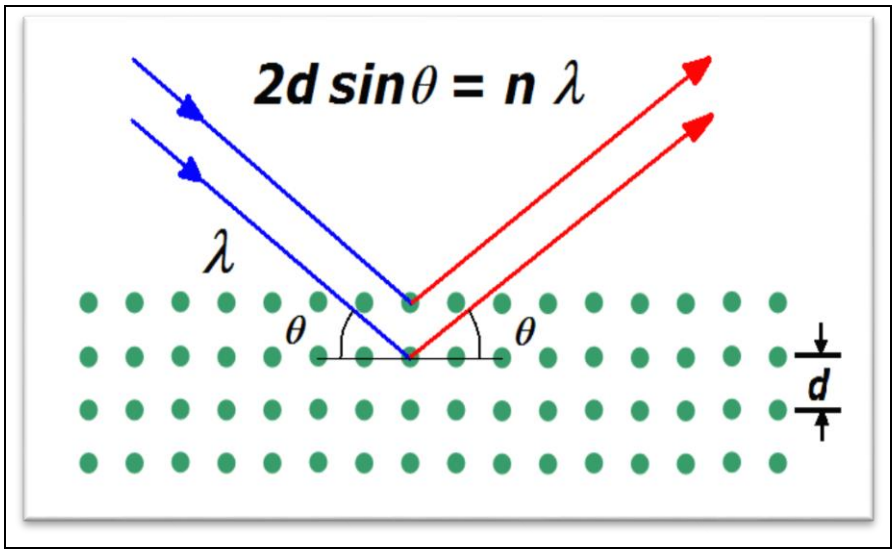

Figure (2-5): Bragg Diffraction [56].

In this method, the angle (θ) is changed continuously during the process of diagnosing the material to know its crystal structure's nature. When the sample is rotated at an angle (θ), the detector has rotated at an angle (2θ). Therefore the angle recorded on the paper strip represents twice the angle

in the law of Bragg provided that the x-rays are of mono wavelength. Thus the value of (d_{hkl}) can be calculated from equation (2-1) if known (λ) and (θ) [57], as shown in Figure (2-6).

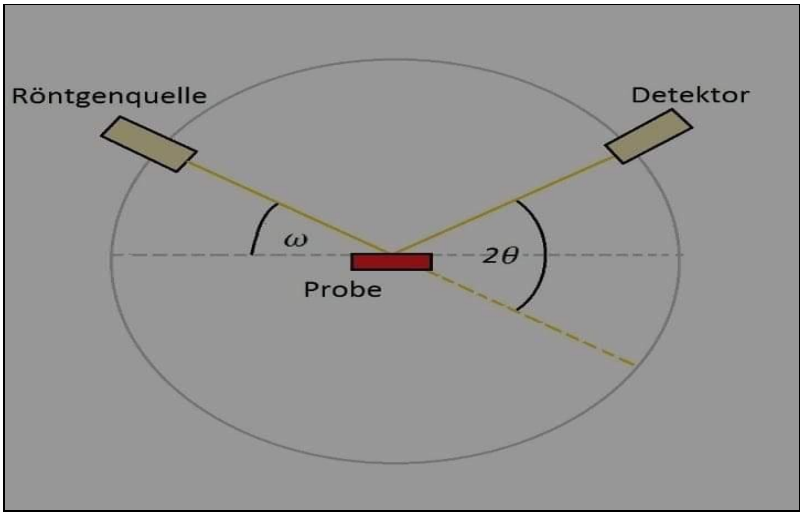

Figure (2-6): Diagram of the XRD device representing the symbol [57].

This technique is often used by researchers when studying the structural properties of precipitated Films [58], can be an advantage of the X-ray diffraction spectrum to get the following:

2.7.1.1.1- Average Crystallite Size

The average crystal size is calculated based on the Debye Scherrer's equation [59, 60].

$$D_S = \frac{0.94\,\lambda}{FWHM\ Cos\theta} \qquad (2\text{-}2)$$

Where :

FWHM: Full Width at Half Maximum in radians units.

θ: Bragg' s angle

2.7.1.1.2- The Density of Dislocations and the Number of Crystals

The dislocations' density has been known as the number of dislocation lines crossing the unit distance in the crystal [50]. and is found by the following relation [51]:

$$\delta_D = \frac{1}{D_s^2} \quad (2\text{-}3)$$

As for the number of crystals (N_o) per unit area, they are found according to the following relation [62]:

$$N_o = \frac{t}{D_s} \quad (2\text{-}4)$$

Where:

t: the thickness of the Thin Film

2.7.1.1.3- Crystal Distortion (Microstrain)

Distortions in the crystal lead to a change in the intermediate distance (d_{hkl}), or in other words that a change in the distance between the atomic surfaces means that there is a deformation in the crystal, which means that ((d_{hkl}) is not equal in every point of the crystal, this leads to each part being reflected of the parts of the crystal X-rays at an angle that differs from the other part, and therefore the reflection resulting from different parts of the crystal will have different angles [63].

The micro-compliance occurs during the growth of the Thin Film as it arises from the expansion or compression of the lattice to make the deviation in the (x) axis of the lattice constant and equal to the value of the standard hexagonal structure. Therefore, the expansion of the strain results from changing the displacement of the atoms with respect to the original lattice position [60], the micro-compliance (S) can be calculated from equation (2-5).

$$S = \frac{FWHM\ COS\theta}{4} \quad (2\text{-}5)$$

2.7.1.1.4- Lattice Constants

The lattice constants of the TiO_2 complex with the quaternary structure of the rutile phase can be calculated from the equation below.

$$\frac{1}{d_{hkl}^2} = \frac{h^2+k^2}{a^2} + \frac{l^2}{c^2} \quad (2\text{-}6)$$

As for the other equations, through which the lattice constants can be found for the TiO_2 compound with the right specific structure of Brookite phase.

$$\frac{1}{d_{hkl}^2} = \frac{h^2}{a^2} + \frac{k^2}{b^2} + \frac{l^2}{c^2} \qquad (2\text{-}7)$$

2.8- Fourier Transform of Infrared Spectrum (FT-IR)

This approach is utilized for obtaining an IR spectrum for a solid, liquid, emission or absorption. The Fourier Spectrophotometer performs a simultaneous collection of the high-resolution spectral data throughout a wide range of spectra. Which has resulted in providing a considerable advantage compared to the spectrophotometer, simultaneously measuring the intensity over a narrow wave-lengths range. This method's operation may be represented by the diagram below [64].

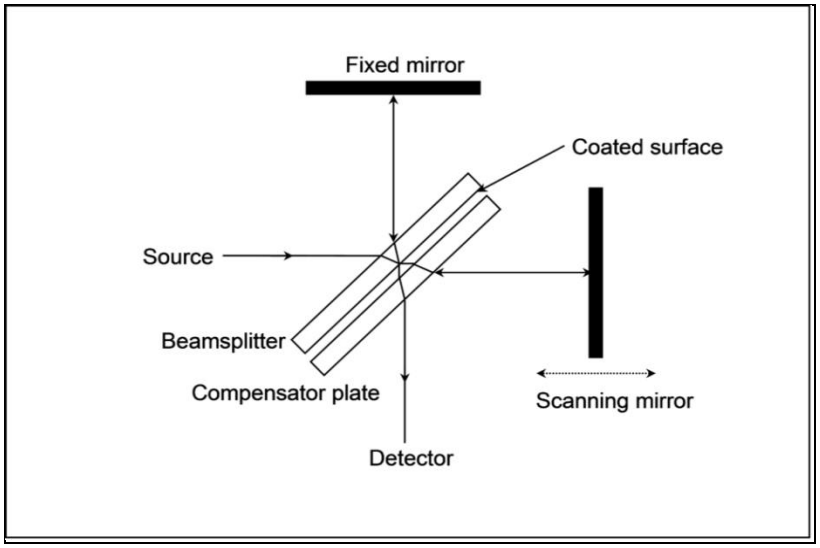

Figure (2-7): Diagram showing the work of FT-IR spectrophotometer [64].

2.9- Structural Properties

Structural Properties is included below:

2.9.1- Techniques that Study Surface Topography: including scanning electron microscopy (SEM), where the SEM is a method for measuring surface roughness of the Thin Film [65].

2.9.1.1- Scanning Electron Microscope (SEM)

It can be defined as a type of the electron microscopy producing images of the sample through scanning that sample by a focused electron beam. Electrons interact with atoms in the sample, resulting in the production of a variety of the signals containing information on the surface composition and topography. A beam of electrons is scanned in general with the use of raster scanning, and the beam location is combined with a signal for the purpose of producing the an image. A separation that is better than 1nm may be accomplished. The samples may be viewed at high and low vacuum, in moist conditions (in an environmental SEM), and at a wide range of very high or very low temperature. The most widely known SEM approach is the detection of the secondary electrons that have been emitted from the atoms that were excited by a beam of the electron. The number of the secondary electrons that may be detected is dependent, amongst other factors, upon the sample's topography. By scanning the sample and collecting secondary electrons that have been emitted with a special detector, an image that shows the surface's topography is created [66].

2.10- Optical Properties Techniques

By studying the optical properties of thin Films, it is possible to understand the composition of the energy bands of the thin Films, as well as to know the values of the energy gap, if direct or indirect. Therefore, the techniques used to study optical properties vary according to the difference in the material is treated with the incident light wave. [67], and used in this research the (UV-VIS) spectrophotometer, which is a technique based on absorbance,as shown in figure (2-8).

Figure (2-8): UV-VIS spectrophotometer [67].

2.10.1- Optical Absorption

It is one of the important methods in the study of the solid state, and the absorption processes of a semiconductors depend on the energy of the incident photon and the optical energy gap. If the photons (hυ) energy is equal to the energy gap (E_g), then the photons are absorbed to generate pairs of (electron - hole), as shown in Figure (2-9 a), if the energy of the photons (hυ) is greater than the energy gap (E_g), then a transition process can occur in the semiconductor and result in an electron excitation from valence to conduction bands, while the additional energy is dissipated (E_g - hυ) in the form of heat, as in figure (2-9b). and both (a) and (b) are referred to as intrinsic transitions or transitions from band to band.

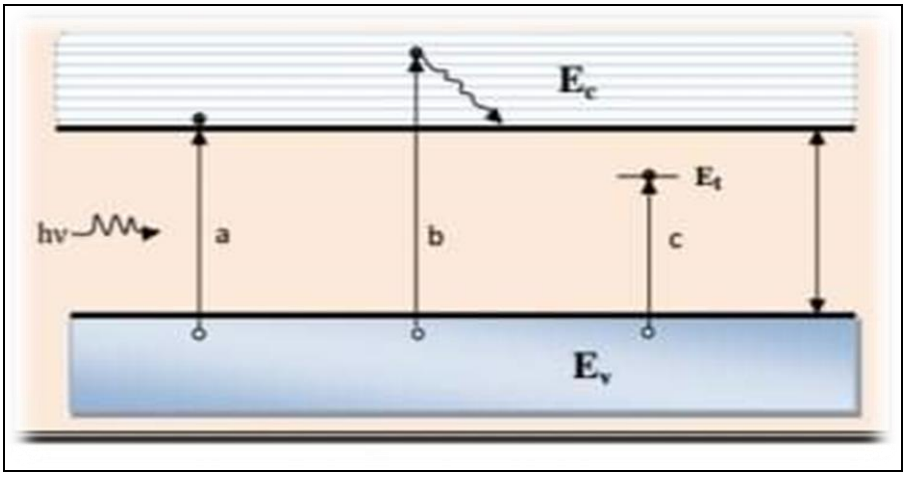

Figure (2-9): Absorption process for semiconductors [67].

If the photons (hυ) energy is less than the energy gap (E_g), absorption will not happen unless there are energy levels in the forbidden gap due to chemical impurities and physical defects, as shown in figure (2-10c). Thus, this process is called non- intrinsic transitions.[٦٧].

2.10.2- Absorbence

When a beam of light with energy hυ < E_g falls on to a semiconductor material with a thickness of (t) as shown in Figure (2-10) with an initial intensity I_0, part of this beam will be absorbed, and the rate of the absorption is dependent upon the wave-length of incident light and the thickness of the sample. The transmitted light's intensity I_T may be computed through the sample from the following relation: [٦8, ٦9].

$$I_T = I_0 e^{-\alpha t} \qquad (2\text{-}8)$$

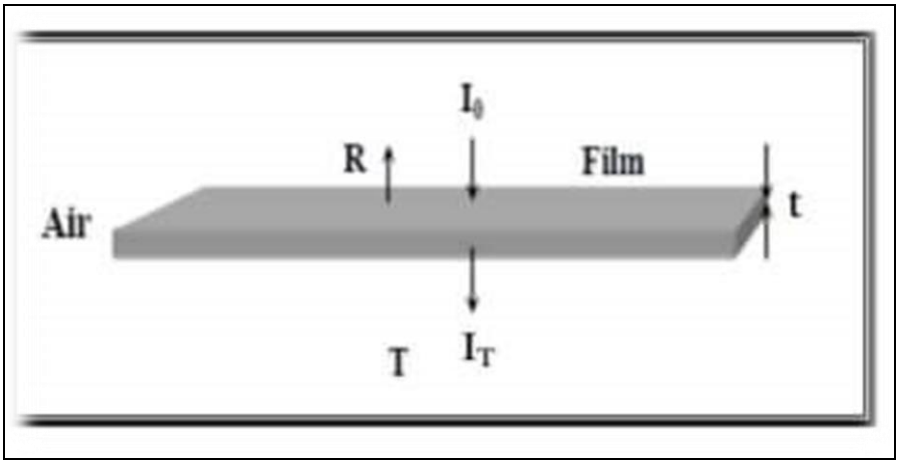

Figure (2-10): Phenomenon of optical absorption[٦٩].

2.10.3- Absorption Coefficient and Fundamental Absorption Edge

The absorption coefficient (α) can be characterized as the ratio of the decrease in the radiation energy relative to the unit distance in the wave propagation direction within the medium, and the coefficient of the absorption is dependent upon the incident photon energy (hυ) and on the properties of the semiconductor from where the energy gap and the

electronic transitions' type that occurs between the bands of its energies in the calculation The absorption coefficient of the Films [٧0]. The energy of the photon is given by the following relation [٧1]:

$$E= h\upsilon \quad (2\text{-}9)$$

When the energy of the incident photon is lower than the energy gap, the photon will penetrate, and the transmittance of the Thin Film has been represented by the following relation [٧2]:

$$T= (1 - R)^2 e^{-\alpha t} \quad (2\text{-}10)$$

Where:

T: transmittance, R: reflectivity

The relation between transmittance (T) and absorbance (A) can be written as follows:

$$T = e^{-2.303A} \quad (2\text{-}11)$$

Substituting the value of (T) into equation (2-10), we get

$$e^{-2.303A} = (1 - R)^2 e^{-\alpha t} \quad (2\text{-}12)$$

In the case of (R) very small, it can be neglected. equation (2-12) is written as follows:

$$e^{-2.303A} = e^{-\alpha t} \quad (2\text{-}13)$$

From them, we get:

$$\alpha = 2.303 \frac{A}{t} \quad (2\text{-}14)$$

The optical absorption spectrum of all semiconductors has the advantage of being common to the rapid increase in absorption that occurs when the energy of the absorbed radiation is equal to the width of the energy gap between the conduction band (C.B.) and the valence band (V.B.) [٧3].The region of the incident ray spectrum, in which the electrons begin to move at the absorption edge, is known as the difference in magnitude between the location of the lowest point in C.B. and the highest point in V.B. [٧4].

From figure(2-11) it is noticed that at the high wavelength that exceeds the value of the absorption edge, the absorption is little, and the wavelength at which the absorption occurs is called the cutter wavelength, as the least energy, an electron can acquire to move from the V.B. to C.B. The edge of the absorption is sharp in mono crystalline semiconductors. In polycrystalline semiconductors, the absorption edge is less severe [٧4].

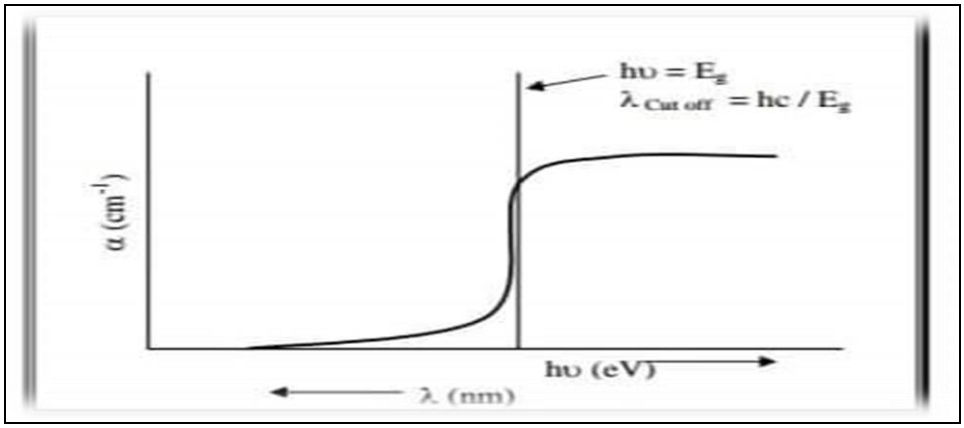

Figure (2-11): Absorption coefficient depending on (hυ) and determines the absorption edge [٧4].

2.10.4- ElectronicTransitions

There are two types of electronic transitions

2.10.4.1- Direct Transition

In this case where an electron moves from the V.B. top to the C.B. bottom at the same point in the vector space (K-space) within the condition ($\Delta K = 0$), That transition will be accompanied by interaction only between incident photon and the valence electron, as each of the momentum and energy is conserved, as in the equation below [72].

$$E_f = E_i - h\upsilon \quad (2\text{-}15)$$

$$K_f - K_i = q \quad (2\text{-}16)$$

Where :

E_i , E_f : represent the initial energy and final energy in both V.B. and C.B., respectively.

K_i and K_f: the vector of the primary and final electron in both the valence and conduction bands, respectively.

q: the vector of the absorbed photon.

and the absorbed photon's vector is very small in comparison with the value of the electron, so it is neglected, and so the above relation is as

$$E_f = E_i \qquad (2\text{-}17)$$

This type of transition is called the Allowed Direct Transition, or it is called the vertical transition, and when the electron transition is from the regions adjacent to the permissible direct transition regions with the condition that the vector value of the vector (K) does not change, then this transition is called the forbidden direct transition, and as shown in Figure (2-12), and in this type of semiconductor, the absorption equation is given by the relation (2-15) to *Taos* [75, 76].

$$\alpha h\upsilon = \beta(h\upsilon - E_g^{opt})^r \qquad (2\text{-}18)$$

Where :

α: optical absorption coefficient (cm^{-1})

β: constant $= \frac{4\pi\sigma_o}{n_o\, c\Delta E_g}$

Where:

σ_o (minimum metal conductivity), c: (speed of light), ΔE_g: (tails width for positional states), n_0: (refractive index), hυ: energy of the incident photon (eV), E_g^{opt} the optical of the energy gap (eV), r: the order of optical transition and depends on the nature of the electronic transition.

Therefore, equation (2-18) clarifies the transition's quality in semiconductors with direct energy gaps, when the (r) value equals (1/2) the transfer is a Allowed direct transition, and in the case where it is (3/2) the transition is forbidden [75].

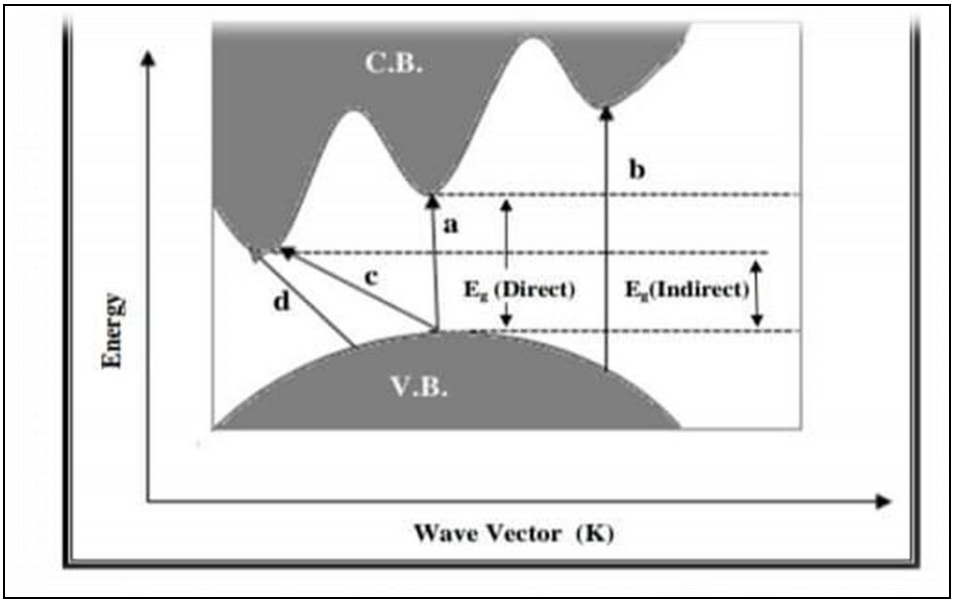

Figure (2-12): Electronic transitions: a = direct allowed, b = direct forbidden c = indirect allowed, d = indirect forbidden [75].

2.10.4.2- Indirect Transition

The indirect transition of electrons occurs when the two energies up of the V.B. and the bottom of the C.B. do not match in the vector space of the vector (K), as a transition between a point in the V.B. and any point in C.B. is non-perpendicular, so the vector's value will be ($\Delta K \neq 0$) [77].This transition includes a change in the crystal momentum as a result of a change in momentum of the transferred electron, and this variation in the crystal's momentum from the lattice is compensated, either by the absorption of a momentum photon [-h (K_c- K_v)] or by the emission of a photon of momentum [h (K_c- K_v)].

where:

K_v: vector of valence band

K_c: vector of conduction band

This, in turn, is necessary to achieve the momentum conservation law.

Which means that:

$$K_i + q = K_f \pm K_p \qquad (2\text{-}19)$$

Where:

q : the photon wave vector

$\pm K_p$: the emitted or absorbed photon wave vector.

By neglecting the photon wave vector due to its smallness, the equation (2-19) is as follows:

$$K_i = K_f \pm K_p \quad (2\text{-}20)$$

Semiconductors that have these transitions are called indirect gap semiconductors, so the absorption equation is given by the following relation: [75].

$$\alpha h\upsilon = \beta(E_g \pm E_q)^r \quad (2\text{-}21)$$

where:

$(+E_q)$: the photon absorption process.

$(-E_q)$: the photon emission process.

These transfers are of two types as well. When an electron moves from the highest point in V.B. and the lowest point in C.B., the transition is from the Allowed indirect type, whose value(r) in equation (2-18) equals (2). and when the transition from the areas adjacent to the highest point in the parity band to the lowest point in the delivery band is called, then the forbidden indirect transition and the value of (r) is equal to (3) in the above equation as shown in Figure (2-13) and the process of emission or absorption is in these transitions, it is dependent on temperature, unlike in direct transitions [75].

2.10.5- Optical Constants

Optical constants is included below:

2.10.5.1- Optical Energy gap

The energy gap is one of the important optical constants, and it is a function of temperature, as its value changes slightly with the change of temperature , as the energy gap value increases in some semiconductors, while it decreases in others. The energy gap of a pure semiconductor is not

completely free, as there are localized levels resulting from structural defects [78].

The energy gap can be calculated from the empirical equation developed by *Taos* with the following formula [79, 80]:

$$(\alpha h\upsilon)^2 = \beta^2(h\upsilon - E_g^{opt}) \quad (2\text{-}22)$$

As the graphical relation between($\alpha h\upsilon)^2$ and ($h\upsilon$) is drawn by extending a straight line that is a cross-extension of the photon energy axis ($h\upsilon$). Where the value of the energy gap is determined from the point of intersection at which $(\alpha h\upsilon)^2 = 0$, as most researchers have adopted this method in determining the energy gap, such as the researcher(*Gordillo*) [81]. and the researcher(*Rusu*)) [82], and the researcher(*Marfai*) and his group [83]. Likewise, the researcher (*Shixing*) [84].

2.10.5.2- Refractive Index

It is the ratio between the light speed in the space and its speed in the medium and is given by the following relation [85, 86].

$$n^* = n_o - ik_o \quad (2\text{-}23)$$

Where:

n^*: complex refractive index

n_o: real refractive index

k_o: Extinction coefficient

The refractive index is related to the reflectivity of the Thin Film according to the following relation [87]:

$$R = \frac{(n_o-1)^2+k_o^2}{(n_o+1)^2+k_o^2} \quad (2\text{-}24)$$

From this equation, the refractive index can be calculated according to the following formula:

$$n_o = [(\frac{1+R}{1-R})^2 - (k_o^2 + 1)]^{1/2} \quad (2\text{-}25)$$

$$R = 1 - (T - A) \quad (2\text{-}26)$$

2.10.5.3- Extinction Coefficient

The extinction coefficient represents the amount of energy absorbed in the thin Film, or more precisely, what the electrons of the material absorb from the incident photons' energy; that is, it represents the extinction or attenuation of the electromagnetic wave inside the material. The extinction Coefficient is given by the following relation [88, 89]:

$$k_o = \frac{\alpha\lambda}{4\pi} \quad (2\text{-}27)$$

It is noted that the extinction Coefficient depends mainly on the incident wavelength and the absorption coefficient (α), which depends on the quality of the material.

2.10.5.4- Dielectric Constant

The interaction between light and the charges of the medium occurs due to the absorption of energy in the material, and this reaction results in a polarization of the charges of that medium.

This polarization is typically described by the complex dielectric constant of the medium (ε), which is known by the following relation [90]:

$$\varepsilon = \varepsilon_r - i\varepsilon_i \quad (2\text{-}28)$$

where:

ε: represents complex dielectric constant

$i\varepsilon_i$: represents imaginary part of the dielectric constant

ε_r : represents real part of the dielectric constant

The relation between the dielectric constant and refractive index is complex.

$$\varepsilon = n^{*2} \quad (2\text{-}29)$$

Substituting the value of (n*) in equation (2-23),and (ε) in equation (2-28) we get:

$$(n_o - ik_o)^2 = \varepsilon_r - i\varepsilon_i \quad (2\text{-}30)$$

By solving equation (2-30), we find that:

$\varepsilon_r = n_o^2 - k_o^2$ (2-31)

$\varepsilon_i = 2n_o k_o$ (2-32)

2.10.5.5- Optical Conductivity

The optical connectivity is related to the refractive index and extinction Coefficient according to the following equation [91]:

$\sigma_o = 2n_o k_o \omega \varepsilon_o$ (2-33)

Where:

ω: angular frequency

ε_o: the permittivity of the space

after substituting in equation (2-32), the equation (2-33) can be written as:

$\sigma_o = \varepsilon_i \omega \varepsilon_o$ (2-34)

2.11- Methods For Measuring the Thickness of the Thin Film

There are many methods for measuring the thickness of thin film.

2.11.1- Optical Method

In this method, a laser with a known wavelength is used, and a red laser with a wavelength is usually used, and through the width of the luminous cilia and the amount of deviation in these cilia, the thickness of the thin film, can be calculated using the relation (2-35),[٩٢].

$$t = \frac{\Delta x}{x} \cdot \frac{\lambda}{2} \quad (2\text{-}35)$$

Where :

t: thickness of thin film

λ: wave length of light of laser

Δx : the amount of deviation

x : width of the luminous cilia

2.11.2- Weight Method

This method is not inaccurate in measuring the thickness of the thin film, but it is used in some cases, from the following relation[92].

$$t = \frac{m}{s.\rho} \quad (2\text{-}36)$$

where:

t :thickness of thin film(nm)

m:Thin film material mass(gm)

s:The area of the substrate on which the thin film is deposited(cm^2)

ρ:Thin film material density(gm/cm^3)

2.12-Dark Current–Voltage Characteristics

Dark (I–V) characteristics have been measured. These measurements usually provide a valuable source of information about the junction properties, such as the rectification ratio(R_F); the ratio of the forward current to the reverse current at a certain applied voltage is defined as the rectification factor, tunneling factor (γ), the barrier height, the reverse saturation current density and the ideality factor (η) analysis of current–voltage (I–V) characteristics of TiO_2/PANI /ITO /Al heterojunction allows us to understand different aspects of current transport. The total dark current of the heterojunctions can be represented as a sum of several components such as generation-recombination current, diffusion current, tunneling current, surface leakage current, and emission current. If generation-recombination and diffusion mechanisms are dominant, then the dark current (I) obeys the following formula [93]:

$$I = I_s[e^{qV/\eta KT} - 1] \quad (2\text{-}37)$$

Where, (I_s) is the reverse saturation current and is given as:

$$I_s = A_j A^* T^2 e^{-q\emptyset_b/\eta KT} \quad (2\text{-}38)$$

Where (A^*) is Richardson constant, (η) is the value of ideality factor, (V) is the applied voltage, ($\emptyset_b$) is barrier height, and (T) is the temperature in Kelvin.

The (η) of PANI/ ITO is calculated from the current-voltage characteristics by using the following equation [93]:

$$\eta = \frac{q}{KT}\left(\frac{dV}{d\ln I}\right) \quad (2\text{-}39)$$

The value of the (η) of the TiO_2/PANI /ITO /Al heterojunction is determined from the slope of the straight line region of the forward bias logarithm of the current as a function of the applied voltage.The current is due to tunnelling that dominates across the junction and it could be represented by the expression[94]:

$$I = I_s e^{\gamma V} \quad (2\text{-}40)$$

This expression is justified for tunneling–recombination mechanism. The reverse bias characteristics of these heterojunction show a linear variation at low reverse voltage [94].

2.13- The Mathematics Factors Affecting on the Efficiency of the Solar Cell

There are several factors that affect the efficiency of the cell, including natural factors such as the intensity of the falling light , the duration of the sunrise , the angle of the cell's inclination relative to the sun, time , temperature, location of the cell, and the abnormal factors such as the efficiency of the battery used to store the output power, occur within the cell, or factors resulting from cell manufacturing, as well as equivalent circuit variables that depend on the manufacturing methods, are:

a- Open- Circuit Voltage (V_{oc})

Is the maximum value of the voltages that can be obtained on both ends of the solar cell when the circuit is open, ($R_L=\infty$) , can be represented by equation [95].

$$V_{OC} = \frac{k_B T}{q} \ln\left(\frac{I_L}{I_o} + 1\right) \quad (2\text{-}41)$$

Where:

q: electron charge, k_B Boltzmann constant, T absolute temperature, I_L current generated from light and I_o saturation current for binary. The open circuit voltages have a clear and direct effect on solar cell efficiency, as it increases the efficiency of the cell.

b- Short Circuit Current Density

In solar cell the current provided plays an important role in determining the final performance of the solar cell**.** Increasing the current can noticeably increase the efficiency of the solar cell. Several parameters affect the production of high current within the solar cell, such as, the light absorbing material (active layer). This layer has the ability to convert light to charge carriers as described earlier in this chapter and therefore provide current to the external load. Four different processes are expected to take place to ensure high current density [96].

1-Absorption of photons from incident light by employing an appropriate absorbing material, taking into consideration the light absorption properties of the material, the band gap and the energy level alignment of donor/acceptor molecules in the case of organic solar cells.

2- Generation of charge carriers (holes and electrons); in the case of OSCs excitons are generated due to light absorption and subsequently conversion of these excited state into free negative and free positive charge carrier pairs.

3- Charge transport mechanism drives the free charge carriers to the respective electrode by the aid of the internal electric field.

4-Finally, the free carriers will be collected by properly selected electrodes, which are mainly ruled by engineering the contact between the electrodes and the active layer[97].

c-Series Resistance and Shunt Resistance

The series resistance (Rs) and shunt resistance (Rsh) are effective parameters which effect the solar cell behavior**,** It deconstructs the solar cell J-V behaviour into four constituent parts: a photocurrent source, diode, series resistance (Rs) and shunt resistance (R_{sh}). The photocurrent source (I_{ph}) is simply the result of converting absorbed photons to free charge by the solar cell, the diode represents electron-hole recombination at the p-n junction, Rs accounts for the internal resistance of the cell to current flow, and Rsh models leakage current through the cells (e.g., via pinholes). Mathematically this model is represented by the following relation [98]:

$$I = I_L - Is\,[e^{q(V-IRs)/nkT} - 1] - (V - IR_s) / R_{sh} \qquad (2\text{-}42)$$

d- Surface Reflection

The reflection of the cell surface has an effect on the decrease in cell efficiency, so it should be greatly reduced by coating the top layer of the cell with a layer or two layers of non-reflective material which has high permeability, this in turn increases the absorbed light and increases efficiency.

e- Load Resistance

Is one of the most important factors that affect the efficiency of the solar cell and directly control the power out of the cell, so the value of this resistance must be known for each intensity and for each specific device and is known as the load resistance at the point of maximum power of the characteristics of current - voltages for cell to desired pregnancy of a certain intensity.

f- Effect of Temperature

The temperature of solar cells varies from place to place. The (Isc) for solar cell's does not rely heavily on temperature because it increases slightly when the temperature increases due to the absorption of light due to the decrease of the energy gap caused by the increase in temperature.

Open circuit voltages decrease as the temperature of the cell increases due to increased saturation current, so the filling factor decreases and this results in reduced output power and efficiency. The power of the solar cell is calculated from the relation,(2-43),The value of the fill factor for the solar cell was calculated from the relation,(2-44), the fill factor was used to calculate the efficiency of the solar cell as in the relation,(2-45).

$P_{max} = V_p * J_p$ (2-43)

$F.F = P_{max}/Voc*Jsc$ (2-44)

$\eta = Voc*Jsc*F.F/1000$ (2-45)

Where:

$P_{max:}$ power of solar cell.

F.F : Fill Factor.

Jsc: Short Circuit Current.

Voc: Short Circuit Voltage.

η: Efficiency of the solar cell.

2.14- Electrical properties

Polymers of unique composition have the properties of semiconductors, while mainly commercial polymers are insulator known that polymers are simply shaped , chemists and physicists happening median the twentieth irregular double century to conduct studies designed to expand conductor polymers characterized by the bonds [99].

2.14.1 - Deposition Electrdes of Solar Cell

Electrical Conductivity (σ_e) of Films that have been prepared account after the measurement of the Films (R) resistivity for every value of the temperature, which starts from the temperature of the room with the use of the equation below [100]:

$$\sigma_e = \frac{d}{AR} \quad (2\text{-}46)$$

Where:

(*R*) represents the Resistant Films that have been practically measured (Ω), (d) represents the width of the Electrde (cm), and (A) represents the distance between opposite electrdes (cm).

3.1- Introduction

In this chapter, the Experimental steps that were carried out in the research were included, starting from the TiO_2 preparation by means of the Sol-gel approach and the thin film deposition process using the Spin-coating technique, then studying the effect of annealing, and then making the optical and structural measurements of TiO_2 as well as the optical measurements of polyaniline, and then apply them in the solar cell, as shown in Diagram (3-1).

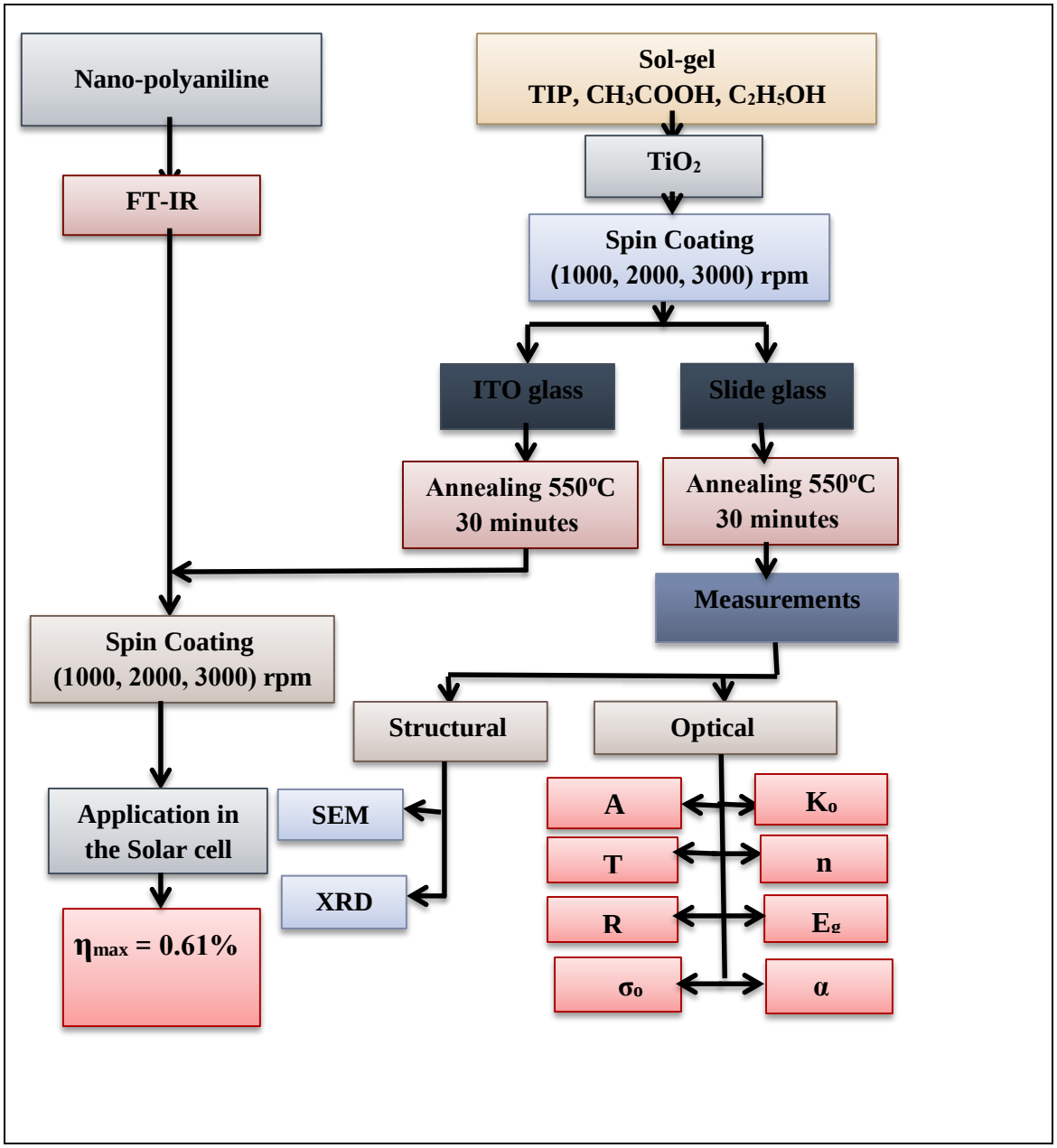

Figure (3-1): Diagram showing the Stages of work.

3.2- Preparation the Material

Titanium dioxide was prepared using three chemicals: acetic acid, titanium isopropoxide, and ethanol alcohol, according to the appropriate chemical conditions for preparation, using the Sol-gel approach as displayed in Figure (3-2).

Figure (3-2): Preparation of TiO_2 using sol-gel method.

3.3- Substrates Cleaning

The cleaning of substrates is a very important process because the influences like oil or dust affect the properties of Thin Films; a clean substrate is also essential to achieve good film adhesion.

3.3.1- Glass Substrate

It can be summarized the glass substrate cleaning as follow:

1. A detergent is used with water to remove any dust or oil that might be attached to the substrate surface; after that, it is placed under distilled water and gently rub.
2. It is placed in a clean beaker that contains distilled water, after that subjected to rinsing in a unit of ultrasound for a period of 15mins.
3. After this, step two will be repeated by using pure alcohol instead of distilled, which is reacting with the contamination like some oxide and grease.

4. Lastly, slides were left to dry with blowing air; after that, a soft paper is used for wiping them.

3.4- Spin Coating Method (Deposition)

Spin coating can be defined as an effective and versatile approach regarding the TiO_2 as well as the polymer films; also, it is a vital approach for preparing a lot of film materials and powders for many industrial applications. Also, the polymer films and TiO_2 were deposited by means of such an approach, which increases the potential of controlling film morphology. The properties and the quality of the films are heavily depending on process parameters. In addition, a spin-coating system (model V T C100), existing in the laboratories of the Department of physics, College of Science, the University of Babylon, used for preparing the Thin Films. Furthermore, the system includes many parts which were arranged for being used to prepare many films on different substrates. Regarding such a system, the prepared films' thickness might be controlled via decreasing or increasing the system's rotation speed. The increase in the system's speed rotation causes a decrease in the film's thickness and the other way around. The prepared film's homogeneity is based on the rotation speed, also the stability, and balance of the system, as displayed in the Figure (3-3).

Figure (3-3): Spin Coating technique used to deposition TiO_2 and PANI films.

3.5- Thermal Annealing

The thermal annealing process regarding the TiO_2 Thin Films which have been prepared through sol-gel approach and deposited by Spin coating method, at a temperature 550 °C and an annealing time of 30 minutes; as in the program of the Figure (3-4 a) the annealing process was carried out using an electric Oven, This electric oven present in the laboratory at the University of Babylon , College of Science , Department of Physics, Figure (3-4 b) Represents the electric oven used.

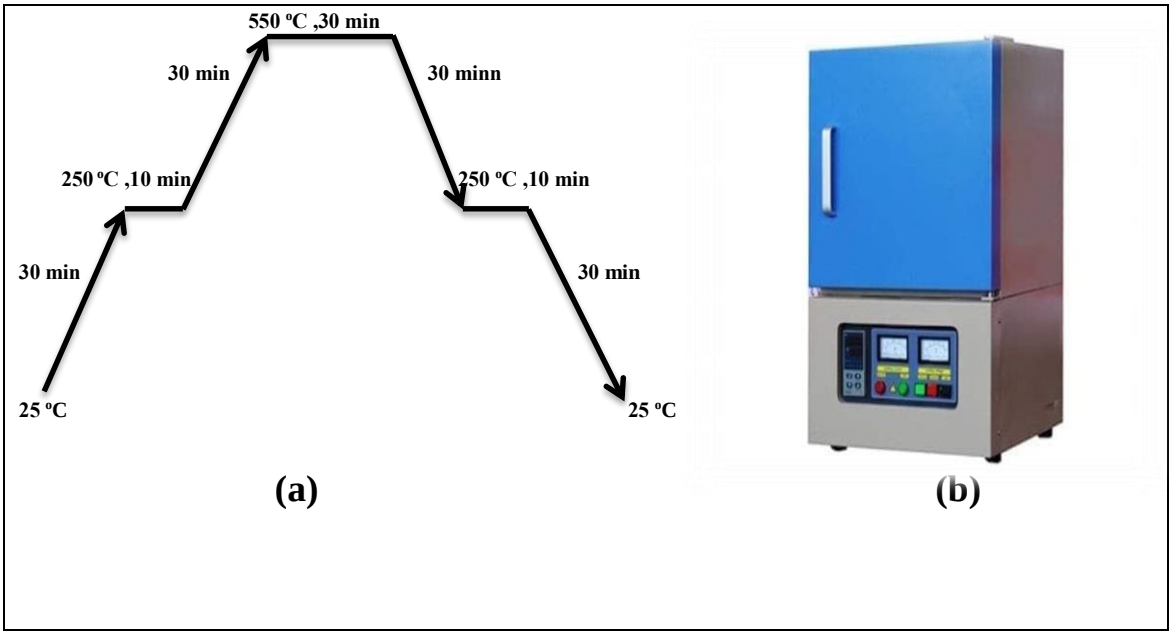

Figure (3-4): Represent (a) annealing program, (b) Electric Oven used for annealing TiO_2 films.

3.6- Measurements and Tests of Films

The measurements are listed below:

3.6.1- Thickness Measurement

There are many methods used to measure the thickness of the films, such as weight, optical and electrical. The optical method was used in our work.

3.6.2- Structural Measurements

After completing the annealing process, a number of Thin Films are chosen that are homogeneous, and it contains no cracks and apparent defects for the measurements, including Structural measurements, knowledge of the crystal structure, and surface topography of the films prepared, using XRD, SEM.

3.6.2.1- X-Ray Diffraction Measurement (XRD)

For knowing the crystalline structures of the prepared titanium dioxide films, we use an X-ray diffraction device. This analysis was carried out in Iran, as shown in Figure (3-5).

Figure (3-5): X-ray diffraction device(XRD).

3.6.2.2- Surface Topography

For knowing the topography and surface nature of the Thin Films, imaging was done using a scanning electron microscope (SEM) with different magnification powers.

3.6.2.2.1- Scanning Electron Microscope (SEM)

Scanning Electron Microscope (SEM) measurements give high-quality images of the material's composition with a very high magnification capacity; through these images, it is possible to identify the homogeneity of the film, and whether it is within the nanoscale structure, the needle is fixed with horizontal support so that it is in a perpendicular position to the sample, when the laser beam passes over the backrest, which is free to move up and down, and this needle is also free to move because it is fixed on this holder and during this movement it gives different pictures. This microscope also gives details of the sample surface, such as the homogeneity of the film and its granular size; this analysis was carried out in Iran, as shown in the following figure.

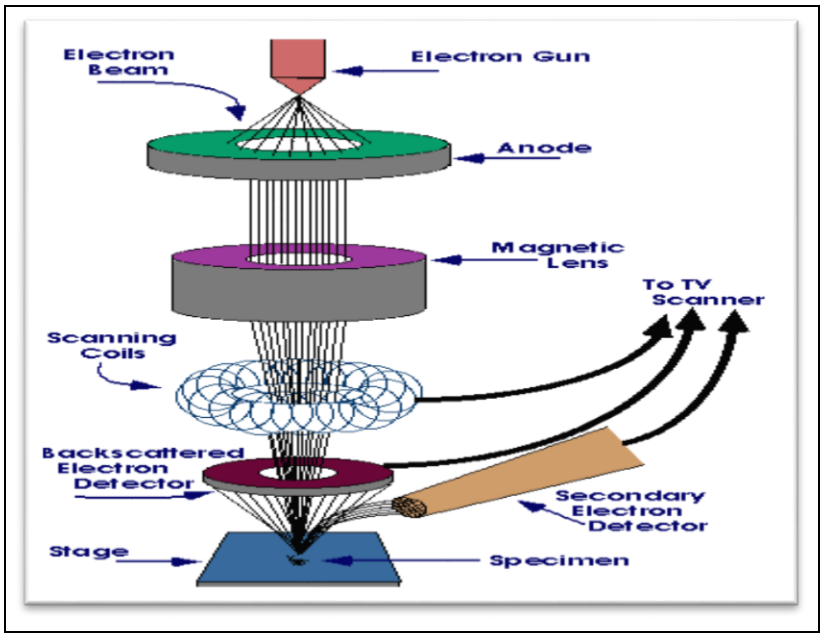

Figure (3-6): Scanning Electron Microscope (SEM) [66] .

3.6.3- FT-IR Analysis

Samples of (PANI) nano films are studied by Fourier Transfer Infrared Spectroscopy (FT-IR) studied samples of (PANI) nano films, using Vertex 70 from broker company, FT-IR Spectrophotometer present in the laboratory of the Department of chemistry, College of Science,

University of Babylon. The Spectrophotometers have recorded as a dispersion of the sample in (potassium bromide) by (IR) disk as (1mg sample in 200mg of the KBr), also a scanning range between ($500cm^{-1}$ and $4000cm^{-1}$) as well as a resolution of ($1cm^{-1}$), as shown in figure (3-7).

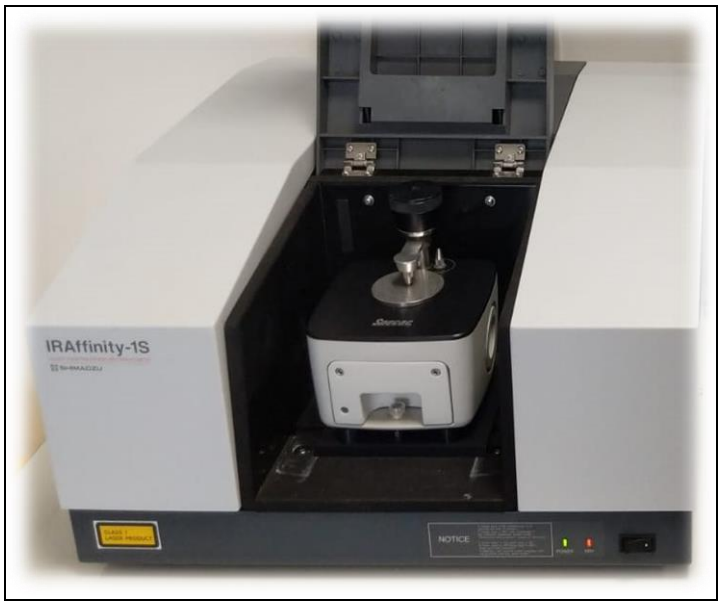

Figure (3-7): FT-IR spectrophtometer.

3.6.4- Optical Measurements

Studying the optical properties starting from optical constants and computing the energy gap are important studies of their relationship to semiconductor materials' behavior and determine their suitability for many applications. The optical measurements included an absorbance and spectral transmittance meter, which was later used to calculate the absorption index, which in turn enables us to compute the energy gap. The optical properties were measured using the SHIMADZU UV-VIS spectrophotometer, and this spectrophotometer is in the laboratory at the University of Babylon , College of Science , Department of Physics, as shown in Figure (3-8), where there are two rays of light placed in a path, one of them is the glass plate that is placed on it the thin film for which the measurement is made. While the second slide is placed on the second track,

it is an unpainted glass plate. Measurements were made of TiO_2 and polyaniline Thin Films in the range of (200-1100) nm wavelengths.

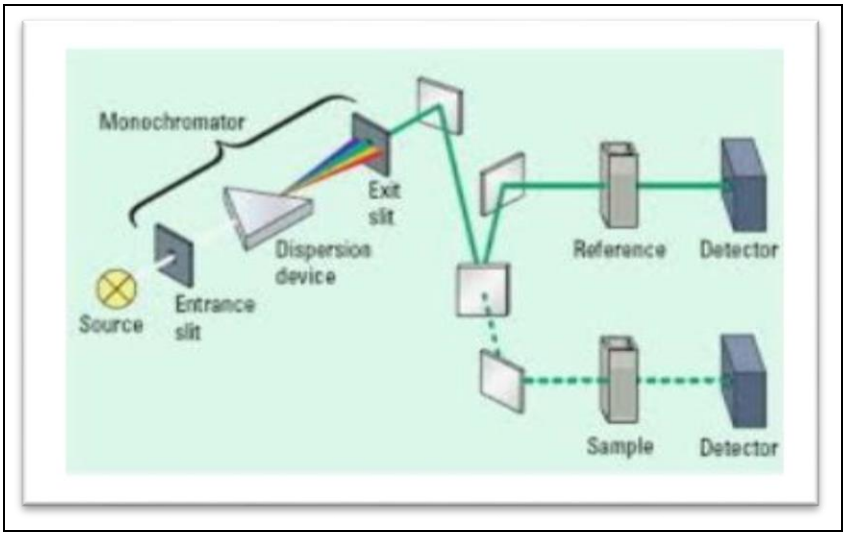

Figure (3-8): Diagram showing the work of UV-VIS spectrophotometer[67].

3.7- Solar Cell Manufacturing (Thermal Evaporation)

The process is done by depositing a layer of aluminum with high purity on ITO slides, then pour polymer on the other side, and then the deposition of aluminum electrdes with masks arranged in a circle, as shown in the diagram (3-9). This deposition was carried out in the laboratories of the Faculty of Education, Department of Physics, University of Babylon.

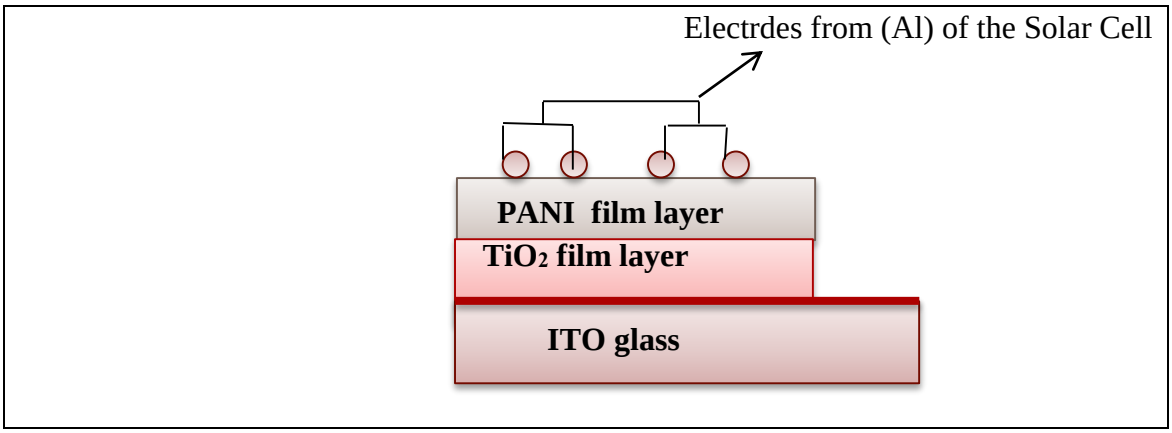

Figure (3-9) Diagram Showing the layers and Electrdes of the Solar Cell

4.1- Introduction

In the presented chapter, a discussion and a review regarding the results of the structural and optical measurements of $TiO_2$and PANI nano films, which were deposited on ITO slides at three different thickess(106,87, 63) nm.

4.2- Results Structural Measurements of TiO_2 Thin Films

Structural Measurements is included below:

4.2.1- Scanning Electron Microscopy (SEM)

The results provided via SEM measurements of TiO_2 nano films deposited with Spin Coating technology at three different thickess (106, 87, 63) nm, respectively, showed that TiO_2 Thin Films are homogeneous and do not contain cracks, as shown in Figures (4-1, 4-2, 4-3), in which there is an evidence that the increase in surface roughness causes an dcrease in thickness, this leads to an increase in the surface area of the films, which leads to an increase in the solar cell's efficiency, which comes in accordance with the results indicated via other works [101, 102].

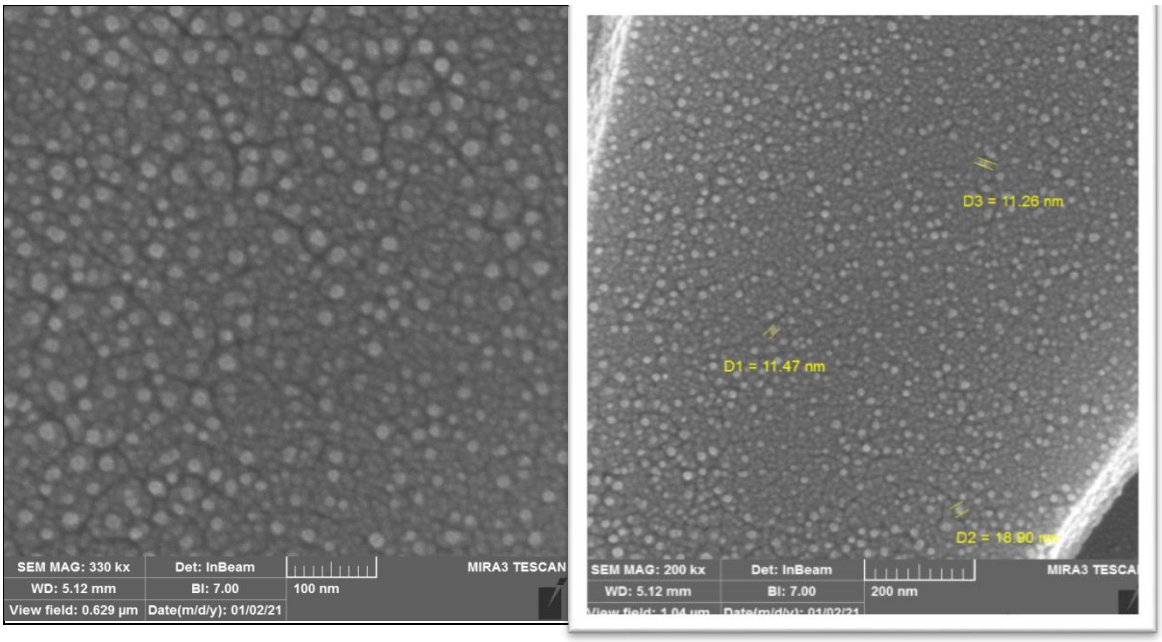

Figure (4-1): SEM images of TiO_2 Thin Films at 106 nm.

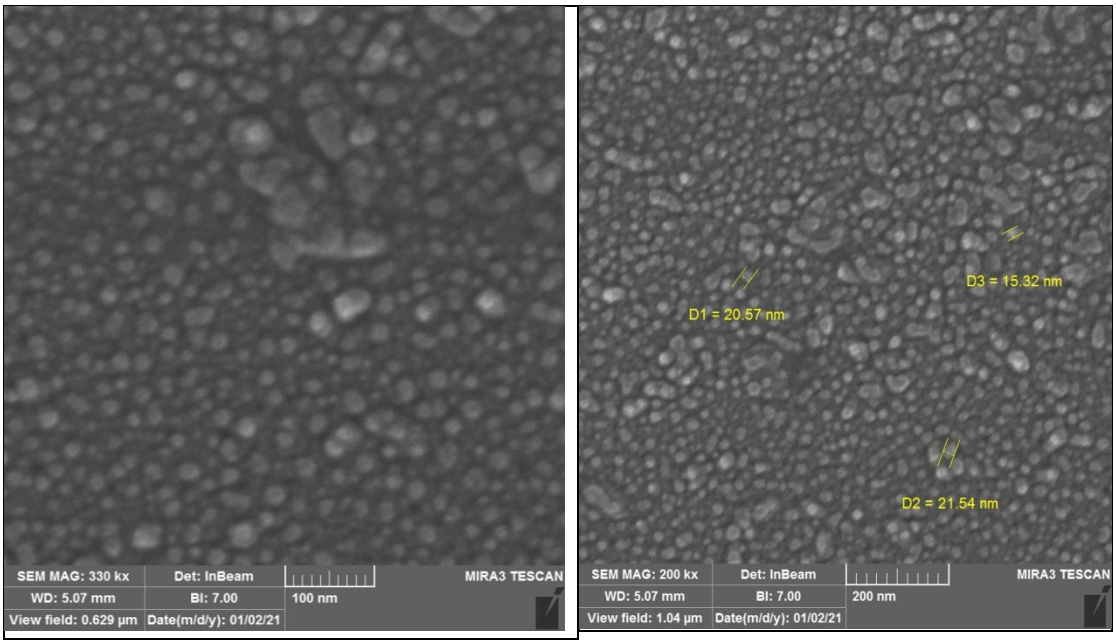

Figure (4-2): SEM images of TiO_2 Thin Films at 87 nm.

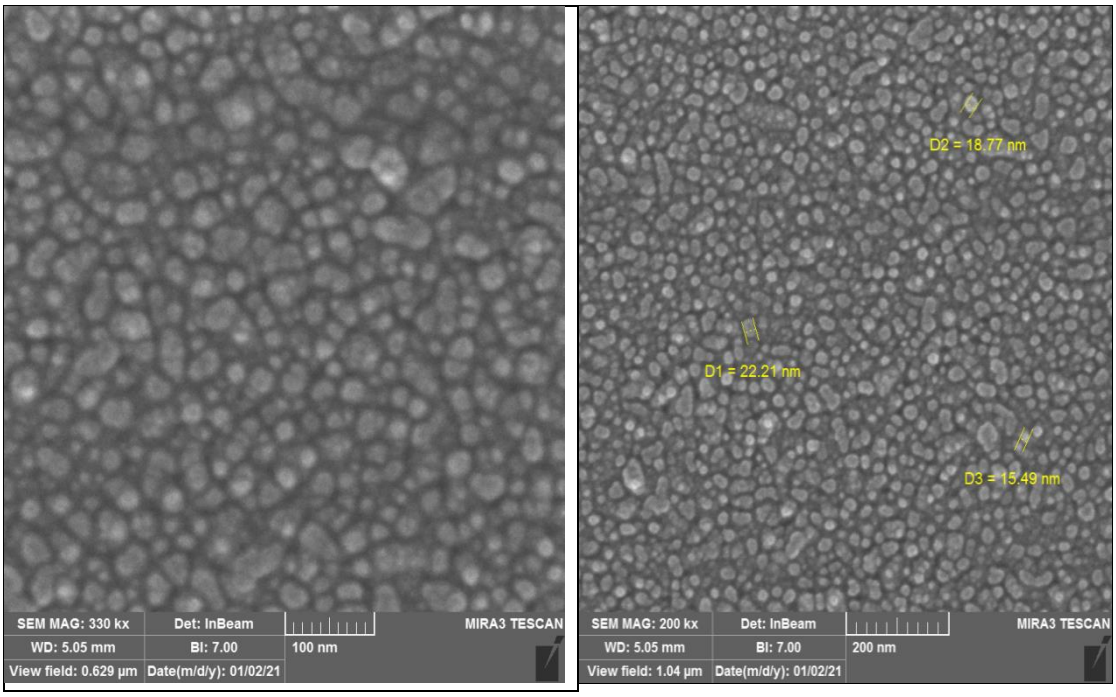

Figure (4-3): SEM images of TiO_2 Thin Films at 63 nm

4.2.2- X-Ray Diffraction (XRD)

When making XRD measurements of titanium dioxide Thin Films that were deposited using the Spin Coating technique at three different thickess

(106, 87, 63) nm respectively and annealing them at a temperature of 550 °C, by figures (4-4, 4-5, 4- 6) observed the formation of an anatase phase at the characteristic peak (2θ = 25º). The figures showed that the brookite phase and the rutile phase did not appear because the anatase phase gradually transformed into the rutile phase at temperature over 550 ºC. The brookite phase was formed at temperatures less than 550 ºC, through the figures, it has been identified that there is a decrease in the peaks intensity when Thickness is dcreased [103].

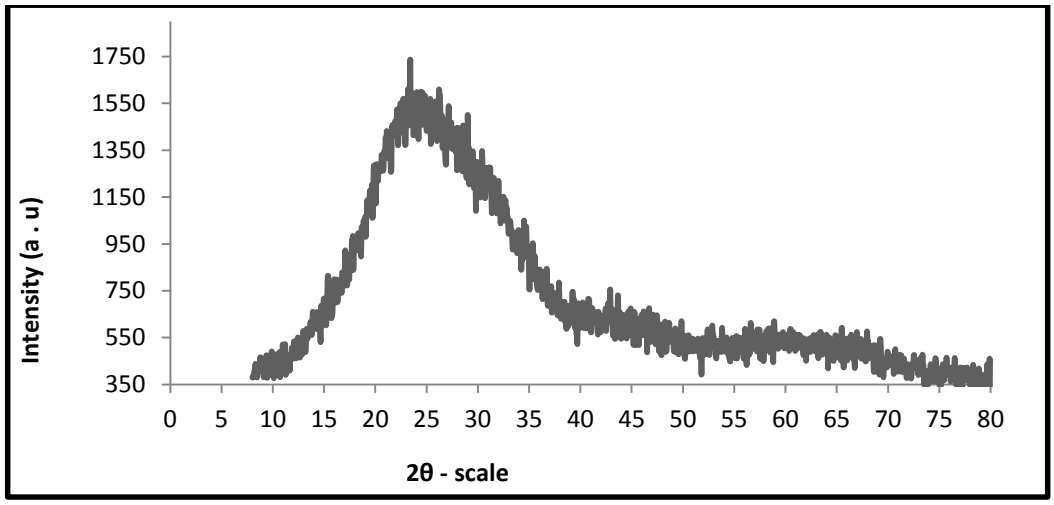

Figure (4-4): XRD of TiO_2 thin film at 106 nm.

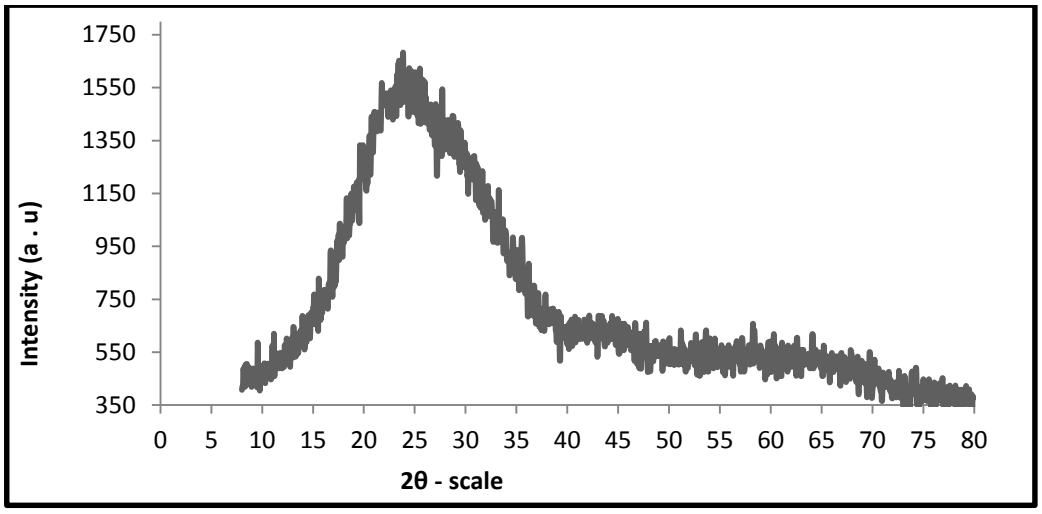

Figure (4-5): XRD of TiO_2 thin film at 87 nm.

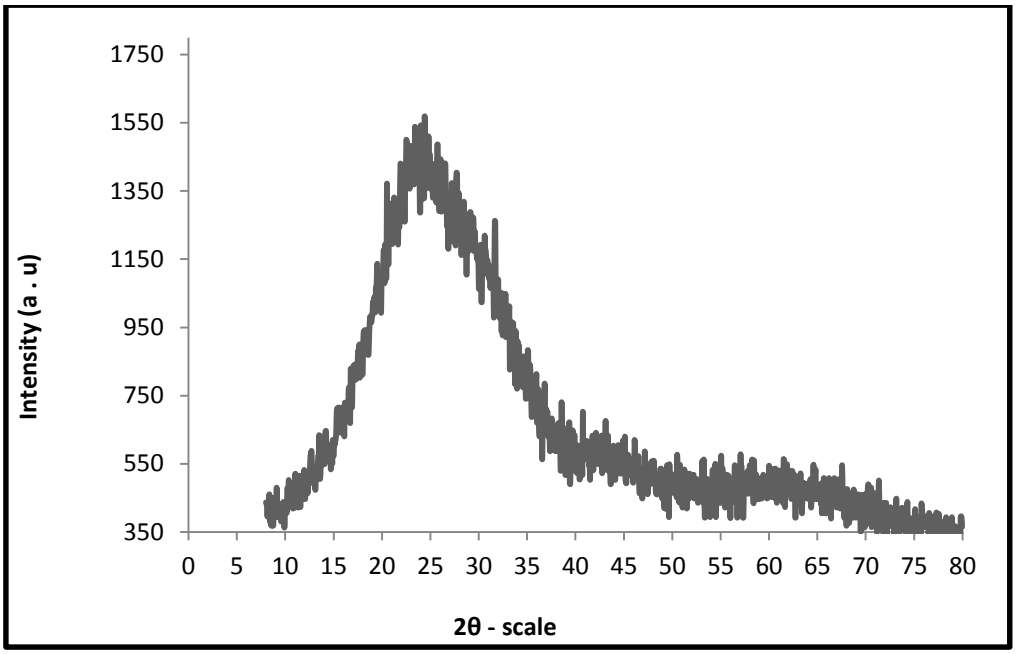

Figure (4-6): XRD of TiO_2 thin film at 63 nm.

4.3- FT-IR Analysis of PANI

The FT-IR spectrum was recorded for the synthesized sample in the wave number range of (4000-500)cm^{-1} figure (4-1) shows the FT-IR spectrum of polyaniline (PANI). The characteristics peaks of PANI including peaks range (3003.17-3529.73) cm^{-1} corresponding to (N–H stretching vibrations of secondary amine) , (2723.49 -2939.52) cm^{-1} corresponding to (C–H vibration of in CH_2) , (1516.05 - 1668.43) cm^{-1} corresponding to (C=C stretching of diamond ring), 1469.76 cm^{-1} corresponding to (C=C stretching vibration of benzenoid ring) , (1313.52-1382.96) cm^{-1} corresponding to (C - N stretching of primary aromatic ring), (1111.00-1157.29) cm^{-1} corresponding to (Aromatic C–H in-plane bending vibrations) and (619.15 – 889.18) cm^{-1} corresponding to (Aromatic C–H out-of-plane bending vibrations) coincides with the literature as well [104].

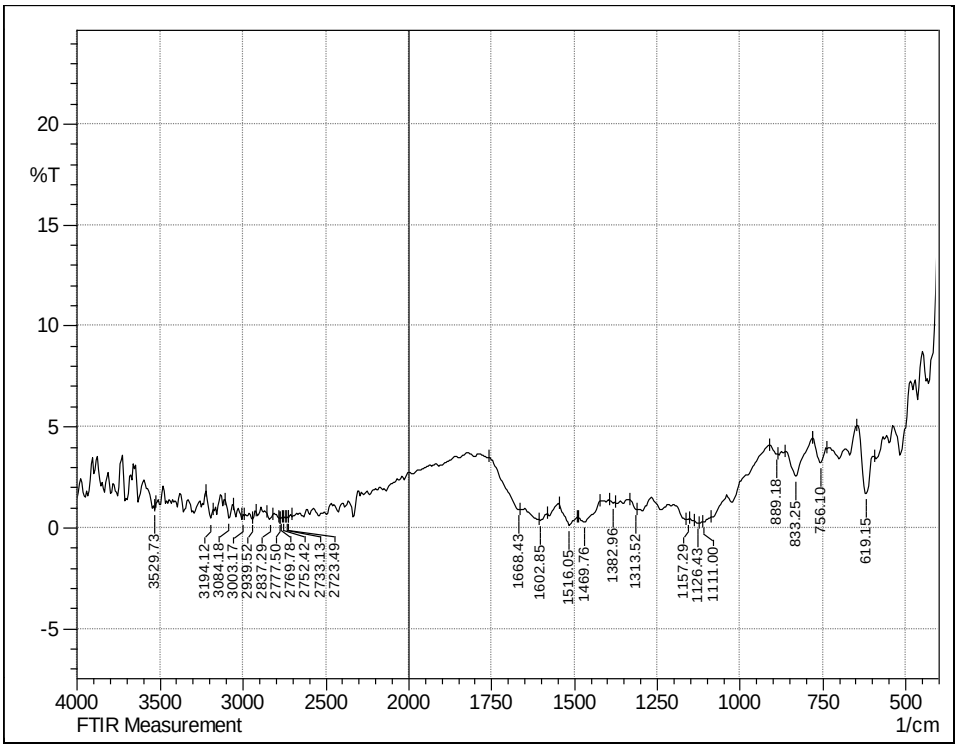

Figure (4-7): FT-IR for PANI.

4.4- Optical Properties of TiO_2 and PANI Thin Films

Optical measurements is included below :

4.4.1- Absorbance Spectrum

Figures (4-8, 4-9) shows the absorbance spectrum as a function related to the wavelength change in range of (200-1100) nm for TiO_2 and PANI Thin Films deposited on glass bases, where it is noticed that the absorbance value decreases with increasing wavelength, and we find that the maximum absorbance is in the uv range of the electromagnetic spectrum, it is noticed that the absorbance value decreases dramatically in the region of high energies with increasing wavelength and decreases slightly in the region of low energies with increasing wavelength. also, we note from the figure that the absorbance decreases with decreasing the Thickness ,this is agreement with [108].

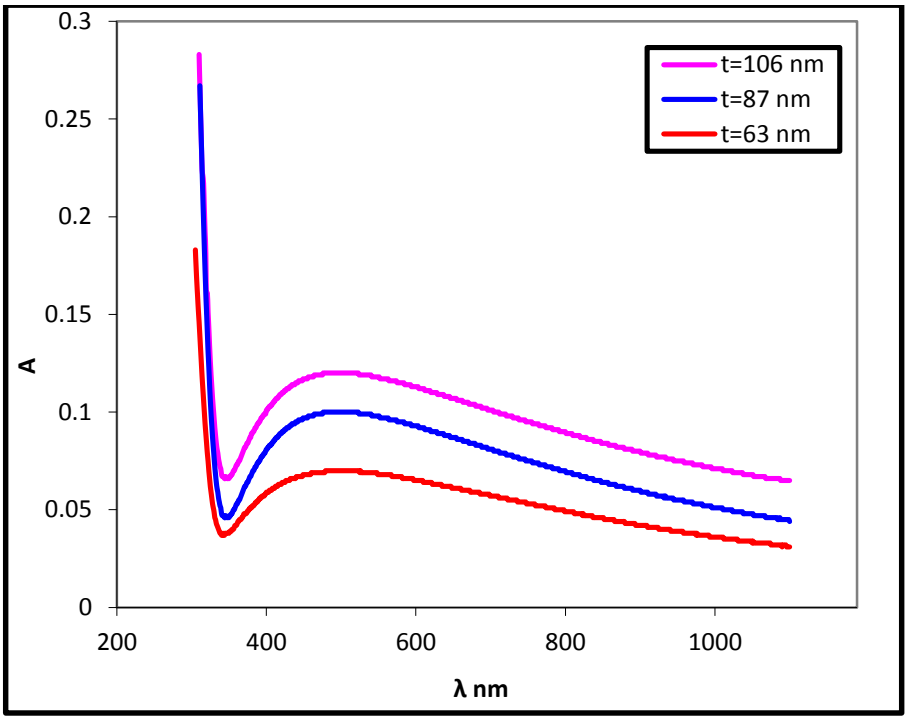

Figure (4-8): The relation between absorbance and wavelength of TiO_2 Thin Films.

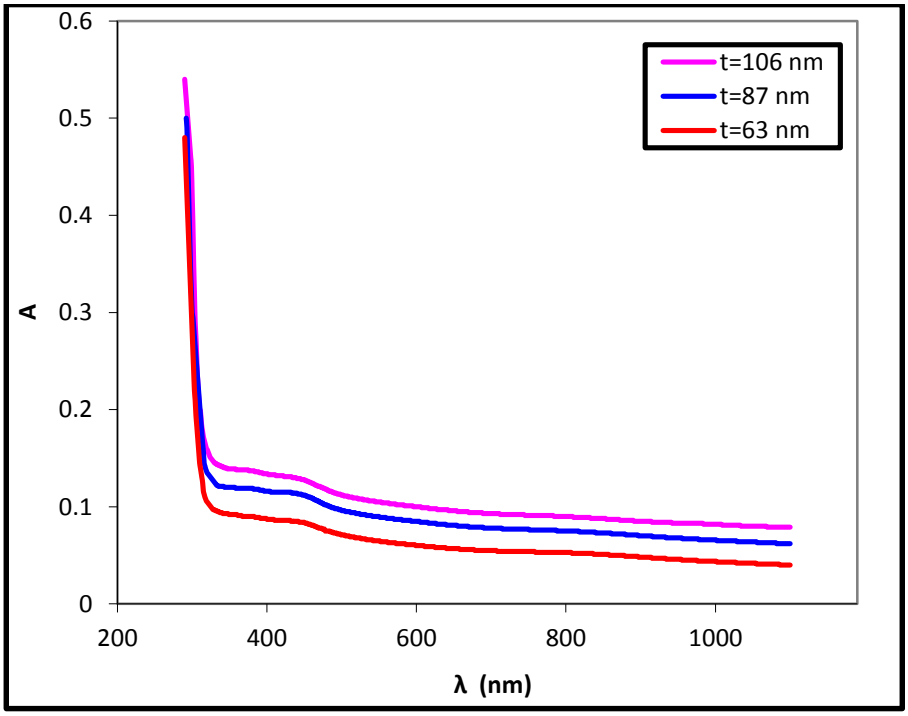

Figure (4-9): The relation between absorbance and wavelength of PANI Thin Films.

4.4.2- Transmittance Spectrum

Figures (4-10, 4-11) show the transmittance spectrum as a wavelength variation's function in range of (200- 1100) nm for TiO_2 and PANI Thin Films deposited on the glass bases where the minimum transmittance regarding TiO_2 Thin Films is in the UV region of the electromagnetic spectrum. The transmittance increases greatly in the high energy's region with the increase in the wavelength and increase slightly in the region of the low energies with the increase in the wavelength. We also note that the TiO_2 and PANI Thin Films' transmittance are subjected to an increase when the wavelength is increased as the transmittance rate exceeds (90%) in the visible and near-infrared region. It indicates the possibility of using TiO_2 and PANI Thin Films as windows in the solar cell. also, we note from the figures that the transmittance increases with dcreasing the Thickness.

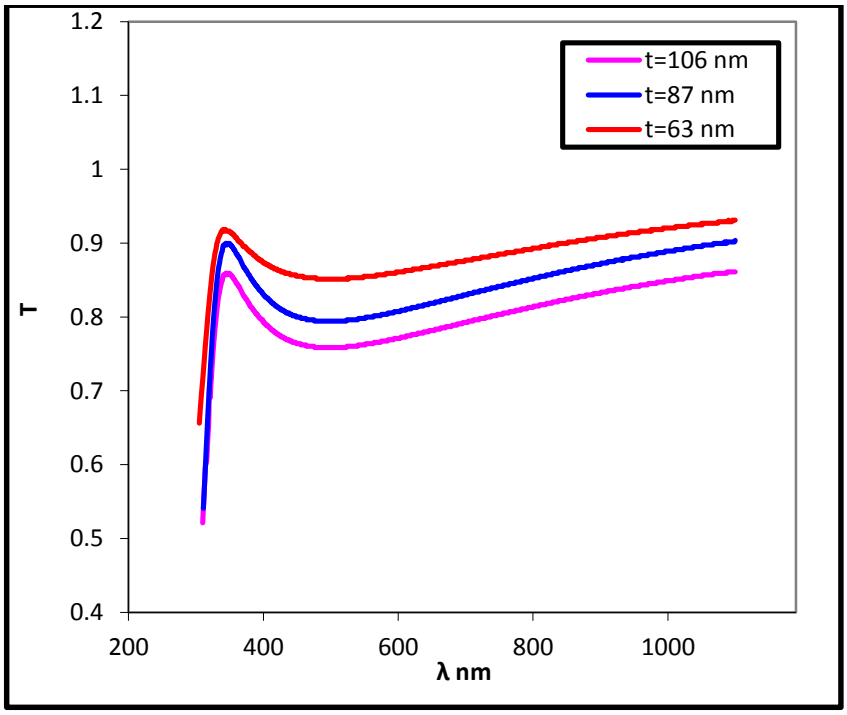

Figure (4-10): The relation between transmittance and wavelength of TiO_2 Thin Films.

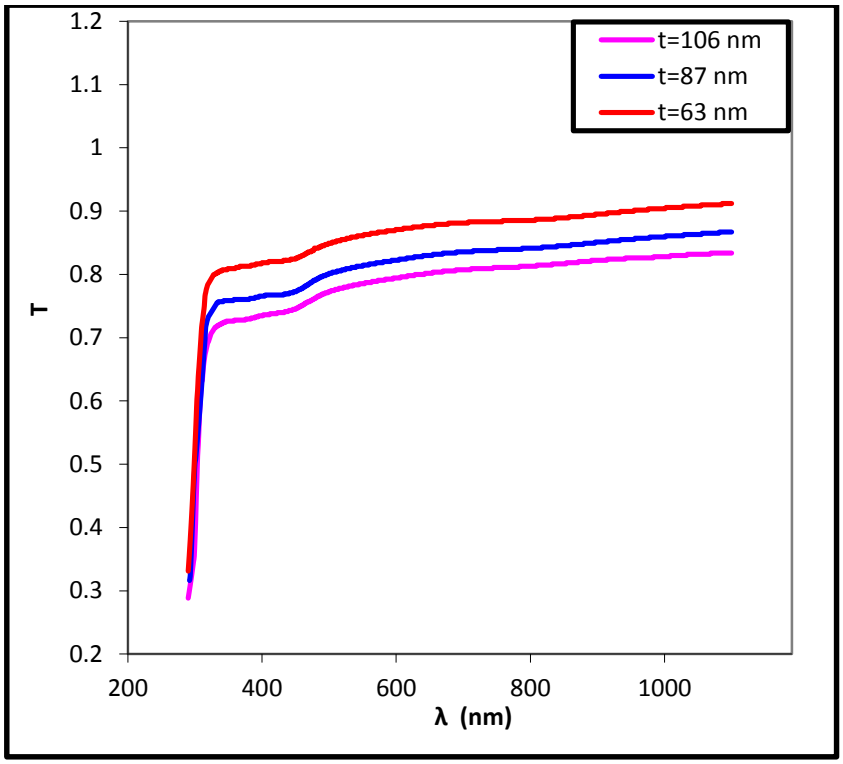

Figure (4-11): The relation between transmittance and wavelength of PANI Thin Films.

4.4.3- Reflectivity Spectrum

Figures (4-12, 4-13) shows the spectrum of reflectivity as a wavelength change's function regarding TiO_2 and PANI films in range of (200 - 1100) nm , where were the reflectivity maximum in the UV region of the electromagnetic spectrum, the reflectivity decreases dramatically in the region of high energies with the increases of wavelength and decreases slightly in the region of low energies with the wavelength increases, also, we note from the figures that the reflectivity decreases with dcreasing the Thickness, the value of reflectivity can be calculated from relation (2-26) which linking reflectivity with absorbance and transmittance.

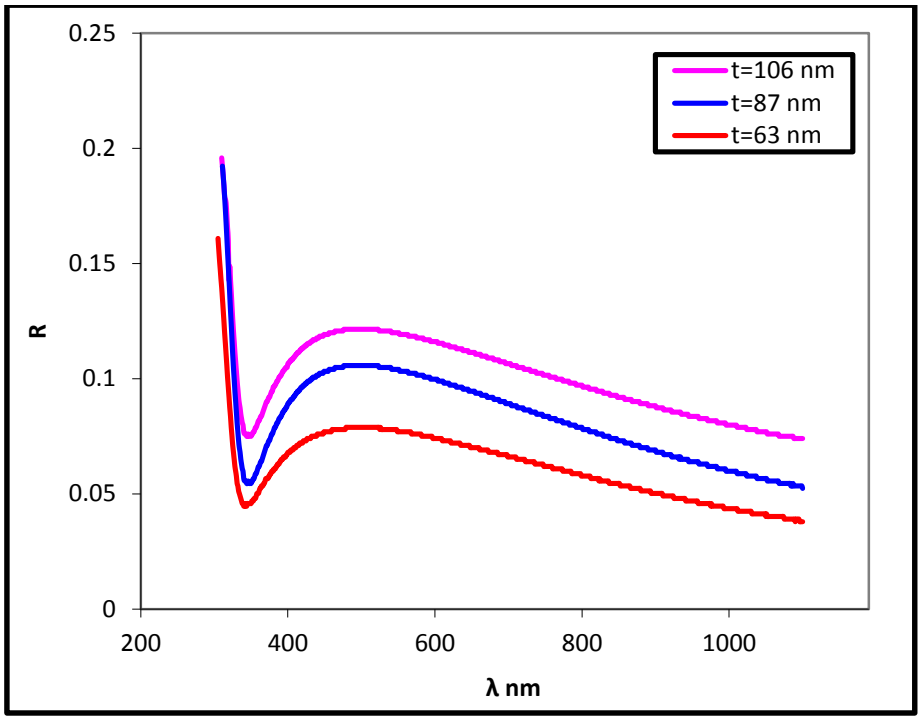

Figure (4-12): The relation between reflectivity and wavelength of TiO_2 Thin Films.

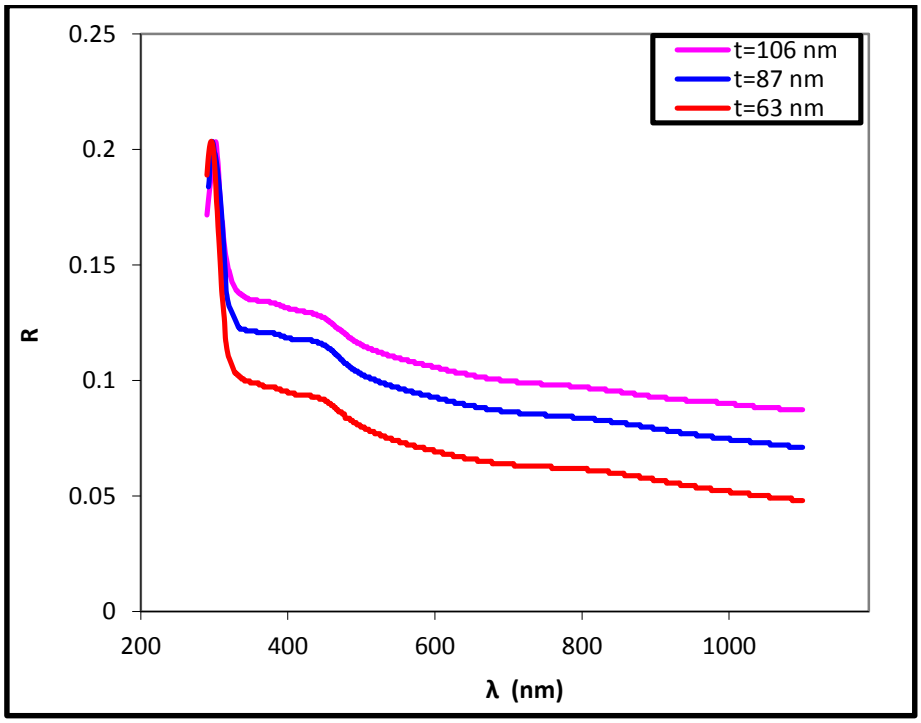

Figure (4-13): The relation between reflectivity and wavelength of PANI Thin Films.

4.4.4- Absorption Coefficient

Figures (4-14 – 4-17) show the absorption coefficient of films TiO_2 and PANI deposited on glass bases as a function of the wavelength. It is noticed that the maximum value of the absorption coefficient in the UV region of the electromagnetic spectrum and a decrease absorption coefficient with the increase in wavelength. Also, the figures are indicating that there is a decrease in absorption coefficient when the thickness is dcreased, the absorption coefficient might be theoretically evaluated from relation (2-14).

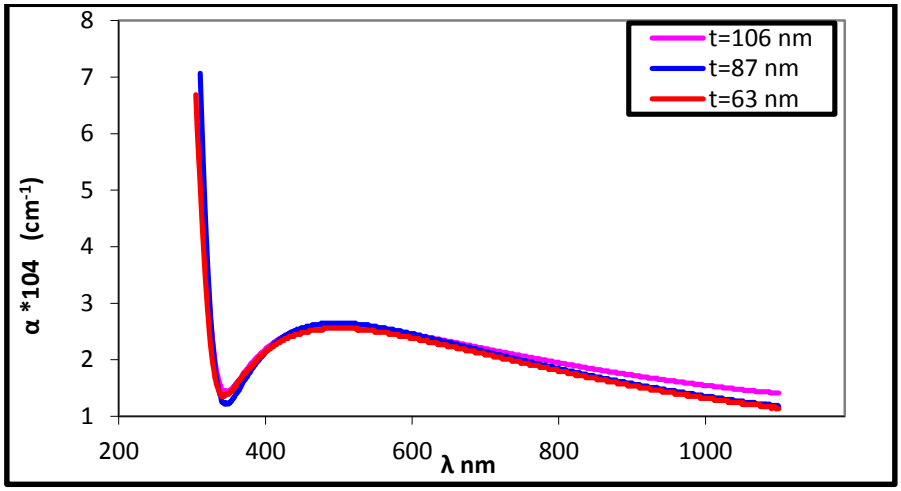

Figure (4-14): Absorption coefficients as a function of wavelength of TiO_2 Thin Films.

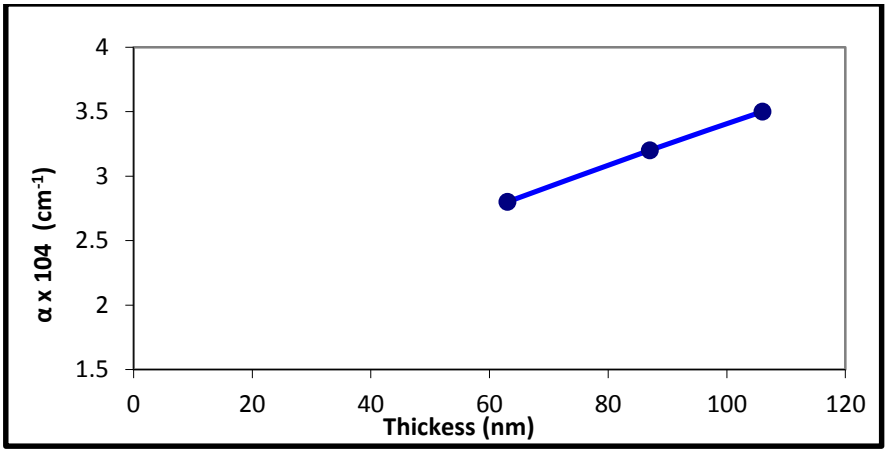

Figure (4-15): Variation of absorption coefficients (α) with Thickness.

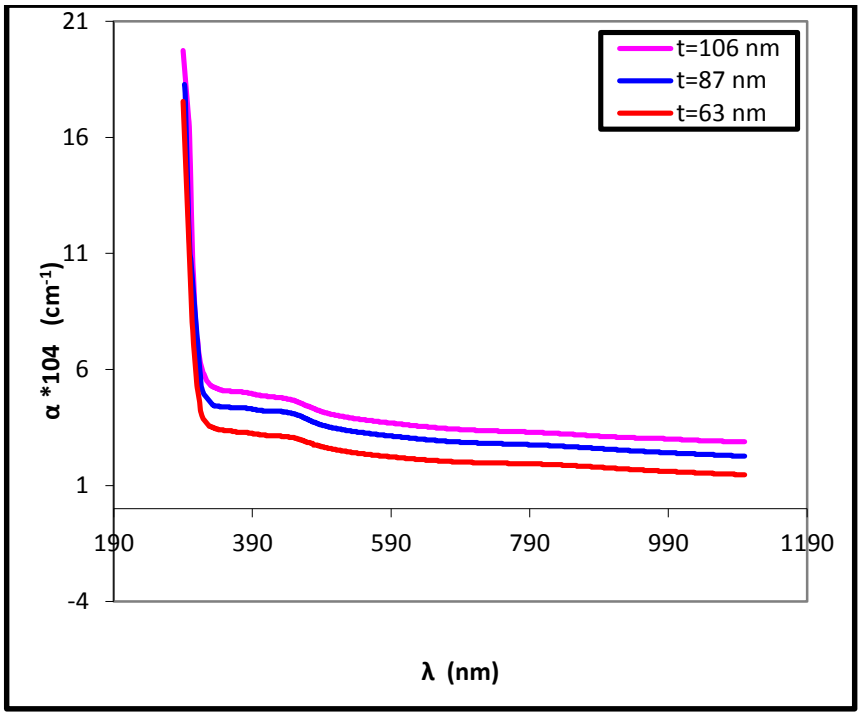

Figure (4-16): Coefficient absorption as a function of the wavelength of PANI Thin Films.

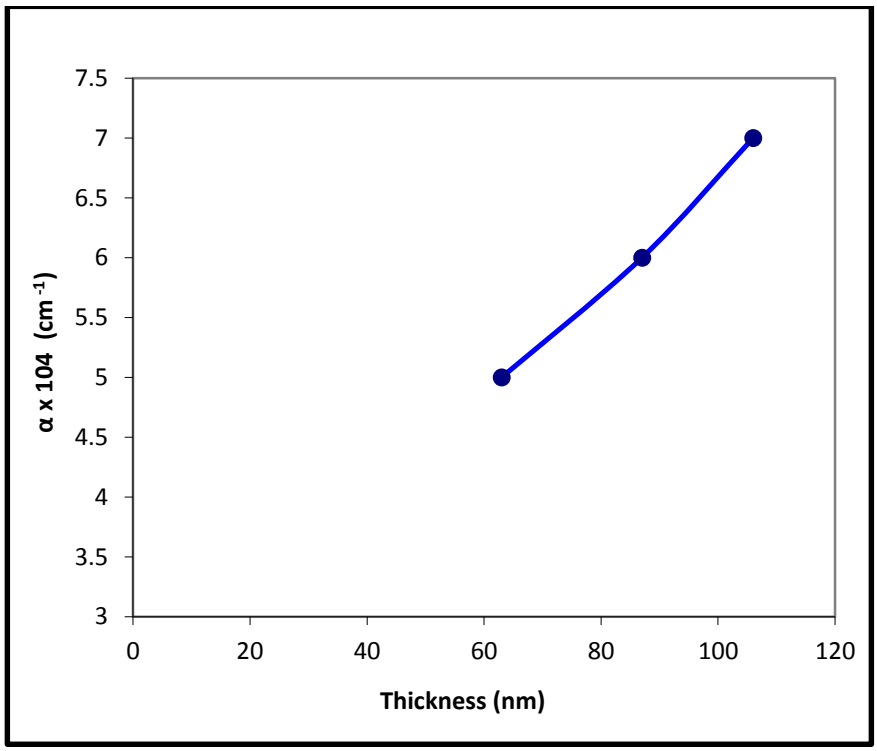

Figure (4-17): Variation of absorption coefficients (α) with Thickness

4.4.5- Extinction Coefficient

Extinction coefficient (k_o) represents the amount of energy absorbed in the thin film, and in a more precise sense, it represents the inactivity of the electromagnetic wave inside the material. Figures (4-18 – 4-21) shows the extinction coefficient change as a function of the wavelength related to Thin Films of TiO_2 and PANI, as it is noticed that the value of the extinction coefficient decrease with the decrease of the wavelength, this decrease in extinction coefficient it is result of an decrease in the absorption coefficient, as it is associated with it in the relation (2-27) , also we note from the figures that there is a decrease in the extinction coefficient with the dcrease in the thickness**.**

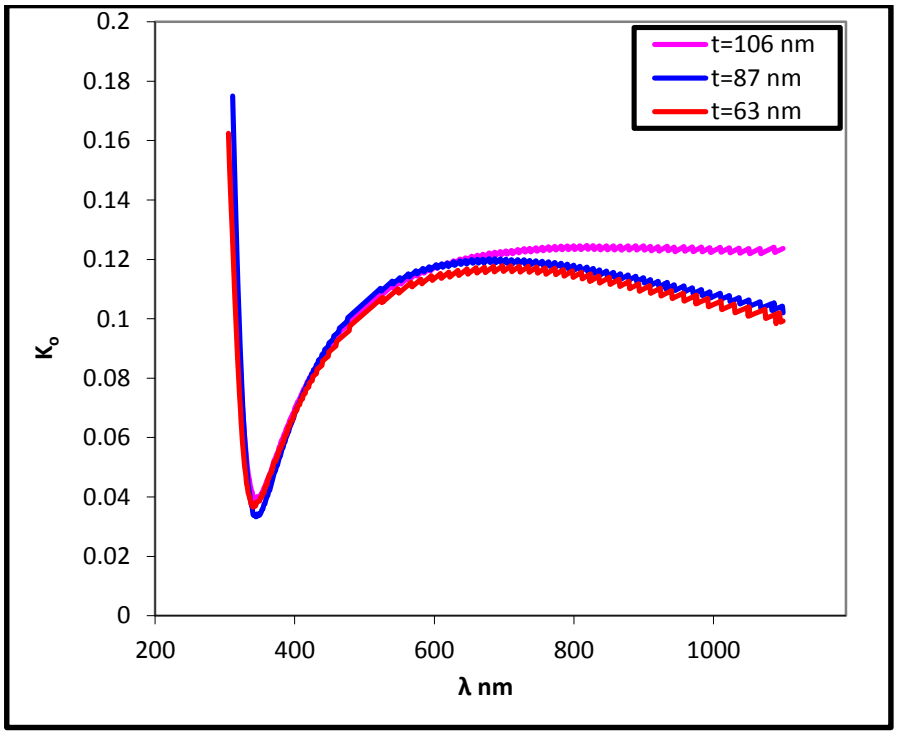

Figure (4-18): Extinction coefficient as a function of the wavelength of TiO_2 Thin Films.

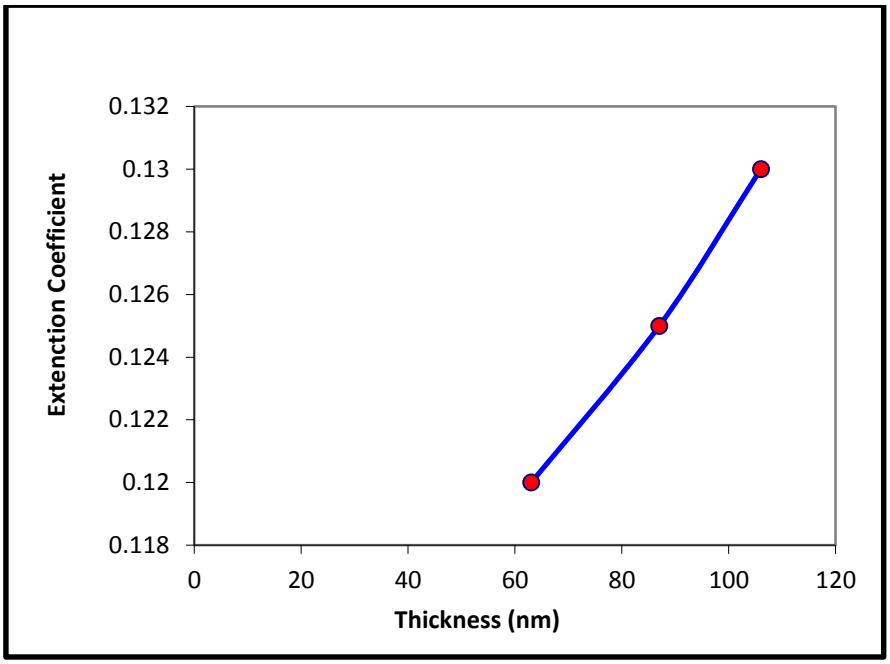

Figure (4-19):The relation between the extinction coefficients (K_o) with Thickness.

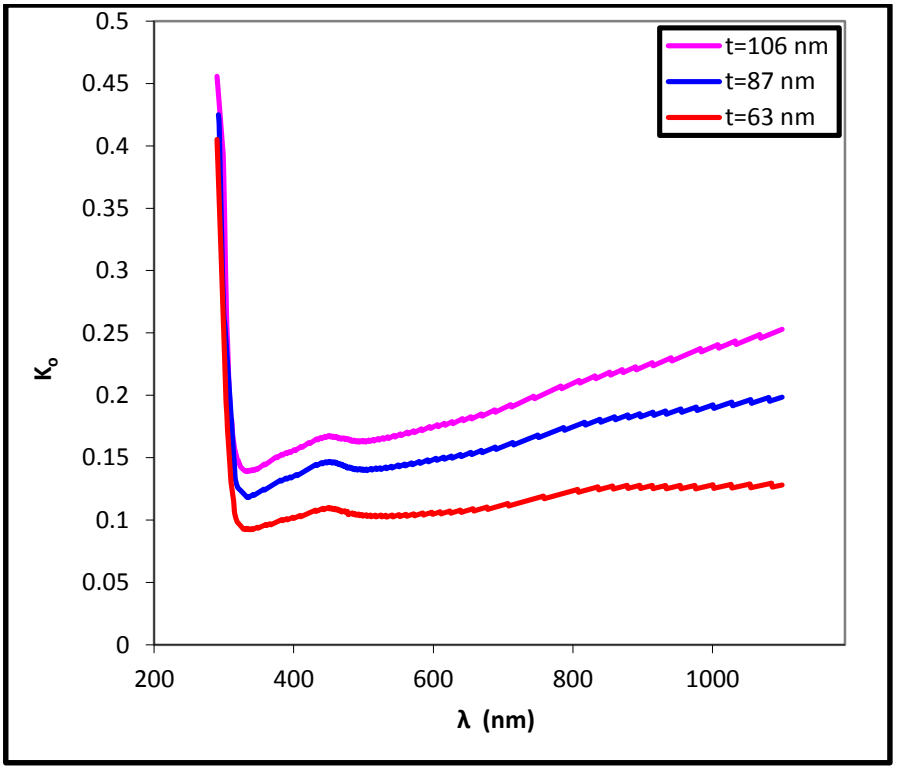

Figure (4-20): Coefficient of extinction as a function of the wavelength of PANI Thin Films.

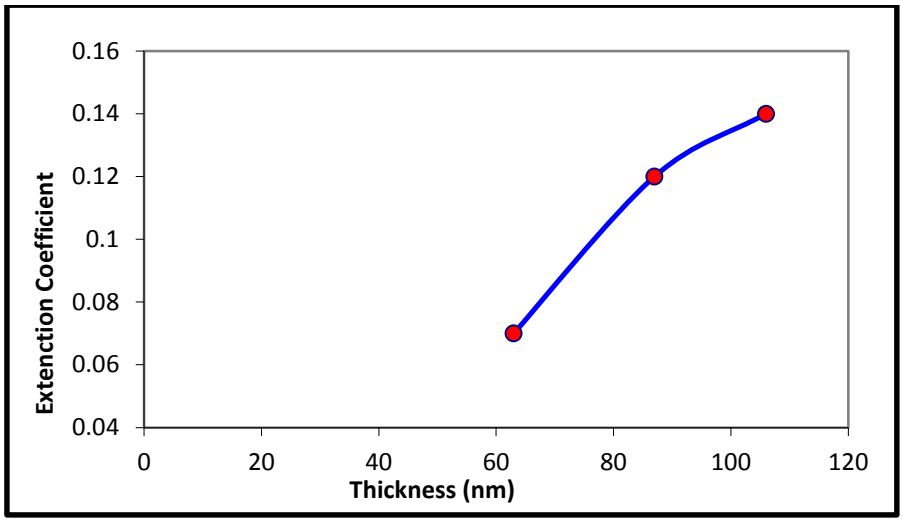

Fig. (4-21): The relation between the extinction coefficients (K_o) with Thickness.

4.4.6- Refractive Index

Figures (4-22 – 4-25) Shows the refractive index change as a wavelength change's function regarding TiO_2 and PANI Thin Films. We also note that the maximum refractive index in the region of high energies, decreases with increasing wavelength due to the decrease of the charge carriers. It has been also indicated that the refractive index was inversely proportional to the Thickness.

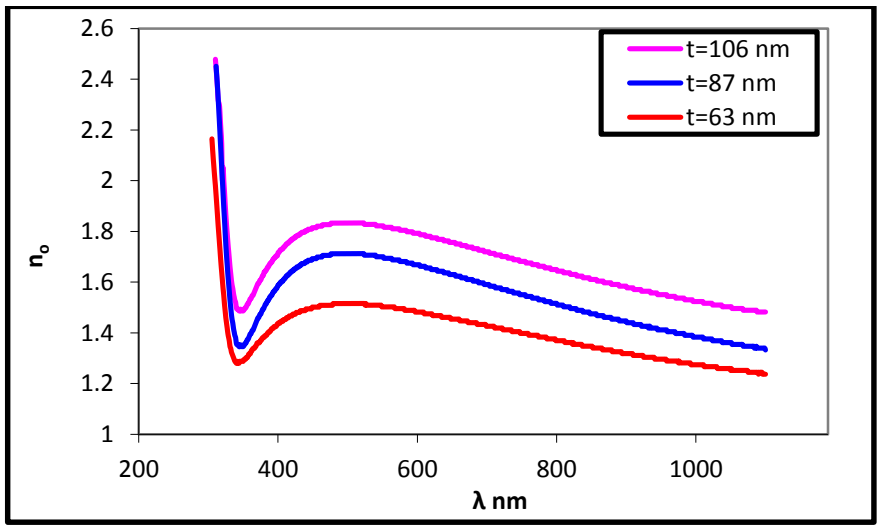

Figure (4-22): Refractive Index as a wave length function of TiO_2 Thin Films.

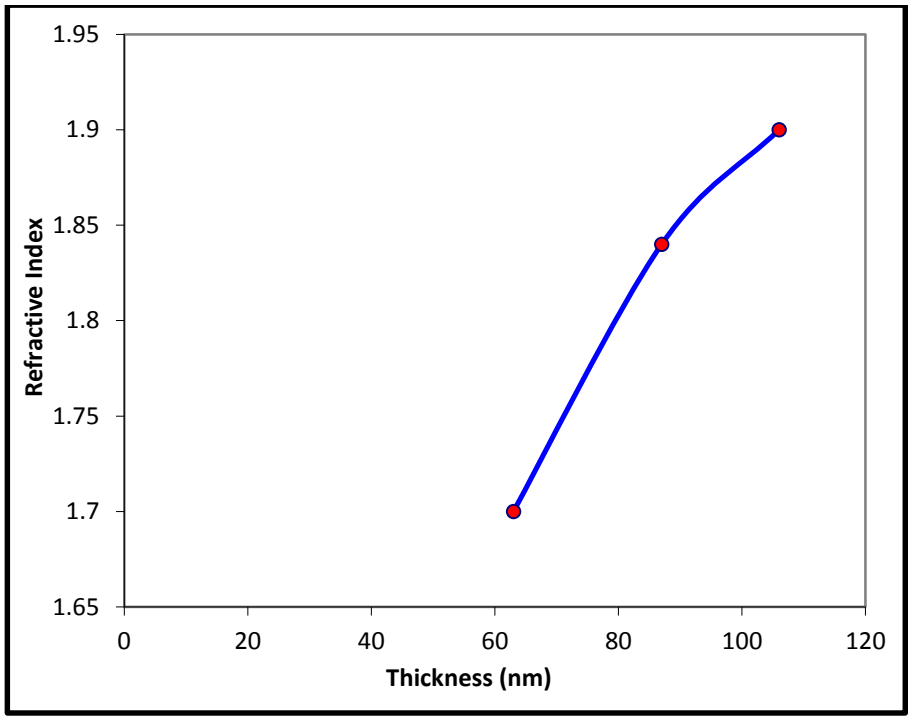

Figure (4-23): The relation between the refractive index with Thickness.

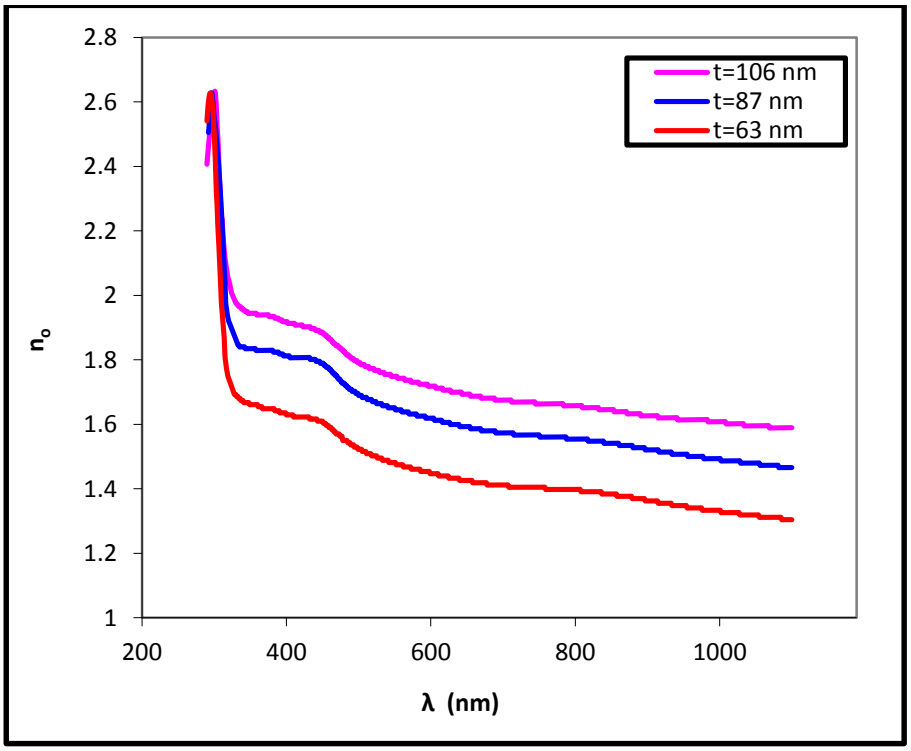

Figure (4-24): Refractive index as a function of the wavelength of PANI Thin Films.

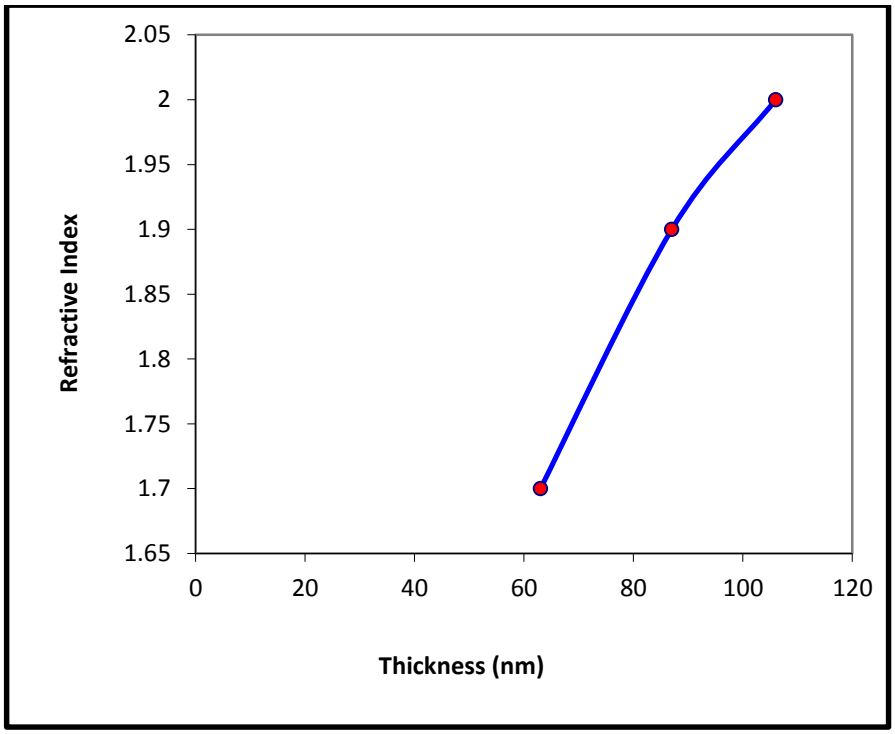

Figure (4-25) : The relation between the refractive index with Thickness.

4.4.7- Dielectric Constant

The interactions between the medium charges and the light are because of the material absorption in the material and then the medium charges' polarization process. Usually, such polarization was indicated via the complex dielectric constant (ε_i).

Figure (4-26a, 4-26b) shows the change of the real part regarding the dielectric constant as a wavelength change's function related to TiO_2 and PANI Thin Films, as we notice that the curves are somewhat similar to the refractive index behavior based on equation (2-31).

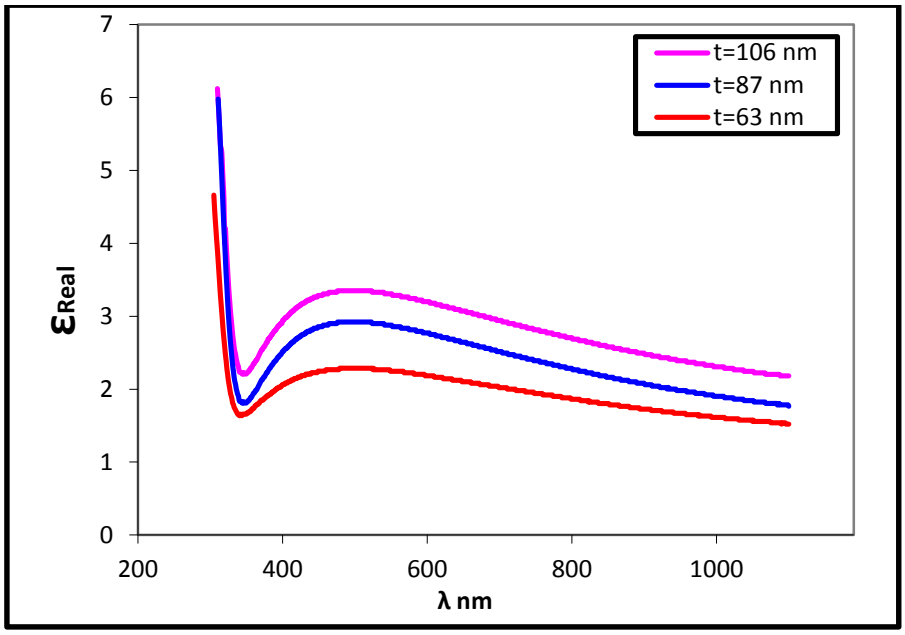

Figure (4-26a): Real dielectric constant as a function of the wavelength of TiO_2 Thin Films.

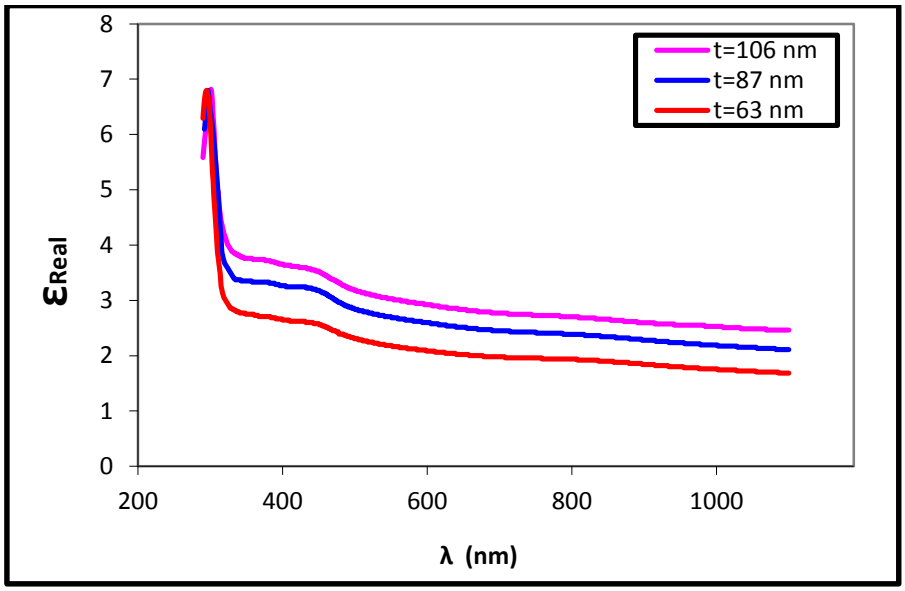

Figure (4-26b): Real dielectric constant as a function of the wavelength of PANI Thin Films.

Figures (4-27a, 4-27b) shows the change related to dielectric constant's imaginary part as a function of changing the wavelength of Thin Films of TiO_2 and PANI, where we observe the curve behavior of the imaginary part that is somewhat similar to the behavior of the extinction coefficient.

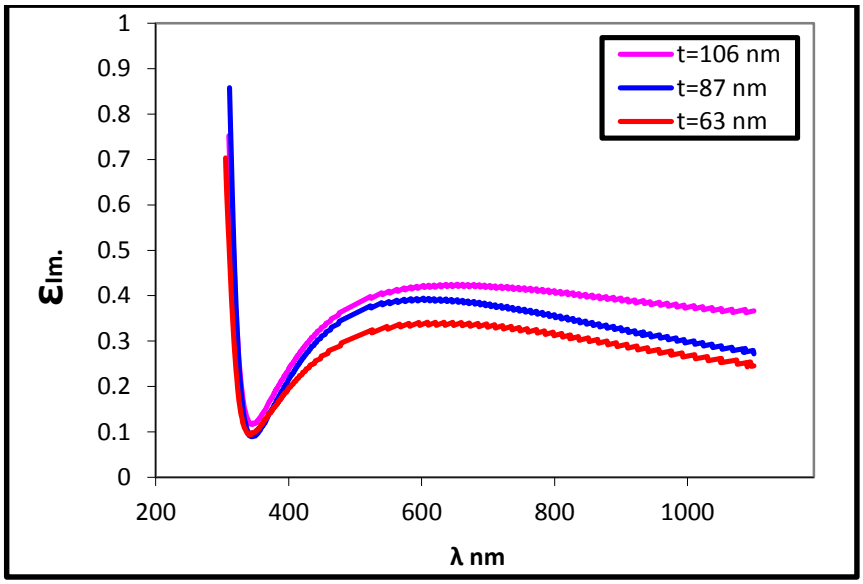

Figure (4-27a): Imaginary dielectric constant as a function of the wavelength of TiO_2 Thin Films.

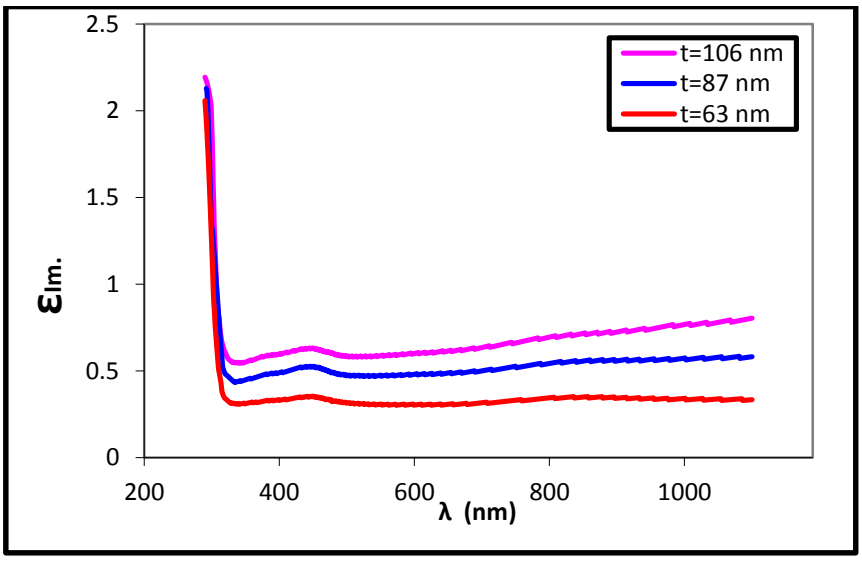

Figure (4-27b): Imaginary dielectric constant as a function of the wavelength of PANI Thin Films.

4.4.8- Optical Conductivity

Optical conductivity was calculated from the relation (2-34) , Figures (4-28 – 4-31) exhibits the changes in optical conductivity as a function of wavelength where the maximum conductivity in the UV region of the

electromagnetic spectrum, and decreases with increasing wavelength, as well as the inverse relation with the Thickness.

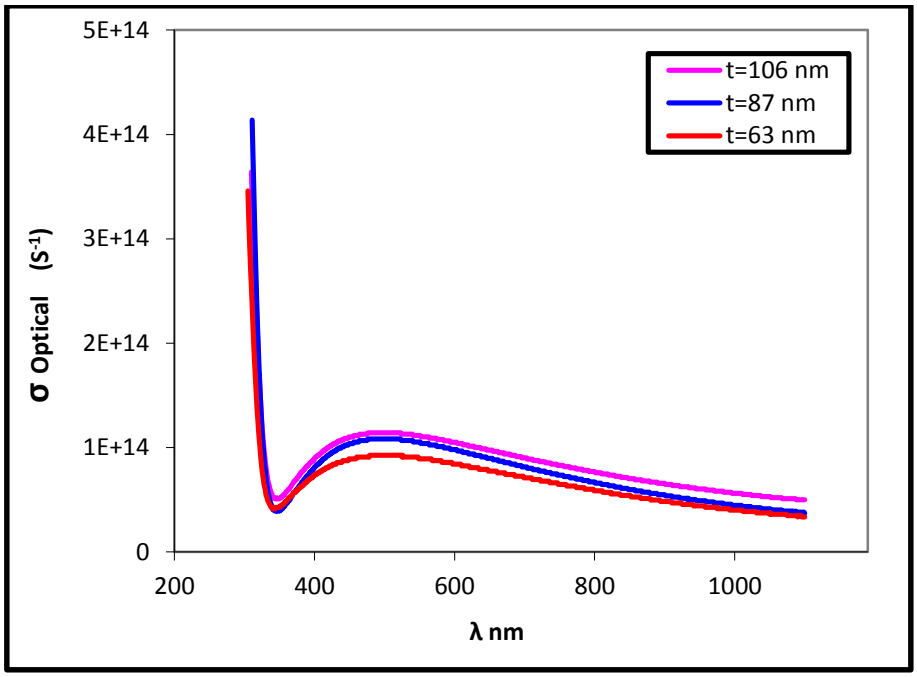

Figure (4-28): Optical conductivity as a wavelength function of TiO_2 Thin Films.

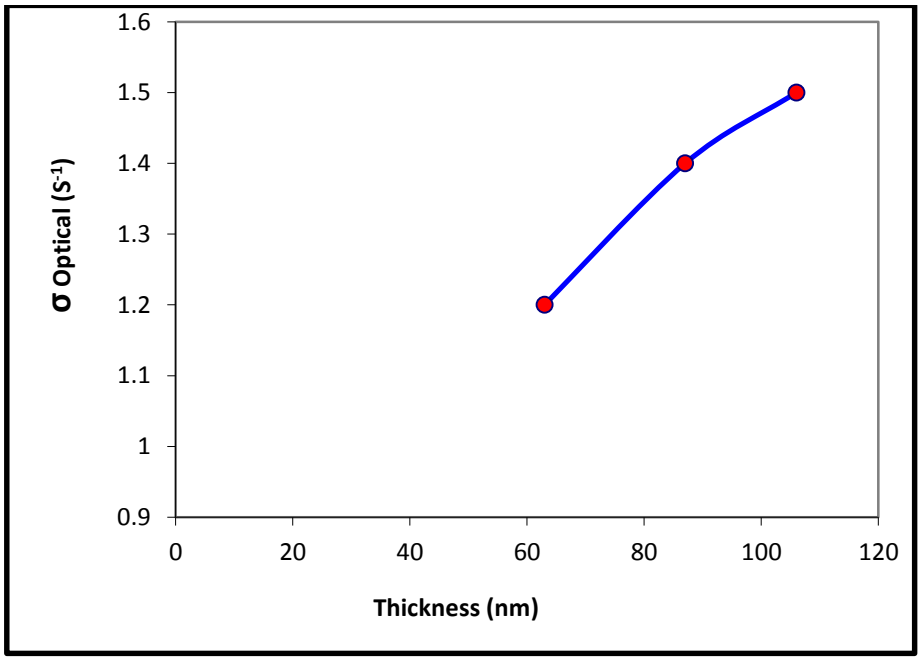

Figure (4-29) : Relation between the optical conductivity (σ) with Thickness.

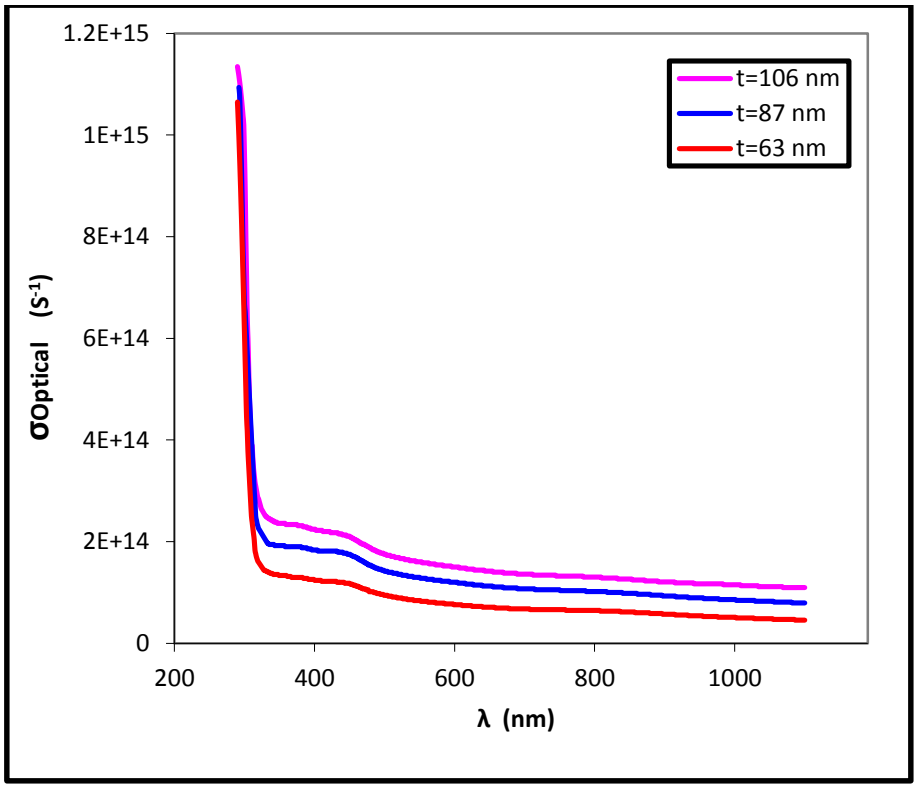

Figure (4-30): Optical conductivity as a wavelength function of PANI Thin Films

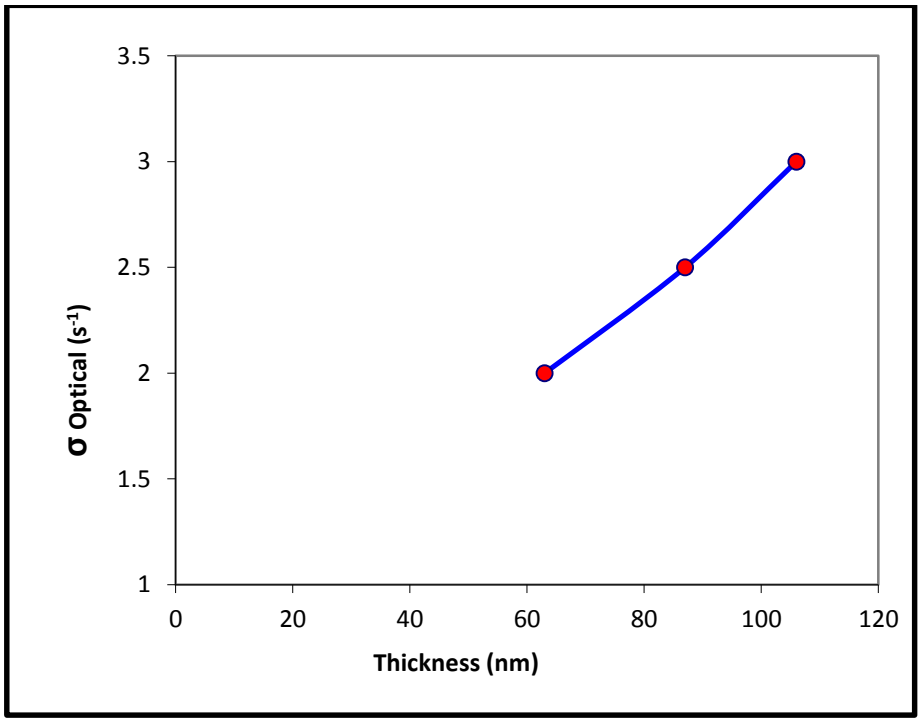

Figure (4-31): Relation between the optical conductivity (σ) with Thickness.

4.4.9- Direct Energy gap

This is a major constant in semiconductor physics, since it is depending on such value of the multiple uses of semiconductors in optical and electronic applications.

The energy gap value is depending on the crystal structure of the material and the energy gap value can be determined by knowing the value of the absorption coefficient and the energy of the incident photon, as shown in Figures (4-32 – 4-35), we note from the figures that the energy gap increases with dcreasing the Thickness, as shown in the tables (4.1, 4.2).

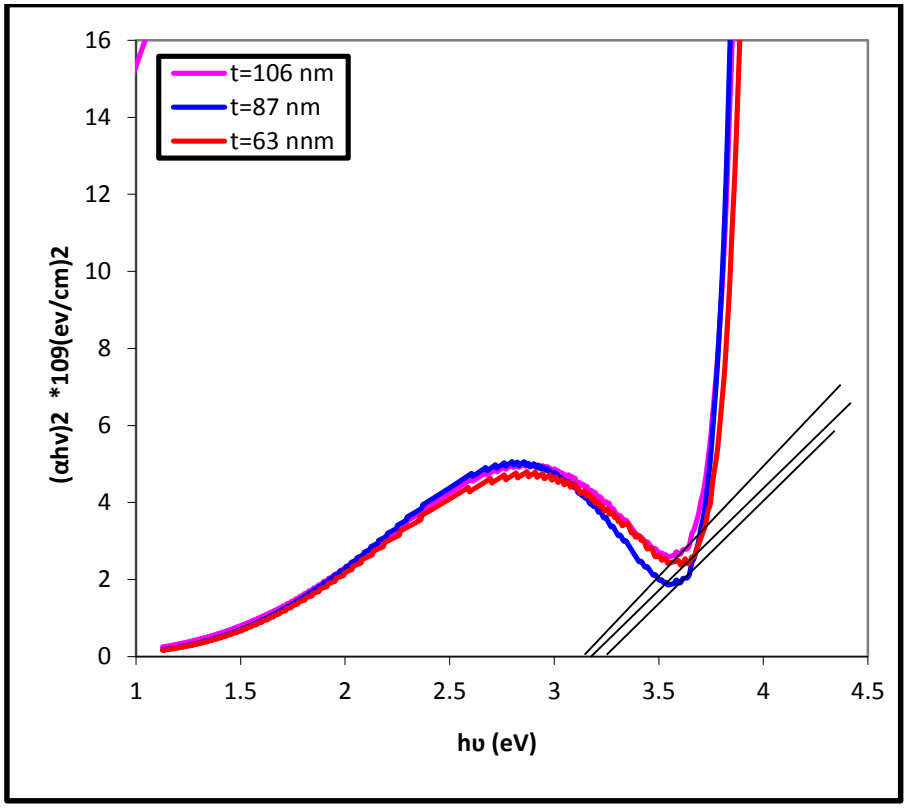

Figure (4-32): Relation between ($\alpha h\upsilon)^2$ versus photon energy of TiO_2.

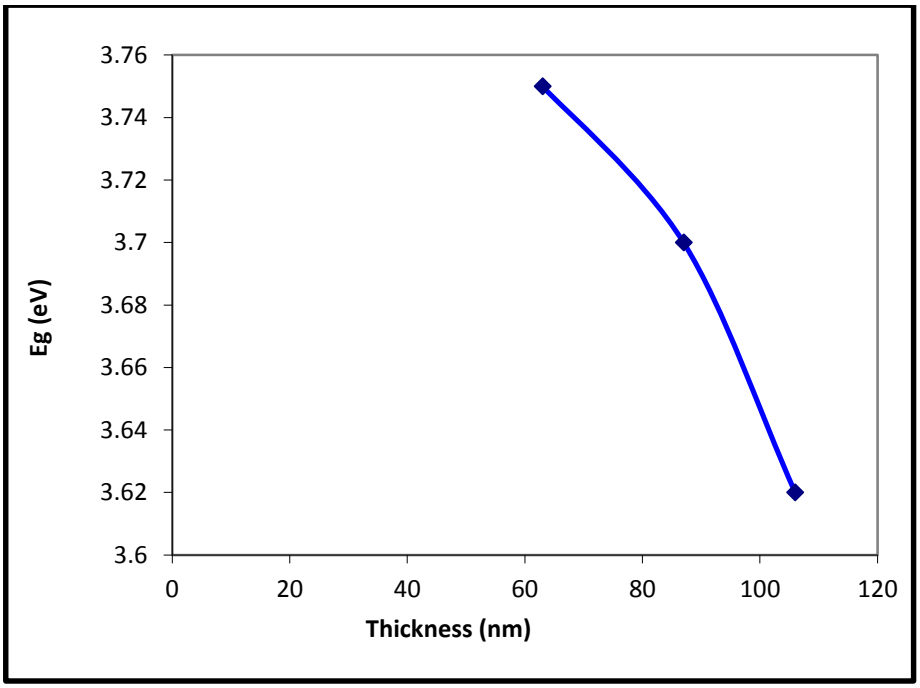

Figure (4-33): Relation between E_g and Thickness.

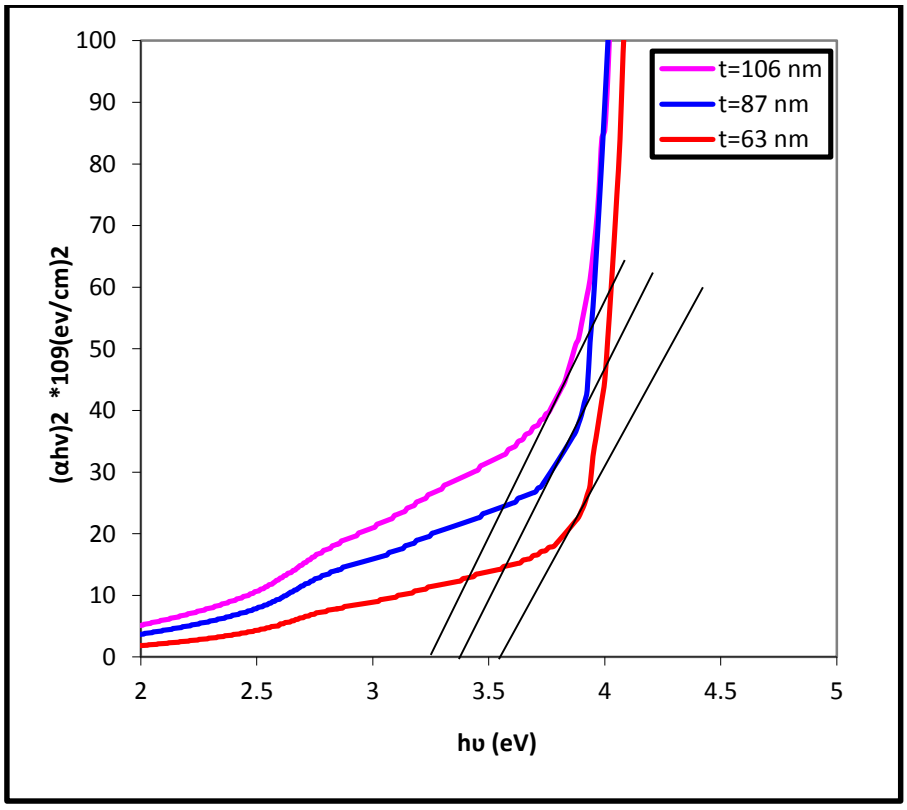

Figure (4-34): Relation between $(\alpha h\upsilon)^2$ versus photon energy of PANI.

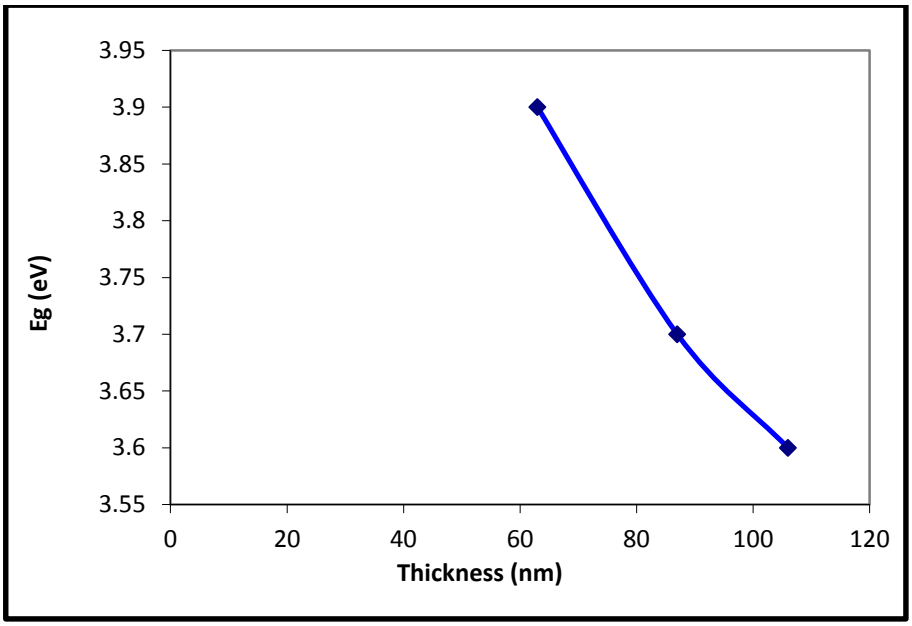

Figure (4-35): Relation between E_g and Thickness.

Table (4.1) Change the direct energy gap with changing Thickness of TiO_2 Thin Films

Thickness (nm)	Direct energy gap(eV)
106	3.19
87	3.2
63	3.25

Table (4.2) Change of the direct energy gap with changing Thickness of PANI Thin Films

Thickness (nm)	Direct energy gap(eV)
106	3.25
87	3.4
63	3.55

4.5 - I-V Characteristic of PANI-TiO_2 / ITO Hetero junction Under Dark and Light Conditions

The results showed that the efficiency value increases when the thickness is dcreased from (106 to 87) nm and then decreases at the thickness 63 nm, as shown in Figures (4-36, 4-37, 4-38). As the efficiency increases from (0.55%) to (0.61%), then it decreases to (0.45%),The reason is due to the decreasing value of the efficiency of the solar cell at the thickness 63nm to 0.45%, where there are in this study several factors that affect the efficiency of the solar cell, where the decrease in the thickness of the thin film due to the increase in the rotation speed leads to an increase in the transmittance, and this factor leads to the increase in efficiency, at the same time With it, the value of the energy gap increases, and this action negatively affects the efficiency, which is the reason for the decrease in the value of the efficiency at a thickness of 63 nm, this efficiency is considered low for two reasons, the large energy gap for both titanium dioxide and the polymer, addition to the low conductivity of the polymer. as in Table (4.3). The power of the solar cell is calculated from the relation (2-43),The value of the fill factor for the solar cell was calculated from the relation (2-44), the fill factor was used to calculate the efficiency of the solar cell as in the relation, (2-45).

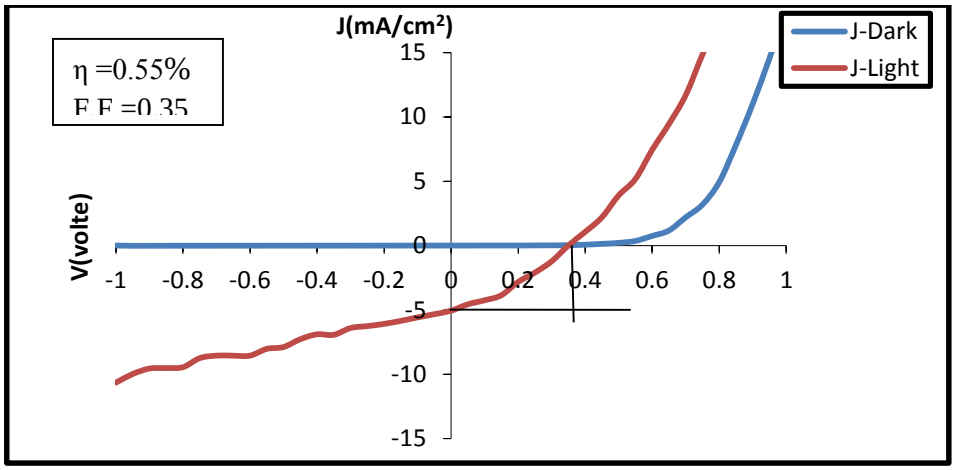

Figure (4-36): J-V characteristic for PANI-TiO_2 at 106 nm / ITO solar cell.

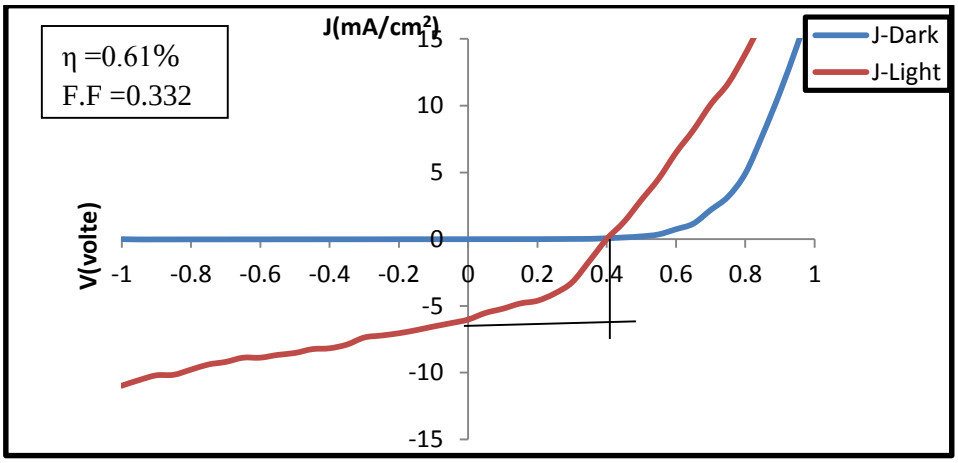

Figure (4-37) : J-V characteristic for PANI-TiO_2 at 87 nm / ITO solar cell.

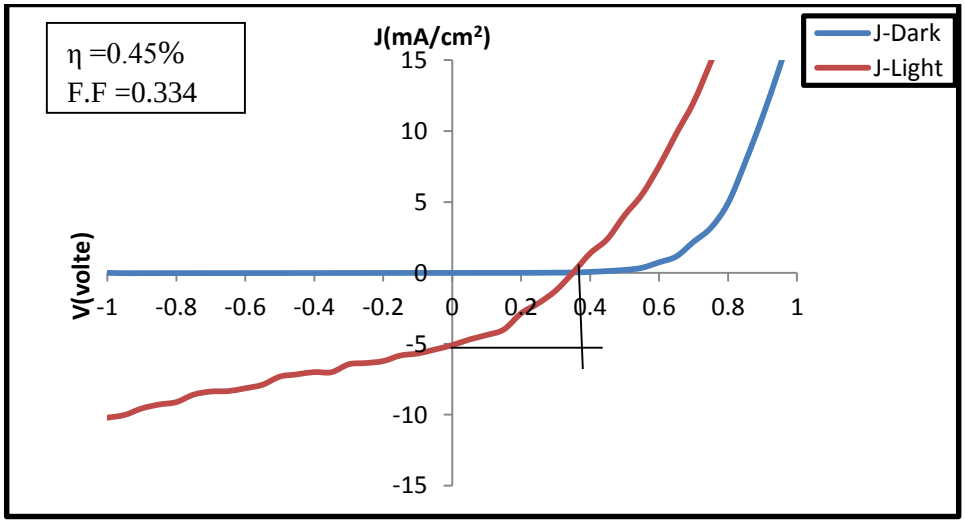

Figure (4-38): J-V characteristic for PANI-TiO_2 at 63 nm / ITO solar cell.

Table (4.3) The results of the J-V for PANI-TiO_2 Thin Films at different Thickness

Thickness (nm)	Jsc (mA/cm^2)	Voc (mV)	I_{max} (mA)	V_{max} (mV)	F.F	η (%)
106	4.44	355	2.7	205	0.35	0.55
87	4.6	400	2.6	235	0.332	0.61
63	4.2	325	2.4	190	0.334	0.45

4.6- Conclusions

By depositing Thin Films of polyaniline polymer on titanium dioxide films on ITO glass using Spin Coating technology and its applications in a solar cell, the following can be concluded:

1. It was found through the study that the anatase phase is formed when the Thin Films of titanium dioxide are annealed at an annealing temperature of 550 °C.
2. The surface roughness of all titanium dioxide films increased at decreasing the Thickness.
3. It was found through the study that the optical properties of titanium dioxide and polyaniline films change with the decrease in the Thickness.
4. Decreasing Thickness leads to increase the Transmittance of titanium dioxide and polyaniline films.
5. Decreasing the Thickness leads to an increase in the energy gap of titanium dioxide and polyaniline films.
6. The maximum efficiency of the solar cell was at the Thickness 87 nm.

4.7- Suggestions for Future Work

Based on the data and the results obtained, we should mention some proposals for future work that could serve as future research.

1. Study of the structural, electrical and optical properties regarding the Thin Films of polyaniline - titanium dioxide by sedimentation on silicon substrates.
2. Improving the efficiency of solar cells by using a polymer with a higher conductivity than that conductivity of polyaniline.
3. Mixing polyaniline with other polymers and studying their optical and electrical properties.

Chapter One

Introduction and Literature Review

Chapter Two

Theoretical Consideration

Chapter Three

Experimental Work

Chapter Four

Results, Discussion ,Conclusions and Suggestions

References

References

1. O. O. Adewoye ," Advances in Engineering Materials Development", Proceedings of Nigeria Materials Congress,Vol.2,No,1,pp.(11-22), (2007).

2. C. X. Shan, X. Hou and K. Choy, "Corrosion Resistance of TiO_2 Films Grown on Stainless Steel by Atomic Layer Deposition" ,Surface and Coatings Technology, Vol. 202, No. 11, pp. (2399-2402), (2008).

3. Z. L. Tang, J. Y. Zhang, Z. Cheng and Z. T. Zhang, "Synthesis of Rutile TiO_2 at Low Temperature", Materials Chemistry and Physics, Vol. 77, No. 2, pp. (314-317), (2001).

4. J. C. Yu, L. Z. Zhang and W. K. Ho, "Photo catalytic Activity of Nano-Sized TiO_2 Powders by Sol Gel Method, Using Titanium Tetraisopropoxide and EtOH/ H2O Solution", Journal of Photochemistry and Photobiology A: Chemistry, Vol. 148, No. 3, pp. (263-271), (2002).

5. Y. Z. Li, N. H. Lee, E. G. Lee, J. S. Song and S. Kim, "Preparation and Characterization of Nano-TiO_2 Powder by Sol-Gel Method", Chemical Physics Letters, Vol. 389, No. 3, pp. (124-128), (2004).

6. A. M. Ruiz, G. Sakai, A. Cornet, K. Shimanoe, J. R. Morante and N. Yamazoe, "Microstructure Control of Thermally Stable TiO_2 Obtained by Hydrothermal Process", Sensors and Actuators, Vol. 103, No.2, pp. (312-317), (2004).

7. S. Qiu and S. Kalita, "Synthesis Processing and Characterization of Nano crystalline Titanium Dioxide", Materials Science and Engineering,Vol. 435,No.2, pp. (327-332), (2006).

8. J.R. Fried ," Polymer Science and Technology " , 3rd. Edition , United States , (2014).

9. P. Ghosh, " Fundamentals of Polymer Science", Polymer Study Centre, Kolkata,Vol.40,No.7,pp.(371-383), (2006).

10. K. Abd Ali Al-Ogaili, " Enhancement of some Physical Properties of Polyethylene Glycol by Adding Some Polymeric Cellulose Derivatives

and its Applications", Ph. D.Thesis ,University of Babylon , College of Science, Department of Physics, (2015).

11. J. Margolis, " Conductive Polymers and Plastics" , Chapman and Hall, Vol. 120 ,No.5,pp,(34-46), (1989).

12. L. Alcacer, "Conducting Polymers Special Applications", Reidel Publishing Company, Vol. 5,No.1,pp.(73-85), (1987).

13. T. Ito, H. Shirakawa and S. Ikeda, " Polymer Chemistry", J. Polym. 2nd. Edition, pp. (11-20),(1974).

14. D. W. Adams and M. Hill, "Nanotechnology Demystified", United States, Vol.9,No.6,p.403,(2007).

15. P. Wurfel," Physics of Solar Cells ", Wiley-VCH Verlag GmbH and CCo. KGaA,Vol.2,No,4, pp. (27-29), (2005).

16. A. E. Pap, "Investigation of Pristine and Oxidized Porous Silico",Ph.D Thesis, University of Oulu, (2005).

17. A. Turner, " Electrolytic Shaping of Germanium and Silicon", Bell Syst. Tech. Journal, Vol. 35,No.9, pp. (33-37), (1956).

18. A. S. Alejandro," Structural Engineering of Nanoporous Anodic Alumina and Applications", University Rovirai Virglli ,Vol.4.No.7,pp.343, (2010).

19. G.E. William ,B.A Aldo and Z. Jinwen ,"Polymer Nanocomposites Synthetic and Natural Fillers",Maderas. Ciencialy tecnología, Vol, 7, No.3, pp.(159-178), (2005).

20. S.B. Legoas, V.R. Coluci, S.F. Braga, P.Z. Coura, S.O. Dantas and D.S. Galvao," Molecular- Dynamics Simulations of Carbon Nanotubes as Gigahertz Oscillators", Phys. Rev. Lett. Vol. 90, No.5,pp.(17-26), (2003).

21. A. Mehto, V . Mehto, J . Chauhan, I . Singh and R .Pandey," Preparation and Characterization of Polyaniline/ZnO Composite Sensor", Journal of Nanomedicine Research, Vol. 5, No.3,pp.(312-320),(2017).

22. D.K. Dwivedi, and M. Dayashankar, "Effect Of Annealing On The Structural And Electrical Properties Of Cdte/Znte Heterojunction Thin Films", Rom. Journ. Phys., Vol. 55, No. 4, pp. (352–359), (2010).

23. A. Hateef, " Studying the Optical and Electrical Properties of (TiO_2) Thin Films Prepared by Chemical Spray Pyrolysis Technique and their Application in Solar Cells", M. Sc. thesis, Science Al- Mustansiriyah University, (2011).

24. D.A. Hanaor, G. Triani and C.C. Sorrell, "Morphology and Photocatalytic Activity of Highly Oriented Mixed Phase Titanium Dioxide Thin Film", Surf. Coat. Tech., Vol. 12,No.7, pp.(59-64) ,(2012).

25. K . M. Ziadan ,H . F . Hussein and K.I. Ajeel , " Study of the Electrical Characteristics of Poly(o-toluidine) and Application in Solar Cell" Energy Procedia ,Vol. 18,No.2, pp. (١٦٤ – ١٥٧ (٢٠١٢).

26. S. Reda Al-Ghannam, "Synthesis and Electrical Properties of Polyaniline Composite with Silver Nanoparticles", Adv. Mater. Phys. Chem. Vol. 2,No,1, PP.(75–81), (2013).

27. M. Abd-Alkadum," Structural, Electrical and Optical Properties of TiO_2 Thin Films Prepared by Pulsed Laser Deposition", M. Sc. thesis, College of Science, Babylon University , (2014).

28. A.N. Daghman, K. Ibrahim, N. M. Ahmed and K. M. Zaidan "Effect of TiO_2 Thin Film Morphology on Polyaniline/TiO_2 Solar Cell Efficiency",World Journal of Nano Science and Engineering ,Vol.5,No.2, pp.(4-41), (2015).

29. Y.M. Evtushenko, S.A. Romashkin, and K.P. Lovetski, "Study Effect of Substrate Type on the Crystallinity of TiO_2 Thin Films", Physics Procedia Vol. 73,No. 10, pp. (100-107), (2015).

30. S. Demirci, T. Dikici, M. Yurddaskal, S. Gultekin, M. Toparli,and E.Celik , "Effect of Temperature on the Efficiency of the Sensors", Applied Surface Science ,Vol. 390,No. 2, pp.(591-601), (2016).

31. S. Mukherjee, S. Chakraborty, A.Samanta, and J. Ghosh, "Effect of Annealing Temperature on Titanium Dioxide Thin Films", Materials Research Express ,Vol. 4,No.9, pp. (165-170), (2017).

32. M.K .Al-hashimi, B.Y. Kadem, and A. K. Hassan , "Study the Crystalline Structure of TiO_2 Nano Particles ", Journal of Materials Science: Materials in Electronics ,Vol. 29,No. 3, pp. (152-160), (2018).

33. M. Q. Hamzah, A. H.Jabbar, S.O. Mezan, A. N. Tuama, and M. A.Agam , "Fabrications of TiO_2 Nano Composite for Solar Cells applications", AIP Conference Proceedings, Vol. 215, No.1, pp. (44 -50), (2019).

34. E. P. Athisayaraj and C. Vedhi, " Composites of copper oxide and polyaniline for solar cell applications", International Journal of Advanced Scientific Research and Management,Vol.16,No.7,pp.(2455-6378), (2019).

35. D.K. Muthee and B.F. Dejene , "Preparation of Thin Films Using Pulsed Laser Deposition", Materials Science in Semiconductor Processing, Vol. 106, No. 2, pp.(104-110), (2020).

36. F. M. El-Hossary , Ahmed Ghitas, A. M. Abd El-Rahman, A. A. Ebnalwaled, and M. A.Shahat, "Characterization and Performance of PAni-TiO_2 Photovoltaic Cells Treated by RF Plasma," IOP Conference Series: Materials Science and Engineering.Vol.4,No.6, pp.956, (2020)

37. A. A. Al Dairy, A.R. Ahmad, A. Qattan , and I.A. Al Fawares, " Synthesis and Characterization of Polymeric(PMMA-PVA) Hybrid Thin Films Doped with TiO_2 Nanoparticles Using Dip-Coating Technique ", Crystals, Vol. 11, No. 4, pp. 99, (2021).

38. P. Chaiyo, B. Duangsing, O. Thumthan, J. Nutariya and S. Pukird, " Electrical and Gas Sensing Properties of TiO_2/GO Nanocomposites for CO_2 Sensor Application", Journal of Physics,Vol.6, No.2, pp. (1-4), (2017).

39. D. F. Timokhov and F. P. Timokhov," Determination of Structure Parameters of Silicon by The Photoelectric Method," Journal of Physical Studies, Vol. 8, No. 2, pp. (173-177), (2004).

40. C. Kittel ,"Introduction to Solid State Physics",6th. Edition, Wiley,(1986).

41. P. J. Brown and j. B. Forsyth, "The Crystal Structure of Solid", Arnold,Vol.8,No.5, p.656,(1973).

42. S. Tarabichi and A. Baghdadi, " Polymers Types, Synthesis, Sensing, Properties and Horizons", Damascus University, Journal of Basic Sciences,Vol.16, No.1,pp.(141-149),(2000).

43. B.L. Mattes, "Polycrystalline and Amorphous Thin Films and Devices", Academic Press,Vol.8,No.9,pp(102-111), (1980).

44. D. A. Neamen , " Semiconductor Physics and Devices", University of New Mexico ,Vol.12,No.2,pp(267-2730, (1992).

45. S. Franssila , "Introduction to Microfabrication" , West Sussex , England , John Wiley and Sons Ltd ,Vol.4,No.2,pp.(16-23), (2004).

46. C. Kittel , "Introduction to Solid State Physics", John Wiley and sons , 5th Edition, (1986).

47. W. D. Callister , " Materials Science and Engineering", 4th Edition, (1997).

48. L. Pawlowski "The Science and Engineering of Thermal Spray Coatings" , John Wiley and sons , 2nd. Edition, France , book, (2007).

49. R.S. Rusu and G .I. Rusu , " The Electrical Properties of TiO_2 Thin Film" , Journal of Optoelectronics and Advanced Materials ,Vol. 7 ,No.5, p.234 , (2005) .

50. M. N. Rahaman, "Ceramic Processing and Sintering" 2nd. Edition , CRC Press, (2003).

51. H. F. Hashim Al-Luaibi ,"Preparation Of Conducting Poly (O-Toluidine) and Study of Its Electrical and Optical Properties for

Application as a Solar Cells " , Ph. D. Thesis University of Basrah , College of Science , Department of Physics , (2010) .

52. E. Li, A. Kim, and L. Zhang, " Modeling Excited States of Fluorescent Compounds with UV-VIS Spectra Calculations", student computational chemistry,Vol.1,No.7,pp.(23-55), (2007).

53. M.D. Tyona,"A Theoretical Study on Spin Coating Technique " Advances in Materials Research, Vol. 2, No. 4 , pp. (195-208), (2013).

54. B. Y. Kadem, "P3HT:PCBM-based Organic Solar Cells: Optimisation of Active Layer Nanostructure and Interface Properties ", Ph. D. Thesis Sheffield Hallam University , (2017).

55. J. Millman ,"Microelectronics", Murray – Hill, Book Company Kogakusha, Vol. 642,No.1, p. 172, (1979) .

56. A. Mihi, M. Oca,A. Mtlide, and H. Míguez, "Oriented Colloidal-Crystal Thin Films by Spin-Coating Microspheres Dispersed in Volatile Media," Adv. Mat., Vol.18,No,2, p. 22, (2006).

57. D. Meyerhofer, “Key Stages in Spin Coating Process”, J. Appl. Phys., Vol. 49,No.9, p. 3393,(1978) .

58. Kaneko and Nakamura, "Photoresponse of a liquid junction polyaniline film", Journal of the Chemical Society, Chemical Communications ,No.6,pp. (346–347), (1985).

59. K. L. Chopra, "Thin Film Devices Application", Plenum Press,Vol.6, No.2,pp.(80-90), (1983).

60. J. L. Comstock," Elements of Chemistry", 4th.Edition. New York, Published by Robinson Pratt, (1858).

61. K. Arshak, E. Moore, G.M. Lyons, J. Harris and S. Clifford," A Review of Gas Sensors Employed in Electronic Nose Applications", Sensor Review, Vol. 24, N. 2, pp. (181-198), (2004).

62. T. A. Miller, S. D. Bakrania, C. Perez and M. S. Wooldridge, "Nanostructured Tin Dioxide Materials for Gas Sensor Applications",

Department of Mechanical Engineering, University of Michigan, Ann Arbor, Michigan Vol.48,No.5,pp.(109-212), (2006).

63. G. Burns, "Solid State Physics", Academic Press,Vol.16,No,5,p.67, (1985).

64. Y.N. Jammal , " Soild State Physics", AL- Mousul University ,Arabic version ,Vol.16,No.7,pp.417, (1990).

65. M. G. Yousif, "Soild State Physics", University of Baghdad book, Vol. 2, (1989).

66. J. Pattar , S. N. Sawant , M. Nagaraja , N. Shashank , K. M. Balakrishna, G. Sanjeev and H. M. Mahesh , " Structural Optical and Electrical Properties of Vacuum Evaporated Indium Doped Zinc Telluride Thin Films", Int. J. Electrochem. Sci., Vol. 4, pp. (369-376) , (2009).

67. M. Dhanam, R.R. prabhu and P.K. Manoj , "Investigations on Chemical Bath Deposited Cadmium Selenide Thin Films" , Materials Ch and Phy, Vol. 107, pp. (289-296), (2008).

68. S. Dimitriev ,"Understanding Semiconductor Devices",Griffth University, New York, Oxford,Vol.5,No.3,p.245, (2000).

69. F. Scholz , "Compound Semiconductors", book, (2009).

70. J. I. Pankove, "Optical Processes in Semiconductors", Prentice-Hall, New Jersey,Vol.2,No.4,pp.(60-71), (1971).

71. A. H. Clark, "Optical Properties of Polycrystalline and Amorphous Thin Films and Devices", Academic press,Vol.3,No.9,pp.(1243-1255), (1960).

72. S.Ben," Solid State Electronic Devices" ,Hall International ,Vol.2,No.6,pp.(87-90),(1990).

73. M. S. Dresselhaus , "Optical Properties of Solids", Part II ,Vol.12,No.4,pp.(261-280), (1998).

74. Y. Sirotin , and Y. M. Shaskolskaya ,"Fundamentals of Crystal Physics ", Mir Publishers , Moscow,Vol.2,No.1,pp.(12-19), (1982).

75. V. Kumar, G. S. Sandhu, T. P. Sharma, and M. Hussain , "Growth and Characterization of Cd1- xZnxTe-Sintered Films" , Research Letters in Materials Science ,Vol.4,No.2,pp.(205-225), (2007).

76. Li Jin , Yang Linyu , Jian Jikang , Zou Hua , and Sun Yanfei , " Effects of Sn-doping on Morphology and Optical Properties of CdTe Polycrystalline Films", Journal of Semiconductors, Vol. 30, No. 11 , pp.(1577-1580), (2008).

77. G. Gordillo, F. Rojas and C. Calderón , " Optical Characterization of Cd(Sx,Te1-x) Thin Films Deposited by Evaporation", Superficies y Vacío , Vol. 16, No. 3 , pp.(30-33), (2003).

78. G. G. Rusu , and M. Rusu , "Optical Behavior of Multilayered Cdte/Cu Thin Films Deposited By Stacked Layer Method" , J. of Opt. and Advanced Materials, Vol. 7, No. 2 , pp. (885 – 889) , (2005).

79. M. Marafi, F. El Akkad, and B. Pradeep , "Properties of R.F. Sputtered Cadmium Telluride Thin Films ",Journal of Materials Science,Vol.14,No.1, pp. (21 – 26) , (2003).

80. S. Weng and M. Cocivera , "Preparation and Properties of Cadmium Telluride Prepared by a Three-Step Process" , Chem. Mater., Vol. 5,No.2, pp.(1577-1580), (1993).

81. J. D. Kraus, "Electromagnetic " , 3rd Edition. , Mc Graw-Hill, (1984).

82. Inoue , Yuasa and Okoshi , "Pd Doped TiO_2 Thin Films Prepared by PLD for Gas Sensors Applications ", Applied surface science ,Vol. 319 ,No.2, p. 686, (2006).

83. G. Korotcenkov , Sang Do Han and D. Fisher ," Doping Influence on Thermal Stability of The Film Structure ", Materials Chemistry and Physics ,Vol. 113 ,No.5, pp.(756–760) , (1997) .

84. A. P. Caricatoa , M. Catalanob , G. Ciccarellac , M. Martinoa , R. Rellab , F. Romanoa , J. Spadavecchiab , A. Taurinob , T. Tunnoa and D. Valerinia, " Matrix Assisted Pulsed Laser Evaporation for TiO_2

Nanoparticle Thin Film Deposition", Journal of Nano materials and Bio structures ,Vol.1,No. 2 , pp. (43 – 47) , (2005) .

85. E. Meyer, "Atomic Force Microscopy", Progress in Surface Science, Vol. 41,No.1, pp. (3-49) , (1992).

86. C. Kittel, "Introduction to Solid State Physics", 5th ed., Willy, New York, (1981).

87. A. Ivashchenko and I. Kerner,"Physical Approaches to Improvement of Semiconductor Gas Sensor Based on TiO_2 Thin Films", Moldavian J. of the Physical Sciences, Vol. 2, No .1, pp. (95-102), (2003).

88. D. Perednis and L. J. Gauckler,"Thin Film Deposition Using Spray Pyrolysis", Journal of Electroceramics,Vol.14,No.3, pp. (103–111), (2005).

89. T. Theivasanthi, and M. Alagar, "X-Ray Diffraction Studies of Copper Nanopowder", Archives of physics research, Vol. 1, No .2, pp. (112-117), (2010).

90. R. Rusu and G. Rusu, "On the Electrical of TiO_2 Thin Film" Journal of optoelectronics and advanced materials, Vol.7,No.5, p. 234, (2005).

91. A.D. Bhagwat , S . S . Sachin and M . M . Chandrashekhar, " Facile Rapid Synthesis of Polyaniline (PANI) Nanofibers", Journal of nano and electronic physics , Vol. 8, No 1, p. 1037 , (2016).

92. C. Srinivas, D. Srinivasu , B. Kavitha , N. Narsimlu and K .S . Kumar, "Synthesis and Characterization of Nano Size Conducting Polyaniline" , IOSR Journal of Applied Physic, Vol.1, Issue 5, pp. (12 – 15) , (2012) .

93. S. Chandraa, R. Bharadwaj and S . Mukherj,"Label Free Ultrasensitive Optical Sensor Decorated with Polyaniline Nanofibers: Characterization and Immunosensing Application" , Sensors and Actuators , Vol. 240 ,No.11, pp. (443–450), (2017).

94. M. B. Chorin , F. Moller and F. Koch, "Band Alignment and Carrier Injection At The Porous-Silicon Crystalline-Silicon Interface" J. Appl. Phys., Vol. 77, No. 9, pp. (82–88) , (1995).

95. J.M. Nunzi "Organic Photovoltaic Materials and Devices" C. R. Physique, Vol. 3 ,No.7, pp.(52–54), (2002).

96. Thornton and R. Andrew," Modern Physics for Scientists and Engineers", 3rd. Edition, Brooks/Cole, (2006).

97. A. J. Moulson and J. M. Herbe, "Electroceramics Materials, Properties ",2nd. Edition Materials, John Wiley and Sons Ltd, p.9, (2003).

98. J. Dessau, "Manual for Biological Remediation Techniques", International Centre for Soil and Contaminated Sites,Germany,Vol.4, No.2, pp.(80-95), (2006).

99. J.I. Kroschwitz, "Electric and Electronic Properties of Olgmers", John Wiley and Sons, INC. , (1988).

100. V. J. Mohanraj and Y. Chen, ,"Nanoparticles- A Review", Tropical Journal of Pharmaceutical Research, Vol. 5, No.1,pp. (561-573), (2006).

101. C. Yosuf "Preparation and Characterizaton of Conducting Polymer and Polyaniline -Titanum(IV) Oxide Composite Blended with Poly (Vinylcohol)", M.Sc. Thesis of Science (Chemistry), Universiti Teknologi Malaysia, (2005).

102. E.T. Abdullah, R . S . Ahmed, S . M . Hassan and A . N . Naje, " Synthesis and Characterization of PANI and Polyaniline/Multi Walled Carbon Nanotube Composite", International Journal of Application or Innovation in Engineering and Management , Vol. 4, No. 9 ,pp.(130-134), (2015).

103. K. M. Ziadan and H. H. Inayh, "Preparation and Characterization of Nanocompocite Conducting Polymers (PANI-DBSA/MWNCT)" , Chemistry and Materials Research , Vol.8, No.8, pp.(35-43) ,(2016).

104. J. G. Fernando , R. M .Vequizo, M . K . G . Odarve, B. R. B . Sambo, A . C . Alguno , R . M . Malaluan , R . T J . Candidato, J . E . Gambe , M . Jabian , G . J . Paylaga , F. R .G . Bagsican and H . Miyata ," Physico-chemical Effects of Supercritical Carbon Dioxide Post Polymerization Treatment on HCl-doped Polyaniline Prepared via Oxidative Chemical Polymerization ", Materials Science and Engineering ,Vol.5,No.2, p.(79), (2015).

105. A.O. Mousa and S. H. Nawfal, " Study of Some Optical Properties of Polyaniline Polymer", International Journal of Chem. Tech. Research, Vol. 10., No.3,pp.(55-64), (2017).

106. S. Ebrahim, A. Kashyout and M. Soliman, "Ac and Dc Conductivities of Polyaniline/Poly Vinyl Formal Blend Films", Current Applied Physics, Vol. 9, No. 2, pp. (44-45),(2009).

107. S. Hamza Trier,"Study of Some Physical Properties of p-MgxZnO_{1}–x/ n-Si Photodetector and Gas Sensor", Ph.D. Thesis, University of Babylon, College of Science,Department of Physics, (2017).